HEART RATE VARIABILITY AND RHYTHMIC INFLUENCES IN HUMAN ENDOTOXEMIA

By

JEREMY D. SCHEFF

A Dissertation submitted to the

Graduate School-New Brunswick

Rutgers, The State University of New Jersey and

The Graduate School of Biomedical Sciences

University of Medicine and Dentistry of New Jersey

in partial fulfillment of the requirements

for the degree of

Doctor of Philosophy

Graduate Program in Biomedical Engineering

written under the direction of

Ioannis P. Androulakis

and approved by

_____

_____

_____

_____

_____

New Brunswick, New Jersey

October, 2013

ABSTRACT OF THE DISSERTATION

Heart Rate Variability and Rhythmic Influences in Human Endotoxemia

by JEREMY D. SCHEFF

Dissertation Director:

Ioannis P. Androulakis

Inflammation is a critical component of the physiological response to stress. Ideally, the endpoint of inflammation is restoration of homeostasis. However, when anti-inflammatory processes fail to appropriately balance pro-inflammatory signals, inflammation can have deleterious effects. Clinically, this is problematic in diseases such as sepsis because therapies to control inflammation are limited. Rhythmic biological signals, ranging in time scale from very fast neural oscillations to very slow seasonal patterns, are ubiquitous in physiological systems, including those linked to inflammation. The characteristics of an oscillatory signal reflect the state of underlying rhythm-generating physiological systems. Through studying homeostatic rhythms and their disruption in inflammation, we gained insight into the underlying mechanisms and potential diagnostic utility embedded in physiologic variability via mathematical modeling and systems biology approaches.

Based on a mathematical model of human endotoxemia, an experimental model of systemic inflammation, we hypothesized that hormones entrain inflammatory mediators and impose circadian patterns on the endotoxemia response. A model of the interplay

between inflammation and circadian rhythms was developed and validated based on the temporal sensitivity of the inflammatory response. In addition to circadian rhythms, ultradian (~1hr) rhythms in cortisol are another prominent hormonal pattern linked to inflammation. By combining models of cortisol production and pharmacodynamics, we evaluated the downstream implications of ultradian rhythms, finding a relationship between the amplitude of homeostatic ultradian rhythms and responsiveness to subsequent stress. Heart rate variability (HRV) has been studied as a potential prognostic marker in inflammation-linked diseases. We modeled the interactions between human endotoxemia and the autonomic nervous system to understand the loss of HRV in response to stress, allowing for the rationalization of experimental observations in the framework of a quantitative model. Finally, we identified a warning signal of transitions between steady states in a mathematical model of chronic endotoxemia, illustrating the potential for our research to be applied in a translational context. These results all point towards the importance of rhythmic patterns in the underlying physiological systems driving the inflammatory response and the potential for useful information about these systems to be derived from the analysis of variability in physiological signals.

ACKNOWLEDGEMENT

First, I thank my advisor Yannis Andoulakis for the bulk of my growth as a researcher throughout my time at Rutgers. It would be difficult for me to overstate how much he helped my perspective on science change and broaden since I arrived here. I would also like to thank my friends and family members who have helped me in tough times and enjoyed life with me in good times.

Table of Contents

List of Tables

List of Illustrations

Chapter 1: Introduction

1.1: The Clinical Problem of Systemic Inflammation

Inflammation is a critical component of the physiological response of an organism to stressors. When the inflammatory response is successful, it leads to the healing of injury or the clearance of infection, and then the inflammatory process self-regulates and returns to homeostasis. However, when anti-inflammatory mechanisms fail to adequately counterbalance pro-inflammatory activity, the body can reach a state of prolonged, unresolving systemic inflammation.

This dysregulated inflammatory state can cause significant harm to the body even in the absence of any exogenous stressor. Further complicating this issue is our general inability to effectively modulate persistent inflammatory states. Clinically, this represents a major challenge. It has long been known the control of inflammatory balances plays a key role in the progression of a variety of inflammation-related disorders (Bone 1996). Yet even general classes of approaches that work in the context of one particular disease may not apply more broadly. For instance, novel therapies aimed at treating rheumatoid arthritis and inflammatory bowel disease with anti-cytokine therapies have shown promise in recent years, but similar strategies have not produced such promising results in treating sepsis (Marshall 2003; Deans, Haley et al. 2005).

Therapies for the management and control of inflammation in septic patients are limited (Martin, Mannino et al. 2003) and the only recently approved novel therapy (activated protein C) failed to show improved outcome in a repeat Phase III clinical trial (Angus 2011). Sepsis is a syndrome resulting fundamentally from the activation of the systemic inflammatory response (SIRS) in the presence of a severe infection (Angus,

Linde-Zwirble et al. 2001; Decker 2004). Sepsis has an immense cost, both in human life lost and in expenditure of healthcare resources. Annually there are more than three quarters of a million cases, having an in-hospital mortality rate of over 25% and an average cost per case of more than $20,000 (Angus, Linde-Zwirble et al. 2001). This leads to over 200,000 deaths annually in the United States, making sepsis one of the leading causes of death nationwide (Kochanek and Smith 2004). Therefore, novel approaches to understand the biological mechanisms behind inflammation and their dysregulation in inflammation-linked diseases such as sepsis is of critical importance (Marshall 2008).

1.2: The Human Endotoxemia Model

Human endotoxemia is the response to the elective administration of endotoxin (lipopolysaccharide, LPS), a component of the outer membrane of Gram-negative bacteria that is recognized by the innate immune system and provokes an inflammatory response. Although acute, systemic inflammation is of course not reflective of all of the physiological changes occurring in complex disease like sepsis, human endotoxemia does precipitate signs and symptoms characteristic of clinical sepsis (Lowry 2005; Andreasen, Krabbe et al. 2008), acute respiratory distress syndrome (ARDS) (Buttenschoen, Kornmann et al. 2008), and trauma (Shanker, Coyle et al. 2010). These physiological changes include transcriptional responses in immune cells, secretion of cytokines and hormones, and changes in autonomic activity (Lowry 2009). All of these effects stem from responses generated by the binding of LPS to Toll-like receptor 4 (TLR4), thus activating innate immune cells and stimulating pathways linked to the production of inflammatory genes such as the NF-κB, JAK-STAT, and MAPK signaling pathways

(Foteinou, Calvano et al. 2009). This transcriptional activity leads to the production and release of both pro-inflammatory and anti-inflammatory cytokines, mediators of the inflammatory response and the return to homeostasis, respectively.

The initial inflammatory response to LPS also propagates through afferent nervous signaling to the central nervous system (CNS), which then forms a feedback loop to regulate the progression immune response through modulating sympathetic and parasympathetic activity, which may be reflected in increased heart rate (HR) and decreased heart rate variability (HRV) (Godin, Fleisher et al. 1996). In particular, central regulation plays a role in governing the inflammatory response both through autonomic activity itself (Tracey 2002) and though the activation of the hypothalamic-pituitary-adrenal (HPA) axis and the subsequent release of anti-inflammatory hormones such as cortisol (Beishuizen and Thijs 2003).

1.2.1: Physiologic Variability in Human Endotoxemia

Many of the components involved in the inflammatory response contain homeostatic rhythmic variability, and advances in clinical and experimental tools make assaying the state of these rhythms increasingly plausible. Figure 1.1 shows several of these homeostatic rhythms, including mediators directly involved in inflammation such as cytokines and immunomodulatory hormones, as well as oscillatory components that give rise to patterns in heart rate variability (HRV) that are disrupted in inflammation such as breathing pattern, blood pressure rhythms, and autonomic activity. Underlying every biochemical oscillator is some type of negative feedback mechanism (Novak and Tyson 2008). Possibly the simplest system to consider is a protein that acts as a transcription factor by inhibiting the transcription of its own mRNA. Given appropriate

time delays in transcription, translation, and translocation, as well as appropriate rate constants, this simple single-gene system oscillates (Novak and Tyson 2008). Real physiological systems typically consist of much more complex networks comprised of multiple feedback loops. Even still, physiological rhythms are of clinical interest because characteristics of those patterns convey information about the underlying system that is producing them, beyond simply measuring the mean value of a signal. For instance, in some cases, the network structure giving rise to rhythms can be reverse engineered from the pattern of rhythmicity (Pigolotti, Krishna et al. 2007). Given that negative feedback loops are critical in maintaining homeostasis and acute responsiveness, perturbations in negative feedback loops culminating in altered rhythmic patterns can reveal information about the integrity of the negative feedback system (Veldhuis, Keenan et al. 2008).

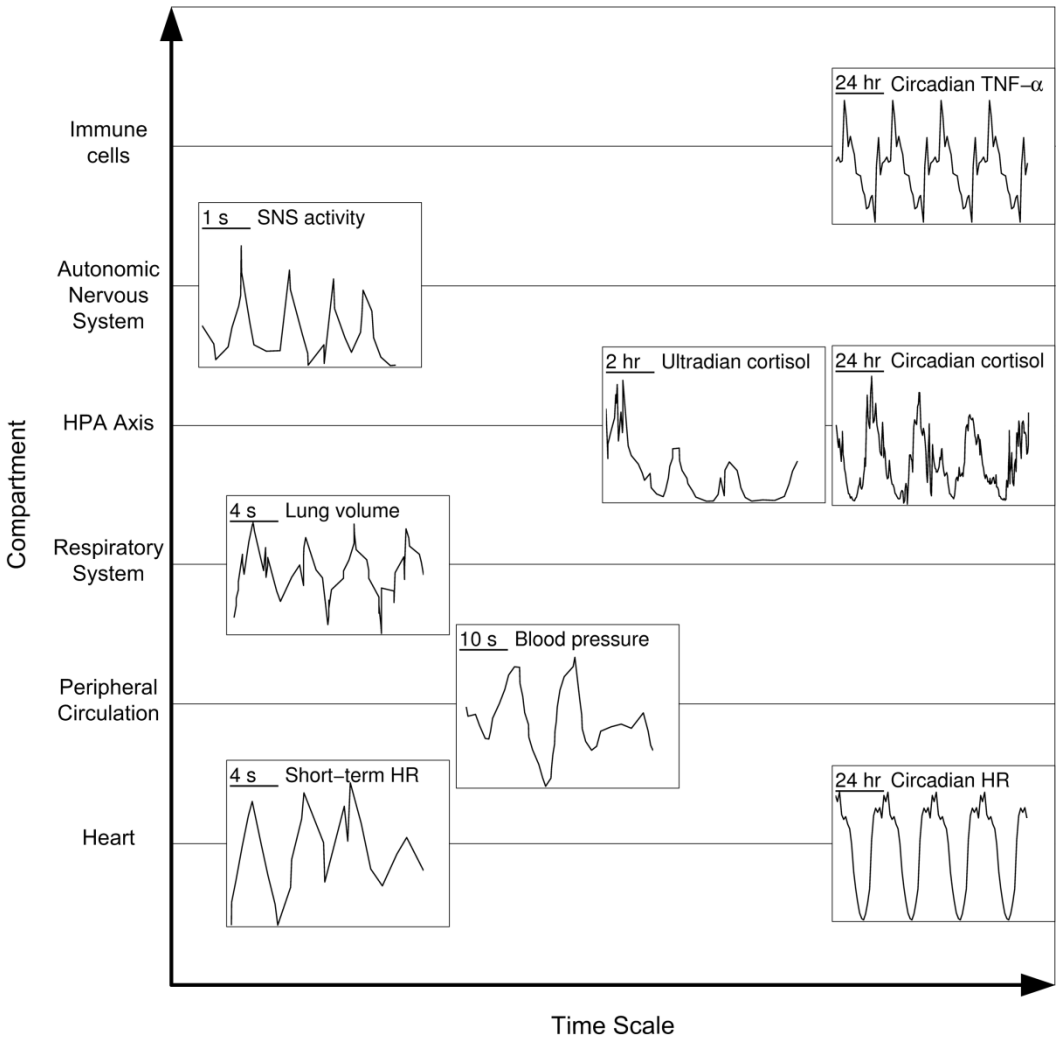

Figure 1.1: Homeostatic rhythms, at a variety of time scales, which contribute to altered physiologic variability in endotoxemia. TNF-α data: (Petrovsky and Harrison 1998). Sympathetic nervous system activity data: (Donadio, Cortelli et al. 2008). Circadian cortisol data: (Brown, Meehan et al. 2001). Ultradian cortisol data: (Charloux, Gronfier et al. 1999). Lung volume, blood pressure, and short-term HR data: (Seydnejad and Kitney 2001). Circadian HR data: (Octavio, Rodriguez et al. 2004). TNF-α is an inflammatory cytokine that has a clear circadian pattern in response to LPS stimulation, and other cytokines also exhibit circadian patterns (Petrovsky and Harrison 1998). Autonomic signaling in inflammation contributes both to changes in cardiac function and modulation of the inflammatory response, and oscillatory activity is inherent in both sympathetic and parasympathetic branches. Cortisol is an anti-inflammatory hormone, with a large circadian rhythm riding on top of an ultradian rhythm. Blood pressure and respiratory rhythms contribute to short-term patterns in HR, which are diminished in endotoxemia

Clinically, patterns in physiological signals represent a broad source of potential diagnostic and prognostic markers. For instance, perturbations in the rhythmicity of heart beats precede the onset of neonatal sepsis (Griffin, O'Shea et al. 2003; Moorman, Carlo et al. 2011). At a much longer time scale, circadian variations in plasma cortisol concentration, a factor that has been linked to immune dysfunction, has been associated with chronic stress resulting from depression (Yehuda, Teicher et al. 1996), obesity (Rosmond, Dallman et al. 1998), psychological stress (Polk, Cohen et al. 2005), and cancer (Mormont and Levi 1997; Sephton, Sapolsky et al. 2000). The loss of rhythmicity in these cases may reflect an underlying loss in the regulation of negative feedback control systems.

1.3: Autonomic Dysfunction and HRV

The autonomic nervous system is commonly divided into two branches, sympathetic and parasympathetic. Although these branches often function antagonistically, under certain circumstances they exhibit complementary behavior; for instance, co-activation of sympathetic and parasympathetic nerves at the sinoatrial region of the heart can produce an increased cardiac output relative to isolated stimulation of either nerve. It is well established that the autonomic nervous system plays a critical role in the progression and resolution of the inflammatory response by communicating through afferent and efferent neural mechanisms with the immune system. In systemic inflammation, activation of the autonomic nervous system leads to the release of immunomodulatory hormones. Furthermore, it has recently been shown that the activity of the parasympathetic nervous system can more directly modulate the inflammatory response in real time (Munford and Tracey 2002).

Clinical measurement of autonomic activity is challenging and imprecise, yet there are a variety of techniques that can give some insight into autonomic function. Analysis of heart rate variability (HRV), generally defined as the quantification of some aspect of beat-to-beat variability in heart rate, is commonly used to develop metrics reflecting autonomic activity. The sinoatrial (SA) node, the pacemaker of the heart, is innervated by both sympathetic and parasympathetic branches of the autonomic nervous system. Thus, changes in autonomic outflow provoke changes in the pattern of heartbeats. These are simple and noninvasive metrics that indirectly reflect cardiac autonomic modulation. Spectral analysis of HRV reveals two distinct frequency bands: low frequency (LF, 0.04-0.15 Hz) and high frequency (HF, 0.15-0.4 Hz). The spectral power in both frequency bands gives some indication of autonomic activity. HF is driven by the respiratory cycle and also responds to vagal signaling. LF responds to changes in both sympathetic and vagal activity. LF and HF are often interpreted as reflecting sympathetic and parasympathetic activity respectively and their ratio is often used to assess autonomic balance. Despite the fact that these metrics are, at best, overlapping and indirect measures of autonomic activity (Karemaker 1999), HRV has still proven to be useful in prognostic and diagnostic applications.

Much has been learned about neuroimmune crosstalk in inflammation from endotoxemia experiments. However, even in controlled human endotoxemia experiments, the extent of correlation between the inflammatory state (*i.e.* cytokine levels) and autonomic dysfunction as assessed by HRV is not clear. One study found a weak correlation between various HRV metrics and TNF-α (Jan, Coyle et al. 2010), yet another found no relationship between HRV and cytokine levels (Kox, Ramakers et al. 2011) and

therapies like exogenous glucocorticoid treatment can alter cytokine responses without a corresponding change in HRV in a dose dependent manner (Rassias, Guyre et al. 2011). These results are not necessarily surprising, as autonomic dysfunction is just one of many physiological changes occurring in inflammation. However, they do suggest that a simple relationship between HRV and inflammatory state is unlikely to be found, particularly in a heterogeneous clinical environment rather than a controlled experimental setting. But even lacking a precise mechanistic interpretation of HRV in inflammation and sepsis, the clinical studies cited earlier show its importance as a prognostic and diagnostic tool.

In an attempt to explain the pathogenesis of multiple organ dysfunction syndrome (MODS), as often occurs in sepsis, it has been hypothesized (Godin and Buchman 1996) that biological networks are collections of oscillatory systems (organs) that are coupled to one other and that the maintenance of healthy homeostasis is based both on the integrity of each oscillator and on the coupling between them. This hypothesis predicts that, when interorgan communication is disrupted and organs become isolated, the loss of oscillatory coupling leads to more regular output. This is supported both by a variety of mathematical models as well as experimental results. For instance, in response to human endotoxemia, the beats of the heart become more regular while autonomic regulation of HR is diminished (Sayk, Vietheer et al. 2008). This type of uncoupling of autonomic regulation of the heart has been implicated in pediatric sepsis (Ellenby, McNames et al. 2001).

A change in autonomic modulation of one tissue does not necessarily imply a similar change has occurred in other tissues. Although much of the results presented here discuss changes in the function of the heart, this is also important in considering the

transition to MODS, as centrally impaired neural signaling impacts many target organs. From this perspective, diminished HRV in sepsis and SIRS may not reflect only modulated autonomic activity but the loss of the ability to convey interorgan signals via the autonomic nervous system.

1.4: Systems Biology and Mathematical Modeling of Inflammation

One of the primary challenges hampering the discovery of effective therapies for inflammation-driven diseases is that multiple interacting pathways regulate the inflammatory response, giving rise to complex dynamics and often unintuitive results (Freeman and Natanson 2000). Approaching this challenge requires a systems-level understanding of inflammation (Seely and Christou 2000; Vodovotz, Clermont et al. 2004) through mathematical and computational models of inflammation (Vodovotz, Constantine et al. 2009). Mathematical modeling facilitates studying the dynamics of a complex system while providing a systematic framework for integrating knowledge from diverse disciplines (Sontag 2004). Through this process, systems-based modeling leverages massive amounts of information, providing insight into both disease progression and potential therapeutic interventions (Rajasethupathy, Vayttaden et al. 2005). In some respects , computational models can be viewed as digital analogs of transgenic animals in that components of the system can be manipulated to investigate a hypothesis (Kitano 2002). Mathematical models represent quantitative, explicit hypotheses of system function at a wide range of scales and levels of detail. Modeling the inflammatory response has the potential to lead to innovations in translational medicine where scientific research is applied for improved clinical care, for instance in rationalizing drug development, designing clinical trials, and optimizing patient care

(Vodovotz, Csete et al. 2008; Foteinou, Calvano et al. 2009). These tasks are all especially important in the context of inflammation-linked diseases like sepsis where mortality rates are high yet novel clinical developments have been slow (Namas, Zamora et al. 2011).

Fundamentally, models of inflammation generally seek to understand the balance between pro- and anti-inflammatory effects. Ideally, the pro-inflammatory response is swift and strong enough to eliminate the inflammatory instigator (*e.g.* a pathogen) and then activate anti-inflammatory mechanisms which restore homeostasis. Additionally, heightened inflammation can also damage healthy tissue, releasing danger signals that further enhance pro-inflammatory signaling (Matzinger 2002). Conversely, it is also problematic if inflammation is not strong enough to eliminate the inflammatory &□&□&□&□&□&□&積&訬&▪&詆&▪&譞&讞&▪&▪&負&□□□□□□□□□□ □□□□□□□□□□□□□□□□□□□□□□□□□□□□□□□□□□□□□□□esponses (pathogen, pro-inflammation, anti-inflammation, damage) may exhibit complex dynamics; simple models of inflammation can produce interesting and biologically relevant dynamical patterns (Kumar, Clermont et al. 2004; Day, Rubin et al. 2006; Reynolds, Rubin et al. 2006). Of course, real biological networks are far larger and introduce further complexities. More complex models can account for spatial heterogeneity and stochasticity (An 2008; Dong, Foteinou et al. 2010) as well as a larger number of components, working towards unraveling the redundant complexity of inherent in inflammation. In addition to the fact that these more complex models contain more assumptions and unknowns which lead to problems with identifiability, larger models often make infeasible the kind of detailed mathematical analysis and intuitive understanding that can be achieved through the study of simpler models.

Much of the work presented in this dissertation is based on a mathematical model of human endotoxemia (Foteinou, Calvano et al. 2009; Foteinou, Calvano et al. 2009; Foteinou, Calvano et al. 2010; Foteinou, Calvano et al. 2011). This model can be considered to be of intermediate complexity, in that it does not attempt a fully detailed molecular description of inflammation, but it has grown to encompass some mechanistic detail, for instance in NF-κB signaling and cortisol pharmacodynamics. At the cellular level, recognition of LPS by TLR4 on immune cells leads to the activation of the NF-κB pathway and ultimately the production of both pro-inflammatory (*P*) and anti-inflammatory (*A*) cytokines, which are proximal mediators of the systemic inflammatory response (Opal and DePalo 2000) and antagonistically work towards the self-regulation and resolution of inflammation. At the neuroendocrine level, the hypothalamic-pituitary-adrenal (HPA) axis and the sympathetic nervous system (SNS) are the primary stress response pathways by which the central nervous system (CNS) regulates the immune response (Sternberg 2006). This was modeled by assuming that the production and release of counter-regulatory anti-inflammatory endogenous hormones cortisol (*F*) and epinephrine (*EPI*) respond to pro-inflammatory cytokines, and then these hormones feed back to modulate the transcriptional response in leukocytes. One notable feature of this model is that it contains no physiologic variability. Either the system is constant at a steady state, or the system is smoothly moving to a steady state in response to an external disturbance (*e.g.* exogenous LPS administration). The network structure is displayed in Figure 1.2 and the model is discussed in more detail, including equations and parameter values, in Appendix A.

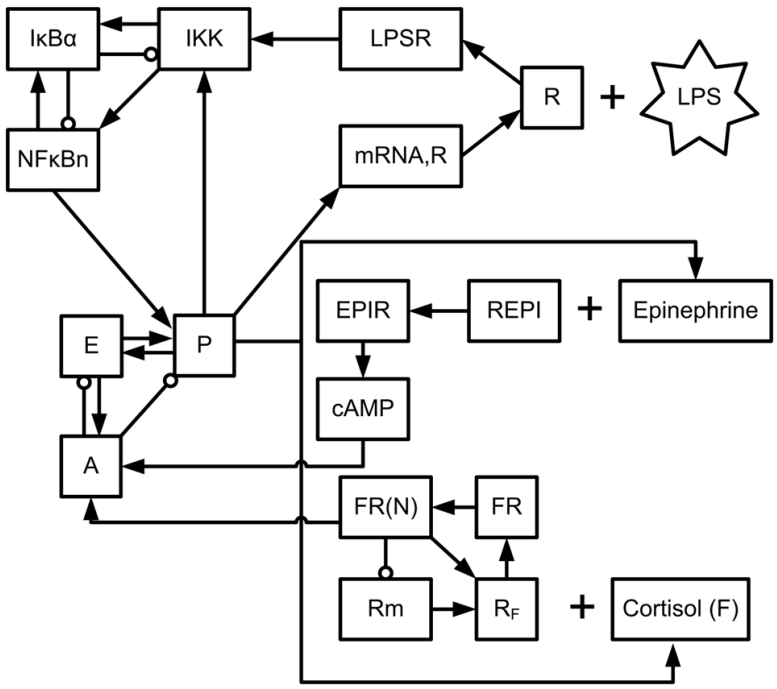

Figure 1.2: Network diagram of the model of human endotoxemia described in Appendix A (Foteinou, Calvano et al. 2010).

1.5: Outline of Subsequent Chapters

Through studying homeostatic rhythms and their disruption in inflammation in the context of mathematical modeling and systems biology, we gained insight into the underlying mechanisms and potential diagnostic utility embedded in physiologic variability.

Circadian rhythms have been shown to play a critical role in the treatment and progression of many diseases. Several of the key components of the inflammatory response, including cytokines and hormones, exhibit significant circadian patterns. Based on the mathematical model of human endotoxemia presented in Appendix A, we hypothesized that central hormonal circadian systems can entrain inflammatory mediators and impose circadian patterns on the response to endotoxemia. As is presented in Chapter 2, a model of the interplay between inflammation and circadian rhythms was developed

and validated by its ability to reproduce diverse sets of experimental data and clinical observations concerning the temporal sensitivity of the inflammatory response.

The circadian pattern of cortisol secretion is fundamentally driven by circadian variations in the characteristics of a faster (~1 hr period) ultradian rhythm; however, the physiological effects of ultradian rhythms are less clear. By combining a model of cortisol by the hypothalamic-pituitary-adrenal (HPA) axis production with a pharmacodynamic model, we evaluated the implications of ultradian rhythms in cortisol in Chapter 3. The downstream transcriptional effects of glucocorticoid pulsatility are reflected by the difference in transcript abundance of glucocorticoid responsive genes when exposed to a normal ultradian glucocorticoid rhythm and a constant level of glucocorticoids with the same area under the curve (AUC) as the ultradian pattern. HPA axis parameter perturbations, altering both the amplitude and frequency of glucocorticoid bursts, diminish the difference between constant and ultradian cases as the ultradian rhythms become flatter. Furthermore, we found a relationship between the amplitude of homeostatic ultradian rhythms and responsiveness to subsequent stress, suggesting that ultradian rhythms may confer desirable properties on the HPA axis.

Heart rate variability (HRV), the quantification of beat-to-beat variability, has been studied as a potential prognostic marker in inflammatory diseases such as sepsis. Chapter 4 focuses on the relationship between HRV and human endotoxemia. We modeled the interactions between human endotoxemia and the autonomic nervous system to understand the loss of HRV in response to stress. Additionally, we explored the dynamics of autonomic-heart coupling to understand experimental data on HRV from human endotoxemia experiments in the framework of a quantitative model. This

produced multiple plausible alternative hypotheses regarding autonomic function in inflammation which give insight into our current state of knowledge regarding autonomic dysfunction in inflammation and will guide future research.

In Chapter 5 we focus on a modality of the potential translational application of systems biology and mathematical modeling. From the perspective of physiology as a dynamical system, an important task is identifying the propensity to transition from one steady state to another, which in practice can occur abruptly. Detecting impending transitions between steady states is of significant importance in many fields, and thus a variety of methods have been developed for this purpose, but lack of data has limited applications in physiology. Here, we propose a parameter-free model-based approach towards identifying critical transitions in systemic inflammation based on a minimal amount of assumptions about the availability of data and the structure of the system. We derived a warning signal metric to identify forthcoming abrupt transitions occurring in a mathematical model of chronic inflammation with a gradually increasing bacterial load. Intervention to remove the inflammatory stimulus was successful in restoring homeostasis if undertaken when the warning signal was elevated rather than waiting for the state variables of the system themselves to begin moving to a new steady state.

These results all point towards the importance of rhythmic patterns in the underlying physiological systems driving the inflammatory response and the potential for useful information about these systems to be derived from the analysis of variability in physiological signals and leveraged through computational modeling.

Chapter 2: Modeling the Influence of Circadian Rhythms on Human Endotoxemia

2.1: Introduction

In recent years, a number of models of inflammation and endotoxemia have been developed by applying different modeling techniques (agent based modeling or equation based modeling), at different scales (molecular, cellular, systemic, or a combination), and focusing on different specific problems (acute inflammation, trauma, or the response to a specific disease) (Jit, Henderson et al. 2005; Lipniacki, Paszek et al. 2006; Prince, Levy et al. 2006; Zuev, Kingsmore et al. 2006; Mi, Riviere et al. 2007; An 2008; Kumar, Chow et al. 2008; Li, Verdolini et al. 2008; Foteinou, Calvano et al. 2009). These models have been developed with the practical goals of impacting healthcare through translational systems biology (Vodovotz, Csete et al. 2008; Foteinou, Calvano et al. 2009) and rationalizing the design of experiments and clinical trials (Clermont, Bartels et al. 2004). Because of the large number of components involved in inflammation, existing models make assumptions about which interactions are most important, either by simplifying or neglecting certain elements. One aspect that has not previously been studied from the perspective of systems biology is the interplay between circadian rhythms and inflammation.

Circadian rhythms are periodic processes that are synchronized to the 24 hour light/dark cycle. This rhythmicity is widely observed in humans from the scale of biochemical reactions, such as hormone production, to behavioral patterns, such as regular sleeping and feeding times. In the context of healthcare, mouse and rat models have shown that the same dose of a drug can be lethal at certain times and ineffective at

others (Levi and Schibler 2007). Thus, it is not surprising that there is also a circadian component to inflammation; in fact, many of the elements typically included in models of inflammation (leukocytes, cytokines, and hormones) are known to have strong circadian patterns (Coogan and Wyse 2008). The importance of these variations is apparent by observing that sepsis patients have a heightened risk of mortality between 2am and 6am (Hrushesky and Wood 1997).

This chapter presents a mathematical model of the interplay between circadian rhythms in inflammation that synthesizes disparate biological knowledge about these systems. Circadian variability is introduced into our previous multiscale model of inflammation (Appendix A) under the hypothesis that the observed circadian variations in the inflammatory response are governed by the hormones cortisol and melatonin and their interactions with immune cells. The model is validated by its ability to reproduce experimental results from a variety of sources and its qualitatively accurate predictions of circadian variability in the strength of the inflammatory response.

2.2: Model

Many of the components described in Appendix A are known to have circadian rhythms. Several studies have shown that numerous pro- and anti-inflammatory cytokines undergo circadian variations in plasma levels, typically peaking in the night (Zabel, Horst et al. 1990; Petrovsky and Harrison 1997; Petrovsky and Harrison 1998; Petrovsky, McNair et al. 1998; Hermann, von Aulock et al. 2006). Plasma cortisol levels also exhibit a circadian pattern, peaking in the early morning. Cortisol is produced by the actions of the hypothalamic-pituitary-adrenal axis, and the circadian production is due to

stimulation from the central circadian clock in the suprachiasmatic nucleus (SCN) (Hermann, von Aulock et al. 2006; Kohsaka and Bass 2007).

Due to the immunomodulatory effects of glucocorticoids and the strong circadian pattern of plasma cortisol levels, cortisol has been implicated in the circadian entrainment of cytokine production (Petrovsky and Harrison 1998). However, exogenous glucocorticoid administration is known to have a differential effect on cytokines; it stimulates the production of anti-inflammatory cytokines while inhibiting the production of pro-inflammatory cytokines (Barber, Coyle et al. 1993; Barnes 1998). Thus, it seems unlikely that cortisol alone could be responsible for the observed fluctuations in cytokine level, especially in light of the fact that a number of other hormones also vary either in or out of phase with cytokine levels (Petrovsky and Harrison 1998).

Of particular interest is the hormone melatonin, due to its potential role as a mediator in the crosstalk between the SCN and the immune system (Coogan and Wyse 2008). Melatonin is tightly regulated to have a peak in production in the night while remaining at very low levels the rest of the day and it has been shown to stimulate the production of cytokines, likely through the melatonin receptors in human leukocytes (Guerrero and Reiter 2002; Skwarlo-Sonta, Majewski et al. 2003). This is supported by experimental evidence showing that pinealectomy leads to decreased cytokine production in mice (del Gobbo, Libri et al. 1989). Thus, in the model presented herein, melatonin is used as the primary circadian regulator of cytokine production. Melatonin and cortisol drive the circadian variation in all of the model variables.

In (Chakraborty, Krzyzanski et al. 1999), six different mathematical models are fit to experimental data to reproduce the circadian profile of plasma cortisol levels. They

found that several of these models were adequately able to capture the dynamics of the cortisol profiles. To assess which circadian cortisol equation is most effective to incorporate into this multiscale model of inflammation, the different circadian cortisol models were tested and shown to produce qualitatively similar results. Ultimately, this work incorporates the "two rates" model due to its simplicity. In this model, a zero-order production term (*RF*) is set to two different values depending on the time of day and the circadian pattern is induced by using a high production rate in the morning and a low production rate the rest of the day (Eq. 2.1a). For comparison, results for the most complex model, consisting of the first three terms of a Fourier series fit to the data (Eq. 2.1b), are also shown.

$$\frac{dF}{dt} = RF + k_{in,F_{en}} \cdot \left(1 + H_{F_{en},P}\right) - k_{out,F} \cdot F$$
$$RF = \begin{cases} k_{in,RF1}, & t_{F1} < \mathrm{mod}(t,24) < t_{F2} \\ 0, & t_{F2} < \mathrm{mod}(t,24) < t_{F1} \end{cases} \quad (2.1a)$$

$$RF = a_0 + \sum_{n=1}^{3}\left[a_n \cos(2\pi nt/24) + b_n \sin(2\pi nt/24)\right] \quad (2.1b)$$

Melatonin is modeled in a similar manner (Eq. 2.2), using *RM* as a zero-order production term that is large during the night and small during the rest of the day and also including a first-order degradation term. More complex models of melatonin production are not investigated because melatonin levels do not have the type of biphasic pattern that is sometimes apparent for cortisol. However, it is well established that pro-inflammatory cytokines can reduce or even fully suppress the nocturnal peak in melatonin (Skwarlo-Sonta, Majewski et al. 2003; Jiang-Shieh, Wu et al. 2005; Fernandes, Cecon et al. 2006; Pontes, Cardoso et al. 2006; Pontes, Cardoso et al. 2007; Couto-Moraes, Palermo-Neto et al. 2009) and corticosteroids can antagonize this effect by stimulating melatonin

production (Ferreira, Fernandes et al. 2005; Fernandes, Cecon et al. 2006; Fernandes, Bothorel et al. 2009). The indirect effect of these two substances on melatonin production is modeled by including an indirect stimulus term for cortisol and an indirect inhibition term for pro-inflammatory cytokines on the production rate of melatonin.

These models for cortisol and melatonin (Eq. 2.1, 2.2) are fit to experimental data (Hermann, von Aulock et al. 2006; Grivas and Savvidou 2007) to ensure that the peak levels of hormones in the model occur at the correct times.

$$\frac{dM}{dt} = RM \cdot \left(1 + \frac{F}{1+F}\right) \cdot \left(1 - \frac{P}{1+P}\right) - k_{out,RM} \cdot M$$
$$RM = \begin{cases} k_{in,RM1}, & t_{M1} < \mathrm{mod}(t,24) < t_{M2} \\ k_{in,RM2}, & t_{M2} < \mathrm{mod}(t,24) < t_{M1} \end{cases} \qquad (2.2)$$

Melatonin has been shown to stimulate the production of both pro- and anti-inflammatory cytokines (Petrovsky and Harrison 1997; Raghavendra, Singh et al. 2001). This is modeled by adding a stimulating term to the production rates of P and A (Eq. 2.3). The strength of these interactions is calibrated based on experimental data for IL-1α (P) (Petrovsky, McNair et al. 1998) and IL-10 (A) (Petrovsky and Harrison 1997).

$$\frac{dP}{dt} = k_{in,P} \cdot (1 + H_{P,NFkBn}) \cdot (1 + H_{P,E}) \cdot (1 + H_{P,M}) / A - k_{out,P} \cdot P \qquad (2.3a)$$

$$\frac{dA}{dt} = k_{in,A} \cdot \left(1 + H_{A,cAMP}\right) \cdot \left(1 + H_{A,E}\right) \cdot \left(1 + H_{A,FRN}\right) \cdot (1 + H_{\mathrm{A,M}}) - k_{out,A} \cdot A \qquad (2.3b)$$

Cortisol produced in the adrenal cortex directly interacts with the adrenal medulla, stimulating epinephrine production (Wurtman, Pohorecky et al. 1972). This matches up well with available experimental data which shows that plasma epinephrine levels lag cortisol levels (Kronfol, Nair et al. 1997; Dimitrov, Benedict et al. 2009). This is modeled by letting cortisol stimulate the production rate of epinephrine (Eq. 2.4a). The normal

circadian pattern of heart rate variability (HRV) is roughly sinusoidal with a peak in the night (Massin, Maeyns et al. 2000); this behavior is likely driven by sleep patterns and a decrease in sympathetic activity at night (Ewing, Neilson et al. 1991). In this model, epinephrine is used as a surrogate for sympathetic activity, which inhibits the production rate of HRV. Experimental data are used to validate the responses of epinephrine (Kronfol, Nair et al. 1997) and HRV (Massin, Maeyns et al. 2000).

$$\frac{dEPI}{dt} = k_{in,EPI} \cdot \left(1 + H_{EPI,P}\right) \cdot \left(1 + H_{EPI,FRN}\right) - k_{out,EPI} \cdot EPI \tag{2.4a}$$

$$\frac{dHRV}{dt} = k_{in,HRV} \ / \ EPI - k_{out,HRV} \cdot HRV \tag{2.4b}$$

It is difficult to draw precise, quantitative conclusions about specific levels of the variables in this model because often, experimental data is not sufficient to calibrate the model. For instance, the measurements of cytokines that are used are indirect measurements that only give relative levels of cytokines (Petrovsky and Harrison 1997; Petrovsky, McNair et al. 1998). Thus, when plotted, all variables are scaled to be between 0 and 1 in the baseline case when there is no inflammatory stimulus by subtracting the minimum and dividing by the difference between the maximum and minimum. These scalings are then consistently used throughout the other figures.

All of the parameters used in the following simulations (beyond those presented in Appendix A) are shown in Table 2.1. After fitting the model to the data, sensitivity analysis is performed to gain insight into the model's dependence on the newly-introduced parameters. As in (Ihekwaba, Broomhead et al. 2004; Yue, Brown et al. 2006), for each parameter, the sensitivity coefficient is calculated as

$$S_p^m = \frac{\delta m / m}{\delta p / p} \tag{2.5}$$

where p represents the parameter that is varied, δp is an incremental perturbation in the parameter, m is the response of the original system, and δm is the incremental change in m due to the perturbation δp. Then, m is defined as the minimum value of *HRV*, i.e. maximum *HRV* depression, throughout the entire time course in response to a low dose of LPS that results in a self-limited inflammatory response. Effectively, this sensitivity analysis measures how the perturbations in the parameter values affect the overall systemic response to the stimulus. Because this model responds differently depending on the time of dosing, due to the circadian nature of the baseline, the sensitivity analysis is run 24 different times to capture the response to LPS at the 24 different hours of the day.

Parameter	Value	Parameter	Value	Parameter	Value
$k_{in,RM1}$	0.406	$k_{P,M}$	0.973	T_{M1}	1.732
$k_{in,RM2}$	0.032	$k_{A,M}$	1.000	T_{M2}	20.149
$k_{out,RM}$	0.421	T_{F1}	12.082	$k_{in,HRV}$	1.185
$k_{in,RF1}$	0.992	T_{F2}	16.530	$k_{out,HRV}$	1.045
$k_{EPI,FRN}$	0.090				

Table 2.1: Parameters for Eq. 2.1-2.4, in addition to those defined in Appendix A.

2.3: Results

Eq. 2.1-2.4, combined with the remaining unmodified equations from Appendix A, comprise a model of human endotoxemia that takes into account circadian variations in most of its variables. A network diagram of these interactions is shown in Figure 2.1. The model consists of several interacting modules representing various different scales; at the cellular level, the three essential transcriptional responses (pro-inflammatory P, anti-inflammatory A, and energetic E) are regulated by NFkB signaling and the recognition of LPS, as shown in the cellular level in Figure 2.1. The circadian hormones section of Figure 2.1 shows how circadian rhythms in the components of the system are

driven by SCN-regulated circadian rhythms in cortisol and melatonin production. Interactions between peripheral inflammation and the neuroendocrine axis are accounted for by incorporating the inflammatory effects of the hormones cortisol, epinephrine, and melatonin along with the systemic level influences on heart rate variability.

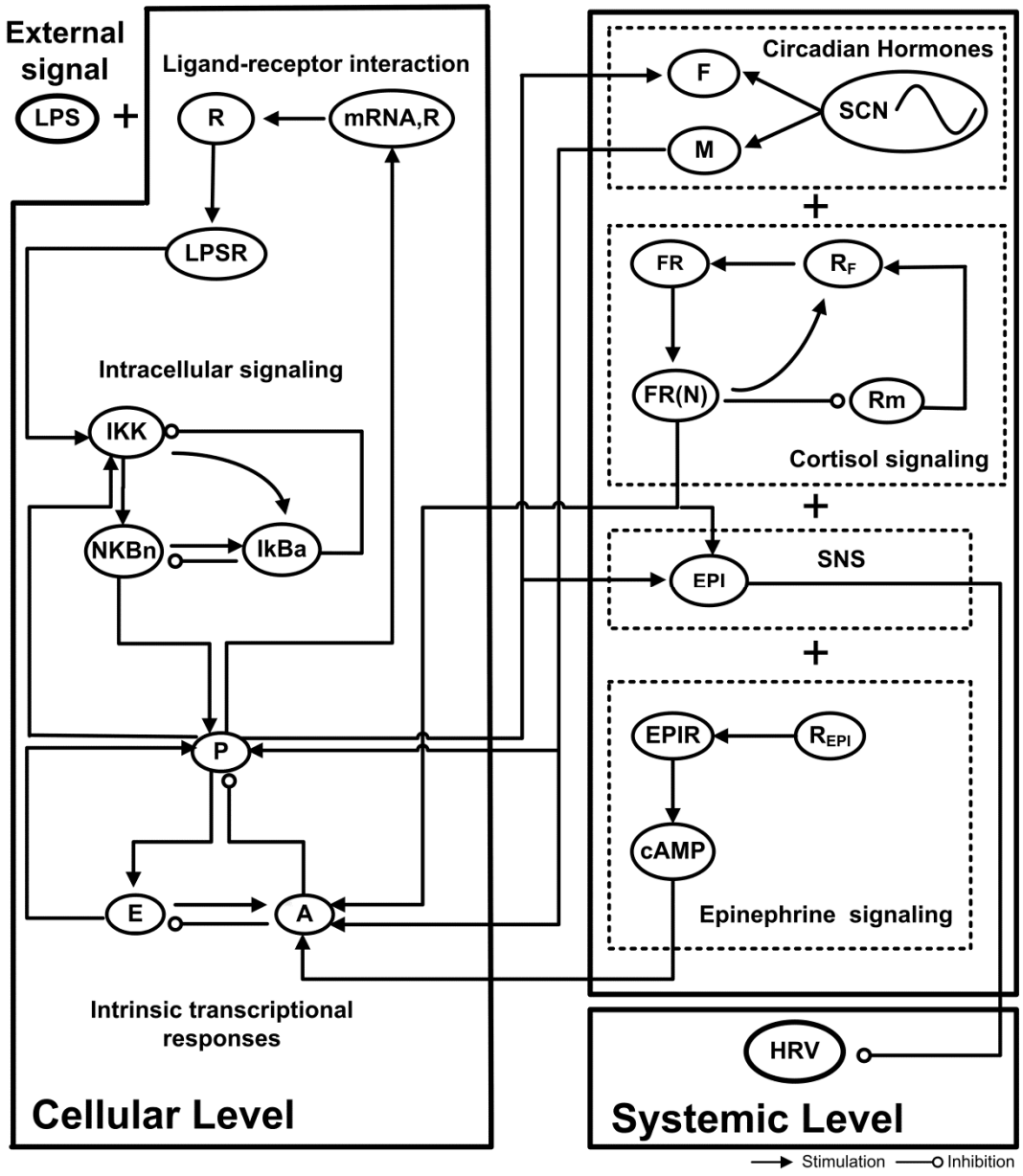

Figure 2.1: Network diagram of the components of the model.

The model is designed to reproduce experimental data from a variety of sources (Kronfol, Nair et al. 1997; Petrovsky and Harrison 1997; Petrovsky, McNair et al. 1998; Massin, Maeyns et al. 2000; Hermann, von Aulock et al. 2006; Grivas and Savvidou 2007), as shown in Figure 2.2. In this figure, a simulation is run with no inflammatory stimulus, giving the normal baseline condition for the model variables. While there is a link between cortisol and the anti-inflammatory response, variations seen in both the pro- and anti-inflammatory responses are primarily driven by melatonin levels. Cortisol is responsible for modulating the production of epinephrine, resulting in epinephrine levels peaking during the day slightly after cortisol does. Then, HRV is inhibited by epinephrine levels.

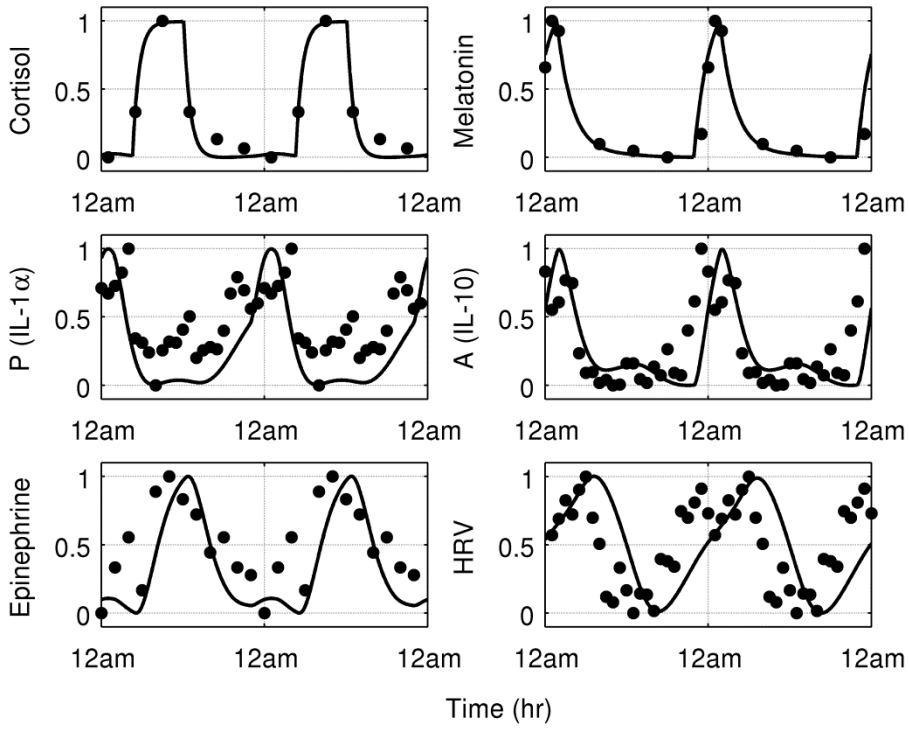

Figure 2.2: Simulation of the model when there is no inflammatory stimulus.

In addition to the simple "two rates" model (Eq. 2.1a) of cortisol used to generate Figure 2.2, a more complex model based on the Fourier series (Eq. 2.1b) was also tested

as shown in Figure 2.3. This model accounts for some of the small deviations from the simpler model, such as the small secondary peak after the circadian decrease in cortisol levels is already underway. This allows for a better fit for the epinephrine data, which shows that the epinephrine levels increase faster than they decline. However, it also leads to a worse fit for HRV. Overall, the predictions do not qualitatively improve when using the more complex model in Figure 2.3; thus, further results presented use the "two rates" model as in Figure 2.2.

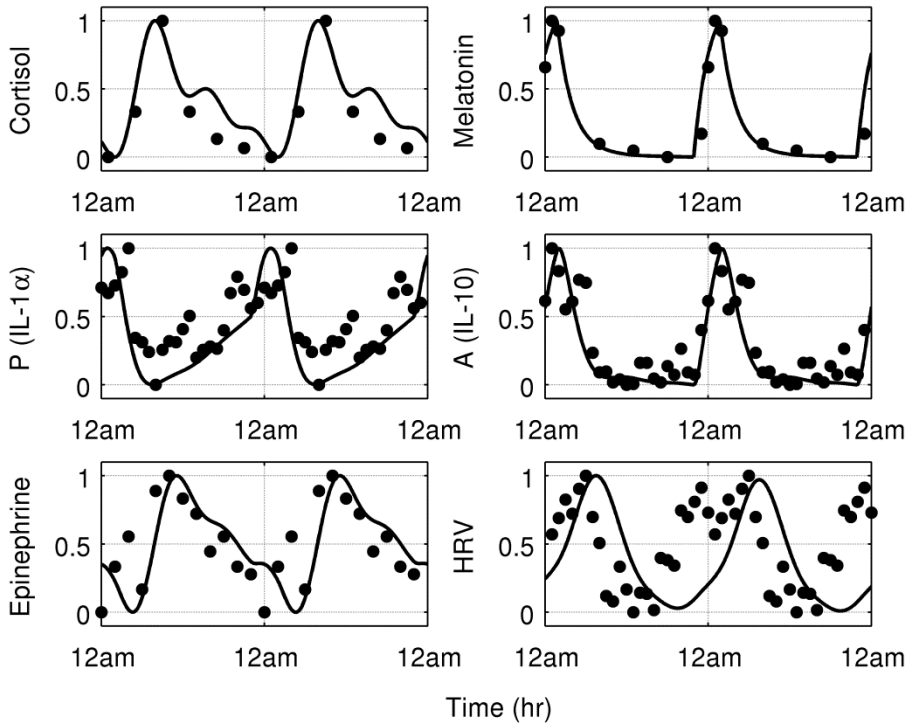

Figure 2.3: Simulation of the model, using an alternative equation for cortisol, when there is no inflammatory stimulus.

To determine the sensitivity of the system with respect to the parameters, sensitivity analysis is performed by calculating the sensitivity coefficient (Eq. 2.5) for each parameter. The simulations are run for the case when the inflammatory stimulus is LPS_0=1, which leads to a self-limited inflammatory response, and the response is tested

for dosing times at each of the 24 hours of the day. Figure 2.4 shows the results, with the large bars equal to the mean sensitivity coefficients and the small error bars equal to the standard deviation.

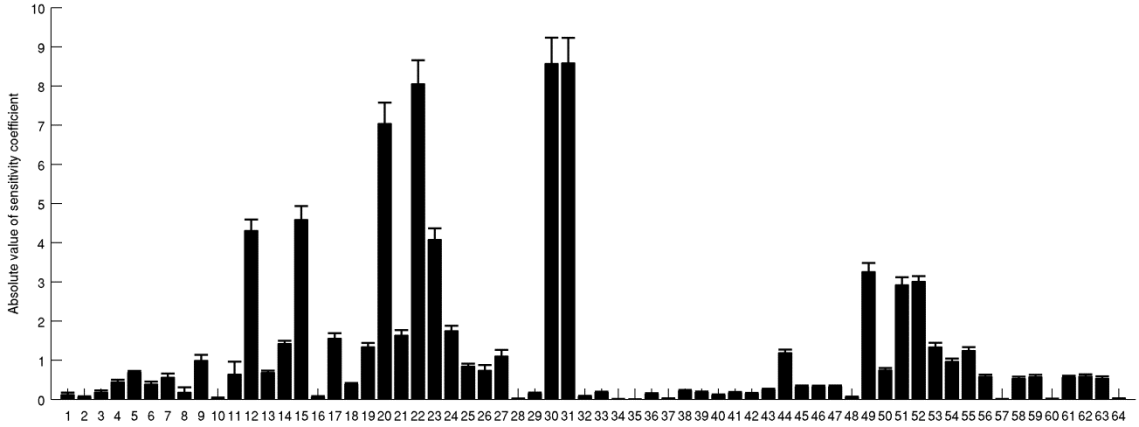

Figure 2.4: Sensitivity analysis on the model parameters. Sensitivity coefficients are calculated by using Eq. 2.5 with δp=0.01. Error bars represent the standard deviation of the sensitivity coefficients for stimuli given at different times during the day.

Figure 2.5 shows simulations of the application of an identical large inflammatory stimulus (LPS_0=10) at two different times. First, at 8am (dashed lines), cortisol levels are high while cytokine levels are low. Thus, the cytokines have less ability to initiate an inflammatory response, and they are countered by the anti-inflammatory influence of cortisol. When the inflammatory stimulus is given at 8am, it provokes an acute response that resolves normally; within several hours, all of the variables have returned to their baseline values. But at midnight (solid lines), cortisol levels are very low and cytokine levels are high; thus, in this scenario, the system is more susceptible to inflammation. This is illustrated by the unresolved inflammatory response that is provoked by the inflammatory stimulus. Interestingly, even in the unresolved inflammatory state, the circadian oscillations persist in cortisol, epinephrine, and the pro- and anti-inflammatory responses. These oscillations are in phase with the normal oscillations in Figure 2.2.

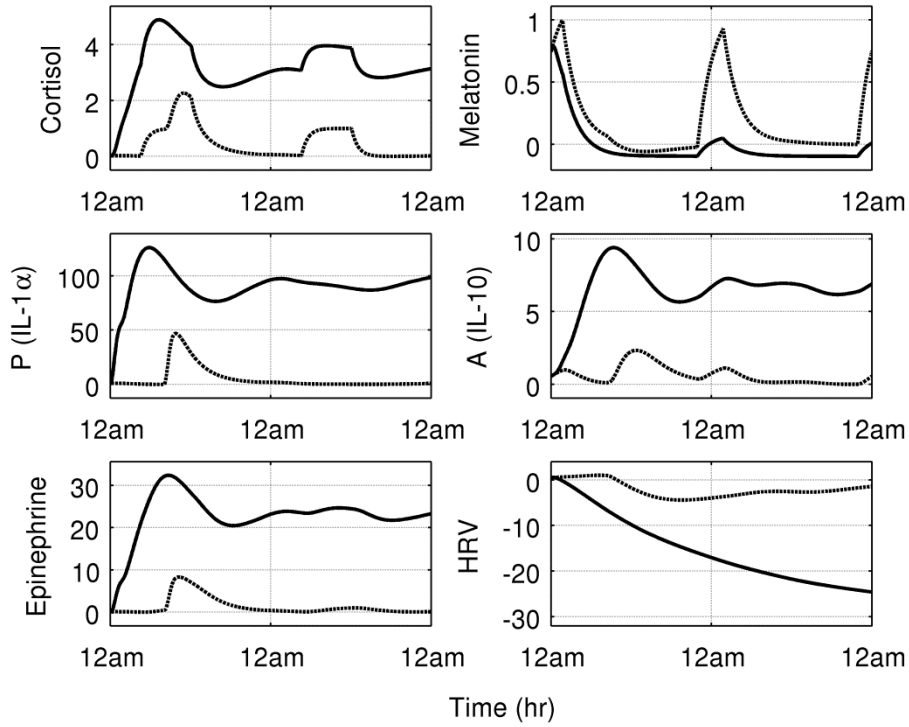

Figure 2.5: Simulation of the model for stimuli at two different times. An inflammatory stimulus is given at 8am (dashed lines) or 12am (solid lines). At 8am, the system is able to recover from the inflammatory stimulus, but at 12am, the same exact stimulus sends the system into an unresolved inflammatory state.

Melatonin levels also respond differently in the two cases in Figure 2.5. In the case when inflammation resolves (dashed lines), there is almost no change in melatonin relative to the normal conditions in Figure 2.2. This is because the transient peaks in P and A occur during the day when melatonin levels are already low, so the cytokines cannot further suppress melatonin production. But in the case when inflammation does not resolve (solid lines), melatonin levels remain suppressed. However, a transient inflammatory response can still lead to a decrease in melatonin production, as shown in Figure 2.6 when the inflammatory stimulus is given towards the beginning of the period when melatonin production is high.

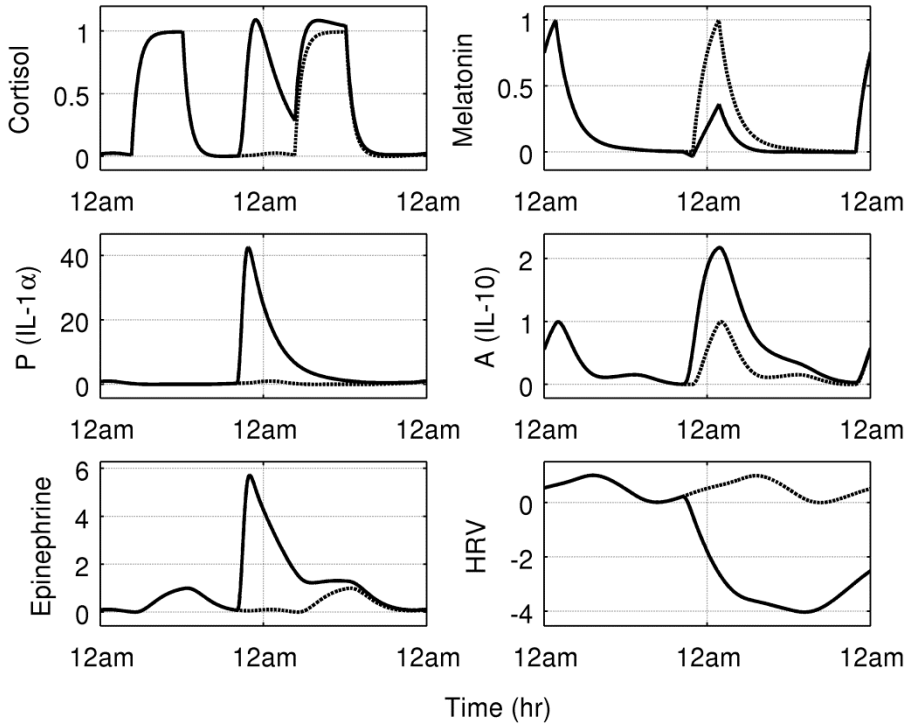

Figure 2.6: The inflammatory response can suppress melatonin levels. The solid lines show an inflammatory response (LPS_0=1) initiated at 8pm so that the inflammation is heightened when melatonin production is beginning to increase. The dashed lines show the baseline conditions (as in Figure 2.2) for comparison. Pro-inflammatory cytokines suppress the production of melatonin, leading to suppressed nocturnal melatonin levels. However, normal melatonin production returns the following night when the pro-inflammatory signal has resolved.

The temporal variation in the inflammatory response to LPS is illustrated in Figure 2.7. In this plot, the model is run as the time of the inflammatory stimulus (LPS_0=1) is varied. Then, the peak of the pro-inflammatory signal (P_{max}) is recorded as a representation of the overall strength of the inflammatory response. There is a significant circadian variation in this signal, which peaks at night and is low during the daytime.

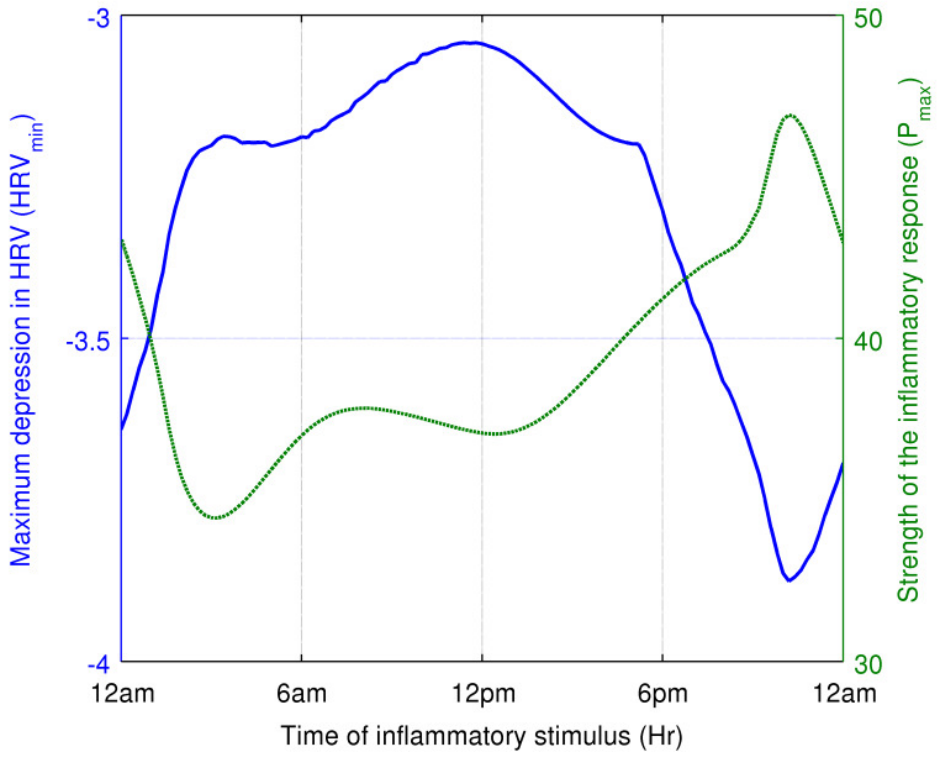

Figure 2.7: Circadian changes in the strength of the inflammatory response. The strength of the inflammatory response varies, as illustrated by monitoring either the maximal response of pro-inflammatory cytokines (P_{max}) or the maximum depression in HRV. Both of these variables have their maximum response in the night when normal levels of pro-inflammatory cytokines are elevated, and the minimum responses occur during the morning when cortisol levels are peaking.

2.4: Discussion

Circadian rhythms are of critical importance in inflammation because so many of the biological components that regulate the outcome of inflammation are themselves under circadian regulation. This work presents the first model that incorporates the effect of circadian variability on the inflammatory response. Proper treatment of inflammatory diseases requires an appreciation of circadian effects (Hrushesky and Wood 1997), so a quantitative understanding of circadian variations on inflammation is important in efforts

to translate computational systems biology approaches in inflammation to clinical relevance (Vodovotz, Csete et al. 2008; Foteinou, Calvano et al. 2009).

The sensitivity analysis shown in Figure 2.4 illustrates the relative influence of the values of all model parameters on the outcome of the model. The outcome is defined as the minimum value of *HRV* after an inflammatory stimulus because heart rate variability is known to have prognostic value in critically ill patients. Because the sensitivity is measured with respect to changes in *HRV*, it is not surprising that some of the most sensitive parameters are in the equations for *EPI* ($k_{in,EPI}$ (20), $k_{out,EPI}$ (22) and k^0_{REPI} (23)), which is closely linked to *HRV* in the model, and *HRV* itself ($k_{in,HRV}$ (30) and $k_{out,HRV}$ (31)). Parameters governing the behavior of both pro-inflammatory cytokines ($k_{in,P}$ (49), $k_{P,E}$ (51), and $k_{out,P}$ (52)) and anti-inflammatory cytokines ($k_{in,A}$ (12) and $k_{out,A}$ (15)) also have high sensitivities. Of the ten most sensitive parameters, eight represent the production and degradation terms for the four variables mentioned (*HRV*, *EPI*, *P*, and A). The other two are k^0_{REPI} (23), the production rate of epinephrine's receptor, and $k_{P,E}$ (51), which links cellular energetic activity to changes in the pro-inflammatory response. Functionally, many of the most sensitive parameters relate to the communication between the different modules of the system. The acute inflammatory response relies on this signaling to activate other components of the neuroimmune system and provoke a systemic response to inflammation, and this is reflected by high sensitivities in parameters governing cytokine and hormonal signals.

The new parameters added to the model to account for circadian rhythms, labeled 1-11 in Figure 2.4, have relatively low sensitivity coefficients compared to the most sensitive parameters from the original model that does not incorporate circadian effects,

indicating that the model retains its circadian response even when the new parameters are not precisely set. Yet although the sensitivities for the circadian parameters are less than the sensitivities of some of the other parameters mentioned earlier, this should not be taken to mean that the circadian components added to the model are unimportant in determining the outcome of the system. This is illustrated by the time-dependent responses found for identical inflammatory stimuli, as shown in Figure 2.5-2.7.

The persistent inflammatory state shown in Figure 2.5 (solid lines) is interesting because this type of persistent inflammation, either along with a persistent infection or after the pathogen is successfully cleared, has been observed clinically (Bone 1996; Alberti, Brun-Buisson et al. 2002). The suppression of the circadian release of melatonin, shown in the simulation in Figure 2.6, illustrates the ability of the model to capture critical aspects of the neuroimmune feedback on the production of circadian hormones. A similar diminished nocturnal melatonin release in response to inflammation has been observed experimentally (Fernandes, Cecon et al. 2006). Furthermore, the observed temporal dependence of the inflammatory response, as shown in Figure 2.5 and Figure 2.7, has important implications in translational medicine, where the goal is to translate current scientific discoveries into tools that can be applied to clinical problems. Specifically, modeling circadian variations in inflammation could lead to optimized clinical treatment times. Models could potentially be used to optimize the treatment of individual patients in an effort towards fulfilling the promise of personalized medicine. In inflammation, this is particularly important because it has been repeatedly observed that patients with sepsis have a significantly increased risk of mortality at night, but if they survive until the morning rise in cortisol levels is underway, they are likely to survive at

least until the next night (Hrushesky and Wood 1997). This qualitatively matches the results shown in Figure 2.7, where the potential for an inflammatory response is greatest at night and is significantly lower during the daytime; furthermore, P_{max} reaches its minimum early in the morning when the risk of death from sepsis is decreased. The observed differences in P_{max} mainly arise due to the variations in cortisol and in both pro- and anti-inflammatory cytokines. When cortisol levels are high, the system is protected from a heightened inflammatory response. But when cortisol levels are low, natural variations in cytokine levels result in periods of time when the system is primed for an inflammatory response.

One key aspect of the interplay between circadian rhythms and inflammation that is not adequately considered in this work is the feedback from inflammation to circadian rhythms. There is some evidence suggesting that immune mediators can directly influence the circadian clock by modulating the strength of expression of clock-related genes and by shifting the phase of circadian rhythms (Coogan and Wyse 2008). Melatonin has been implicated mediating these processes; additionally, inflammatory cytokines are known to influence the production of melatonin (Mundigler, Delle-Karth et al. 2002; Fernandes, Cecon et al. 2006), likely facilitating bidirectional information transfer between the neuroendocrine and immune systems.

The relationship between circadian rhythms and inflammation may be of particular importance in understanding the effects of chronic stress. In response to chronic stress from a variety of stimuli, such as depression (Yehuda, Teicher et al. 1996), obesity (Rosmond, Dallman et al. 1998), psychological stress (Polk, Cohen et al. 2005), and various types of cancer (Mormont and Levi 1997), circadian variations in plasma

cortisol concentration are diminished while overall cortisol levels remain high. The loss of the circadian nature of autonomic and neuroendocrine signaling in chronically stressed patients may be linked to a patient's overall potential to mount a healthy response to an inflammatory stressor (Lowry 2009). Furthermore, an extended period of stress hormone exposure results in diminished anti-inflammatory capacity as manifested by dynamic alterations in circulating levels of the anti-inflammatory cytokine IL-10, similar to subjects exposed only to LPS (van der Poll, Barber et al. 1996; van der Poll, Coyle et al. 1996). The clinical relevance of the circadian component of inflammation, particularly as it relates to chronic stress, is illustrated by the fact that diminished circadian variability in cortisol is associated with increased mortality in patients with breast cancer (Sephton, Sapolsky et al. 2000). The model presented here provides a solid foundation towards future work exploring the intricacies of these interactions.

Chapter 3: Transcriptional Implications of Ultradian Glucocorticoid Secretion, in Homeostasis and in the Acute Stress Response

3.1: Introduction

Glucocorticoid hormones, corticosterone in rats and cortisol in humans, are released from the adrenal cortex as a general response to stress. The secretion of glucocorticoids is regulated by the hypothalamic–pituitary–adrenal (HPA) axis: corticotrophin-releasing hormone (CRH) released from the hypothalamus stimulates adrenocorticotropic hormone (ACTH) secretion in the pituitary gland, which provokes the production of glucocorticoids by the adrenal gland. Glucocorticoids then complete feedback loops by inhibiting the release of both CRH and ACTH. Circadian rhythms in CRH, ultimately originating from exogenous cues of light and feeding (Reppert and Weaver 2002), drive circadian rhythms in plasma glucocorticoid levels. Feedback between glucocorticoids and ACTH production leads to ultradian (roughly hourly) rhythms in glucocorticoid release (Walker, Terry et al. 2010).

Experimentally, discrete ultradian bursts of glucocorticoid release can be determined, and the amplitude, timing, and regularity of these bursts can be assessed (Veldhuis, Iranmanesh et al. 1989; Veldhuis, Iranmanesh et al. 2001). These pulse properties can be differentially regulated in disease (Lightman and Conway-Campbell 2010), motivating interest in understanding the origins of HPA pulsatility, the relationship between pulsatility and stress responsiveness, the modulation of ultradian rhythms, and the mechanisms of downstream effects.

Several experiments have shown the importance of glucocorticoid pulsatility in regulating the transcription of glucocorticoid responsive genes (Lightman and Conway-Campbell 2010). Rapid binding and dissociation between glucocorticoid receptor (GR) and DNA (McNally, Muller et al. 2000) leads to gene pulsing in response to pulsatile glucocorticoid treatment (Stavreva, Wiench et al. 2009). Even in the absence of a difference in concentration between pulsatile and constant cortisol treatment, broad differential transcription persists (McMaster, Jangani et al. 2011). These experimental results are complimented by models of the HPA axis that have attempted to explore the origins of the pulsatile release of glucocorticoids (Brown, Meehan et al. 2001; Keenan, Licinio et al. 2001; Walker, Terry et al. 2010). From the perspective of pharmacology, pharmacokinetic and pharmacodynamic models of glucocorticoid action have been developed and applied towards quantitatively understanding the behavior of endogenous and exogenous glucocorticoids (Ramakrishnan, DuBois et al. 2002).

It has been hypothesized that pulsatile secretion of glucocorticoids is important in governing the behavior of the GR signaling pathway without desensitizing the system, thus maintaining the responsiveness of the HPA axis to acute stress without inappropriately elevating glucocorticoid responsive systems in homeostasis (Desvergne and Heligon 2009). It has been further hypothesized that, if the normal pattern of ultradian glucocorticoid rhythms is lost in stress (Lightman and Conway-Campbell 2010), then the new homeostatic equilibrium defined by altered pulsatility may exhibit dysregulation of glucocorticoid responsive genes, potentially leading to glucocorticoid resistance through constitutive exposure to glucocorticoids (Desvergne and Heligon 2009). Modeling the mechanisms that underlie both the loss of pulsatility and the

differences in downstream responses caused by altered glucocorticoid secretion patterns is important in understanding the physiological relevance of ultradian rhythms in both homeostatic and stressed conditions.

We previously presented the basic elements of a mathematical model combining the pulsatile release of glucocorticoids by the HPA axis (Walker, Terry et al. 2010) with the downstream pharmacodynamic effects of glucocorticoids on target genes (Yao, DuBois et al. 2006) in homeostasis (Scheff, Kosmides et al. in press) This integrated model now allows us to investigate the importance of pulsatility not only in homeostasis, but also with respect to perturbations in the form of altered parameter values and acute stressors. The downstream transcriptional effects of glucocorticoid pulsatility are reflected by the difference in transcript abundance of glucocorticoid responsive genes when exposed to a normal ultradian glucocorticoid rhythm and a constant level of glucocorticoids with the same area under the curve (AUC) as the ultradian pattern. HPA axis parameter perturbations, altering both the amplitude and frequency of glucocorticoid bursts, diminish the difference between constant and ultradian cases as the ultradian rhythms become flatter. Through these computational simulations, the mechanistic origins of glucocorticoid pulsatility and peripheral responses to pulsatility are explored within the framework of a mathematical model. This is of importance both in evaluating pathophysiological HPA axis behavior and in considering the clinical use of glucocorticoids, which are typically not given in an ultradian manner. Additionally, we study the concept of HPA axis pulsatility as it relates to the stress response by testing system responsiveness to acute CRH exposure as it relates to the phase and amplitude of ultradian rhythms. The observed positive relationship between ultradian amplitude and

peak responsiveness to stress provides computational evidence that the loss of homeostatic ultradian rhythms may have adverse effects on the response to stressors.

3.2: Methods

3.2.1: Linking Glucocorticoid Production and Pharmacodynamics

To study the impact of ultradian rhythms on downstream processes regulated by glucocorticoids, we need to account for both the rhythmic production of glucocorticoids by the HPA axis and the pharmacodynamic action of glucocorticoids in peripheral cells.

3.2.1.1: The HPA Axis and Glucocorticoid Secretion

Several prior models have been published in an attempt to investigate ultradian rhythms in HPA axis function, particularly with respect to the mechanistic origins of ultradian rhythms. These prior studies consider the origin of ultradian rhythms as due to either discrete bursting (Keenan, Licinio et al. 2001; Keenan and Veldhuis 2003) or an unstable fixed point driving oscillatory dynamics (Liu, Hu et al. 1999; Jelic, Cupic et al. 2005; Kyrylov, Severyanova et al. 2005; Savić and Jelić 2005; Bairagi, Chatterjee et al. 2008; Walker, Terry et al. 2010). The latter class of models rely on either unphysical parameter values or time delays to induce oscillations, as illustrated by Vinther et al. (Vinther, Andersen et al. 2010).

Still other models represent the HPA axis without rhythmicity. For instance, in (Gupta, Aslakson et al. 2007), a model of the HPA axis was developed linking the primary hormone determinants of glucocorticoid secretion: stress stimulates hypothalamic CRH, which stimulates pituitary ACTH, which stimulates adrenocortical glucocorticoids. Then, the HPA network is completed by accounting for negative feedback via glucocorticoids to both CRH and ACTH. In addition, the pituitary

concentration of GR is considered. GR, when activated by glucocorticoids, stimulates both the production of more GR and the inhibition of ACTH.

In (Walker, Terry et al. 2010), the model described above was modified to capture the pulsatile dynamics of glucocorticoid secretion. First, it is assumed that the dynamics of CRH are not critical in the origin of ultradian rhythms. Despite the fact that pulsatile release of CRH has been observed in rats and macaques (Ixart, Barbanel et al. 1991; Mershon, Sehlhorst et al. 1992), glucocorticoids are known to have a slow effect on CRH (Ma, Levy et al. 1997) and sheep whose hypothalamus and pituitary were surgically disconnected maintained pulsatile glucocorticoid release (Engler, Pham et al. 1989). Therefore, the model was simplified to consider CRH only as a constant parameter p_1, reducing the system to only three differential equations: pituitary ACTH (a, Eq. 3.1a); the availability of pituitary GR (r, Eq. 3.1b); and adrenal glucocorticoids (o, Eq. 3.1c). ACTH stimulates the production of glucocorticoids, and glucocorticoids (mediated by GR) inhibit the release of ACTH, forming a negative feedback loop. However, the mechanisms behind these hormone releases are not the same, which is important in the origin of pulsatility. ACTH is synthesized and stored in the pituitary gland, ready to be released rapidly when an appropriate signal is received. Glucocorticoids are synthesized by the adrenal cortex in response to ACTH signaling, which results in a time delay between ACTH release and glucocorticoid release. This time lag is incorporated into the equation representing the release of glucocorticoids from the adrenal gland, thus producing a delay differential equation (DDE) system, shown in Eq. 3.1. p_1 in Eq. 3.1a represents the effect of CRH on the system and τ in Eq. 3.1c is the time delay. Eq. 3.1d translates the dimensionless variable o into the concentration of glucocorticoids in the

plasma in nM, D_p, by scaling the oscillations by the normal homeostatic ultradian amplitude, represented by the parameter A. Parameter values are given in Table 3.1.

$$\frac{da}{dt} = \frac{p_1}{1 + p_2 \cdot r \cdot o} - p_3 \cdot a \tag{3.1a}$$

$$\frac{dr}{dt} = \frac{(o \cdot r)^2}{p_4 + (o \cdot r)^2} + p_5 - p_6 \cdot r \tag{3.1b}$$

$$\frac{do}{dt} = a(t - \tau) - o \tag{3.1c}$$

$$D_p = \frac{o - o_{min}}{o_{max} - o_{min}} \cdot A \tag{3.1d}$$

HPA axis model				Glucocorticoid pharmacodynamics model			
Param	**Value**	**Param**	**Value**	**Param**	**Value**	**Param**	**Value**
p_1	36 *	τ	0.25 *	α	0.0175 †	k_{prod} (hr^{-1})	1
p_2	15 *	A (nM)	650	B_{max} (fmol/mg)	44 †	k_{deg} (hr^{-1})	10
p_3	7.2 *	$p_{1,stress}$	200	K_d (nM)	5.13 †,‡	k_S (mg/fmol)	1
p_4	0.05 *	$t_{CRH,start}$ (hr)	47.5	τ_{DR} (hr)	1.13 †		
p_5	0.11 *	$t_{CRH,end}$ (hr)	47.6				
p_6	2.9 *						

Table 3.1: Model parameter values. * Taken from (Walker, Terry et al. 2010). † Taken from (Yao, DuBois et al. 2006). ‡ Taken from (Wolff, Baxter et al. 1978).

As in (Walker, Terry et al. 2010), the time delay is set to 15 minutes. Although this time delay is larger than experimentally measured delays (Papaikonomou 1977), this may be due in part to the deterministic simulations performed here, as noise in the system facilitates noise-induced oscillations at lower time delay values (Walker, Terry et al. 2010).

3.2.1.2: Glucocorticoid Pharmacodynamics

The model represented by Eq. 3.1 culminates in the release of glucocorticoids by the adrenal cortex into systemic circulation. To assess the downstream effects of glucocorticoids, the concentration of glucocorticoids in circulation must be related to the transcriptional regulatory activity of GR. To do this, the model of glucocorticoid release

from the HPA axis in Eq. 3.1 is combined with the glucocorticoid pharmacodynamic model (Yao, DuBois et al. 2006) shown in Eq. 3.2.

Glucocorticoids are neutral, lipophilic hormones, so they freely diffuse across cell membranes to the cytoplasm, where they interact with GR. At rest, GR are sequestered in the cytoplasm where they are bound to or chaperoned by various heat shock proteins (HSP). Upon binding between glucocorticoids and GR, HSP are released. Then, the activated GR-glucocorticoid complex translocates into the nucleus and binds to glucocorticoid responsive elements (GRE) on DNA as a dimer, promoting the transcription of many genes, including inflammatory genes. These steps are summarized in Eq. 3.2: movement of glucocorticoids across the cell membrane is assumed to be linear (2a); binding between glucocorticoids and GR to form the activated complex DR , based on B_{max}, the concentration of cytosolic GR, and K_d, the dissociation constnant (2b); translocation of the complex to the nucleus where DR_1 represents the nuclear regulation and τ_{DR} is the mean transit time (2c); and transcriptional regulation of a prototypical glucocorticoid responsive gene, denoted *mRNA* (2d). Table 3.1 lists the parameter values used in Eq. 3.2.

$$D_c = \alpha \cdot D_p \tag{3.2a}$$

$$DR = \frac{B_{\max} D_c}{K_d + D_c} \tag{3.2b}$$

$$\frac{dDR_1}{dt} = \frac{1}{\tau_{DR}}\left(DR - DR_1\right) \tag{3.2c}$$

$$\frac{dmRNA}{dt} = k_{prod}\left(1 + k_S \cdot DR_1\right) - k_{deg} mRNA \tag{3.2d}$$

In all cases, DDE system was solved by using the `dde23` function in MATLAB (Shampine and Thompson 2001) and setting the assumed history of a prior to the initial time point to be a constant equal to the initial condition.

3.2.2: Modulated Glucocorticoid Patterns

The model described in Eq. 3.1-3.2 spans both the production of glucocorticoids and the pharmacodynamic effects of glucocorticoids. This quantitative, mathematical system facilitates the study of how modulations in HPA axis function are propagated through to peripheral transcriptional regulation. The nondimensionalized HPA axis model in Eq. 3.1 contains seven parameters (p_1 through p_6 and the time delay τ) which, when perturbed, alter the output of the adrenal cortex. In the context of our model, altering any of p_1 through p_6 changes the amplitude of ultradian rhythms, while altering τ changes the frequency of ultradian rhythms. Therefore, in this chapter, two HPA axis modulations are explored: (1) altered ultradian magnitude by perturbing the feedback from adrenal glucocorticoid secretion to pituitary ACTH secretion, p_2; and (2) altered ultradian frequency by perturbing the time delay from pituitary ACTH secretion to adrenal glucocorticoid secretion, τ. These two modulations are assumed to be representative of perturbations to HPA axis feedback loops in general, which have been explored experimentally with respect to altered ultradian behavior (Veldhuis, Iranmanesh et al. 2001).

3.2.3: Acute Stress Response

The parameter p_1 in Eq. 3.1a represents CRH's influence on the pituitary gland. To mimic the acute stress response, this parameter is acutely elevated as in Eq. 3.3, provoking transient responses in the other model variables which resolve within 5 hours.

$$p_1' = \begin{cases} p_1, & t < t_{CRH,start}, t > t_{CRH,end} \\ p_{1,stress}, & t_{CRH,start} < t < t_{CRH,end} \end{cases} \quad (3.3)$$

It has been shown experimentally that responsiveness to noise stress varies as a function of ultradian phase (Windle, Wood et al. 1998; Windle, Wood et al. 1998). In an attempt to model this phenomenon, Eq. 3.3 was applied for different time cutoffs, spanning the entire ultradian cycle (1 hour, sampled every 6 minutes).

In the previous section, individual parameters were perturbed to modulate the amplitude and frequency of ultradian rhythms. An advantage of a computational modeling approach is that large scale surveys of the parameter space can be performed to more generally assess the performance of the system under what could be considered genetic or environmental perturbations. Based on this concept, 100,000 random sets of parameters p_2 through p_6 were generated based on Eq. 3.4, where *N(1,1)* is a random number sampled from a normal distribution with mean 1 and standard deviation 1, with the goal of studying the relationship between pulsatility and stress responsiveness.

$$p_i' = p_i \cdot \mathcal{N}(1,1) \quad (3.4)$$

This produced model parameterizations with a wide range of behaviors, including ultradian rhythms at a variety of amplitudes. To assess the general relationship between pulsatility and the stress response, these systems with random parameters were tested by applying an acute stressor as defined in Eq. 3.3. Then, the peak values of the responses were measured with respect to ultradian rhythmicity.

3.2.4: Circadian Rhythms

Circadian rhythms in glucocorticoid concentration have been observed experimentally. In contrast to ultradian rhythms, which are largely assumed to arise due

to dynamics internal to the HPA axis, circadian rhythms are typically viewed as a centrally mediated external signal which drives 24 hour variability in glucocorticoid secretion (Reppert and Weaver 2002). For this reason, prior models that have considered this issue typically drive a model parameter by an imposed sinusoid with a 24 hour period (Jelic, Cupic et al. 2005; Kyrylov, Severyanova et al. 2005; Bairagi, Chatterjee et al. 2008; Vinther, Andersen et al. 2010; Walker, Terry et al. 2010). This has previously been applied to the HPA axis model in Eq. 3.1 (Walker, Terry et al. 2010) by setting the parameter p_1, representing CRH drive, to a sinusoid, as in Eq. 3.5.

$$p_1 = 26 + 10\sin(2\pi t / 24) \tag{3.5}$$

This results in the ultradian rhythms in HPA hormones having circadian amplitudes.

3.3: Results

The integrated DDE system given in Eq. 3.1-3.2 comprises the production of glucocorticoids by the HPA axis and glucocorticoid pharmacodynamics culminating in the transcription of glucocorticoid responsive genes; the components and interactions involved in this system are shown in a network diagram in Figure 3.1.

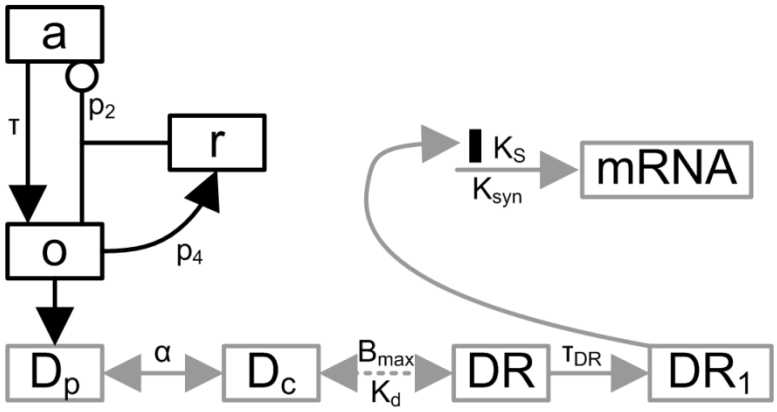

Figure 3.1: Network diagram of pituitary-adrenal interactions (Eq. 3.1, black lines) and glucocorticoid pharmacodynamics (Eq. 3.2, gray lines). Lines ending in arrows represent stimulation, and lines ending in open circles represent inhibition. The black box in front of *mRNA* represents the stimulus in the first term of Eq. 3.2d. The dashed line represents the nonlinear dose-response relation in Eq. 3.2b. Production and degradation rates are not shown for clarity. ACTH (*a*), released by the anterior pituitary, stimulates the release of glucocorticoids (*o*) from the adrenal cortex. Glucocorticoids have two effects in the model: (1) negative feedback onto ACTH production in the anterior pituitary via pituitary GR (*r*); and (2) transcriptional regulation of glucocorticoid responsive genes in peripheral tissues. In a peripheral cell, GC diffuses into the plasma (D_p), binds to its receptor forming the drug-receptor complex (*DR*), translocates into the nucleus (DR_1), and regulates the transcription of glucocorticoid responsive genes (*mRNA*).

To evaluate the difference in transcriptional responses to constant or pulsatile glucocorticoid exposure, two cases are shown in Figure 3.2. First, the model is evaluated, as described in Eq. 3.1-3.2 and Table 3.1, producing a pulsatile pattern in the components of the glucocorticoid pharmacodynamic model, culminating in gene pulsing observed in the mRNA variable. This pulsatile scenario is compared to a simulation in which a constant amount of glucocorticoids is imposed, equal in total to the amount of glucocorticoids secreted in the pulsatile case described above. In this constant case, the mRNA production stimulated by the glucocorticoid pharmacodynamic model is greater than the mRNA in the rhythmic case.

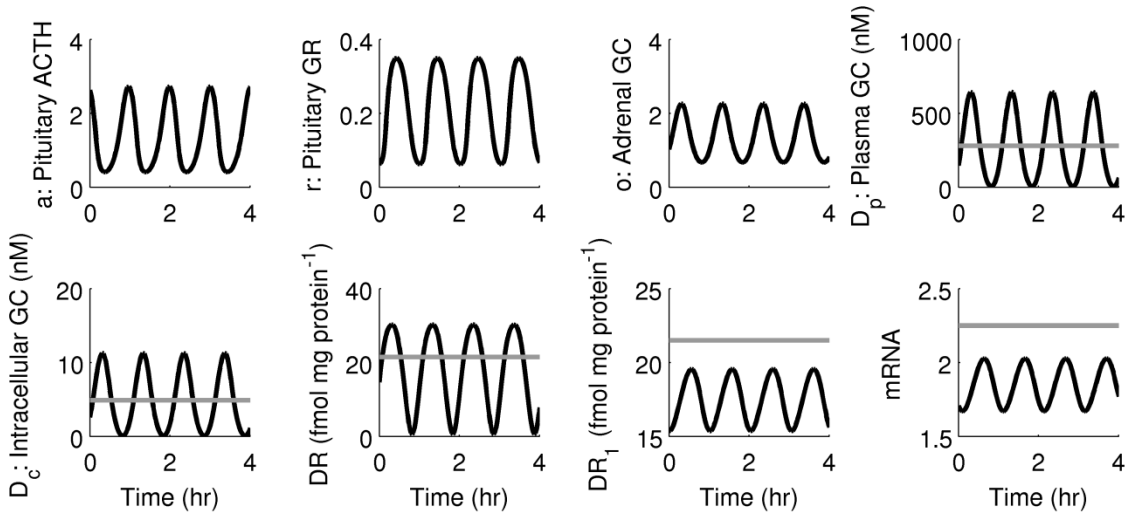

Figure 3.2: Two simulations are shown, representing the ultradian model propagation through the glucocorticoid pharmacodynamic model (black lines) and a constant level of glucocorticoids with the same AUC imposed on the plasma GC variable (gray lines). Despite the fact that the same total amount of glucocorticoids is equal in both cases, there is a significant difference in the mean levels of glucocorticoid responsive mRNA.

The integrated model developed here allows for the assessment of HPA axis dysfunction on homeostatic gene regulation. As the feedback from adrenal glucocorticoids to pituitary ACTH release (p_2) is decreased, the amplitude of oscillations in HPA axis variables, and thus in glucocorticoid responsive mRNA, are progressively diminished, as shown in Figure 3.3. A similar response is observed in Figure 3.4 as the time delay for the effect of ACTH on glucocorticoid secretion (τ) is decreased. Decreasing the time delay provokes increased oscillatory frequency along with a lower amplitude.

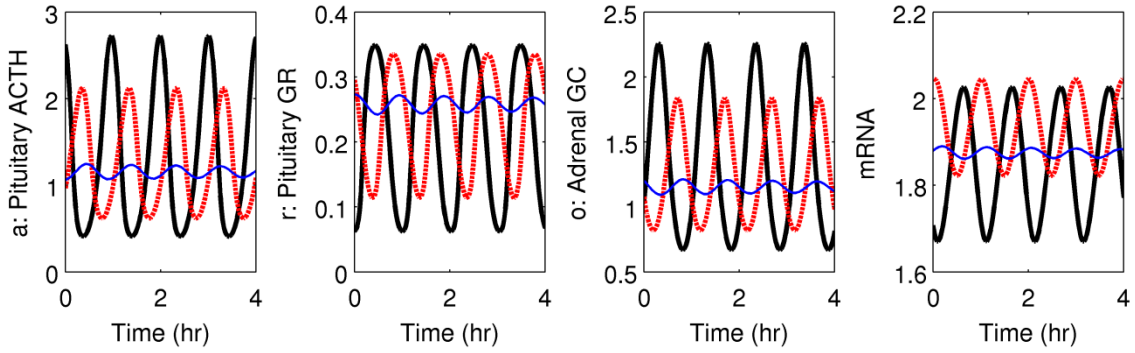

Figure 3.3: Ultradian oscillations in ACTH, GR, and GC as the feedback between GC and ACTH is decreased. Thick solid lines: normal feedback (default parameter value, Table 3.1), highest pulsatility; dashed lines: 20% decreased feedback, intermediate pulsatility; thin lines: 25% decreased feedback, lowest pulsatility. As the feedback is further decreased, the system eventually produces a flat output.

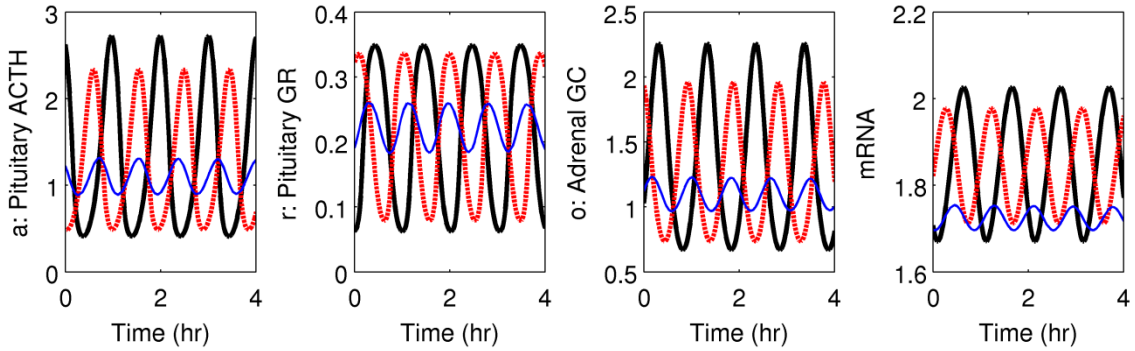

Figure 3.4: Ultradian oscillations in ACTH, GR, and GC as the frequency is altered by decreasing the time delay for feedback from GC to ACTH relative to the default value in Table 3.1. Thick solid lines: normal time delay (default parameter value), highest pulsatility and lowest frequency; dashed lines: 12% decreased time delay, intermediate pulsatility and frequency; thin lines: 28% decreased time delay, lowest pulsatility and highest frequency. As the time delay is further decreased, the system eventually produces a flat output.

Quantifying the effect of pulsatility on downstream responses within the context of HPA axis modulation is complicated by the shifting mean value of glucocorticoid levels shown in both Figure 3.3 and Figure 3.4 as the ultradian amplitude decreases. One approach to separate the effects of pulsatility and the changing mean is shown in Figure 3.5. Comparing a particular pulsatile output of the HPA axis and a constant

glucocorticoid level with the same AUC, the distance between the mean glucocorticoid responsive mRNA in those two cases represents the effect that the pulsatile secretion pattern is exerting. As pulsatility is lost, this difference (D in Figure 3.5) in means decreases until it is exactly zero when ultradian rhythms disappear.

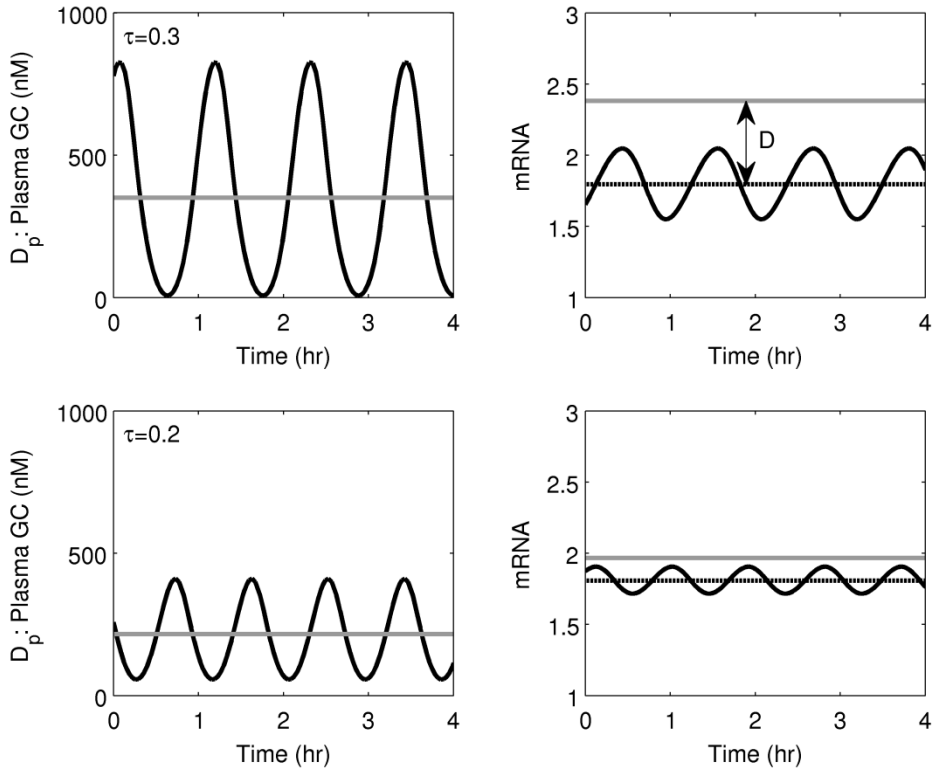

Figure 3.5: As the time delay from ACTH secretion to GC release (τ) is decreased, the frequency of ultradian rhythms increases and the amplitude decreases. Decreased ultradian amplitude corresponds with a smaller difference (D) between glucocorticoid responsive mRNA when comparing pulsatile (black lines) and constant (gray lines) glucocorticoid levels with the same AUC.

Although the results presented above concern, for simplicity, the case where no circadian rhythms are present in the model, Figure 3.6 shows that the significant transcriptional difference between constant and pulsatile cases persists even in the presence of both ultradian and circadian rhythms. The presence of pulsatility still leads to

the suppression of glucocorticoid-responsive mRNA, only now with a circadian dependence on the magnitude of suppression.

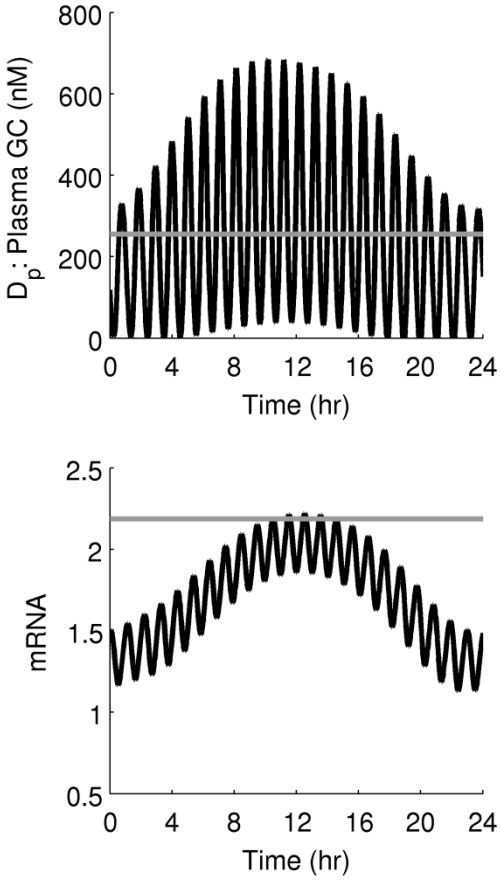

Figure 3.6: Top: Circadian (black) and constant (gray) plasma glucocorticoid levels, at the same AUC. The circadian rhythms are defined by imposing circadian variability in the parameter p_1 via Eq. 3.5. Bottom: mRNA output from the pharmacodynamic model (Eq. 3.2). As in Figure 3.2, there is a significant transcriptional difference in model output depending on the presence or absence of ultradian rhythms.

Applying an acute stimulus at different time points relative to the ultradian phase revealed a significant ultradian dependence in the acute stress response, shown in Figure 3.7. When the stimulus was given during the rising phase of the ultradian rhythm, a robust response was generated. However, during the falling phase, the response was severely blunted.

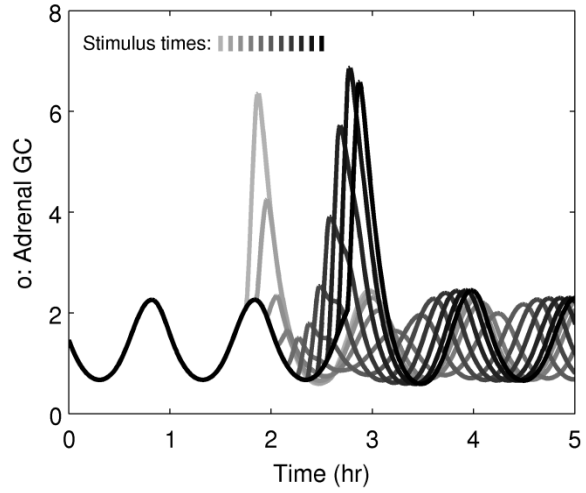

Figure 3.7: HPA axis responses, quantified by GC values, to stimuli at various time points relative to the ultradian phase. These time points range from 1.5hr (lightest gray color) to 2.5hr (darkest black color), incrementing by 0.1hr (6 minutes), as indicated by the vertical bars at the top of the figure. As has been seen experimentally (Windle, Wood et al. 1998; Windle, Wood et al. 1998), there is a strong dependence on the response to a stressor depending on whether the stressor occurs in the rising of falling GC phase.

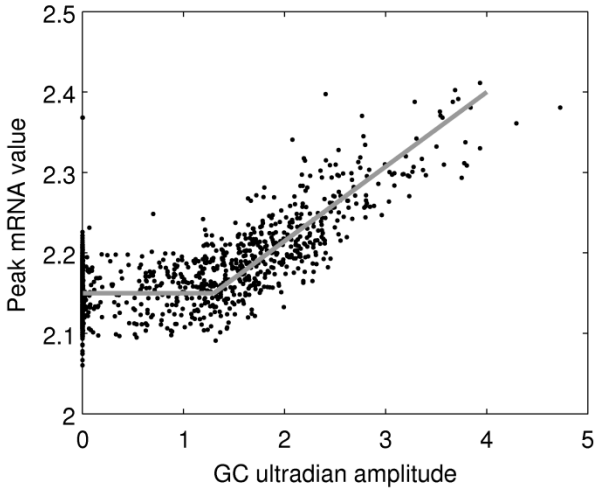

Figure 3.8: Scatter plot of peak mRNA values versus homeostatic GC (*o*) amplitude for 2,092 of 100,000 parameter sets which have homeostatic mean mRNA values close to those produced by the default parameters in Table 3.1.

The application of an acute stressor to the HPA axis model with random parameters produced a wide range of responses. To narrow down these 100,000 different

responses, parameter sets were selected if the mean homeostatic level of *mRNA* was near (difference of less than 0.05) the value obtained from the default parameters (Table 3.1). This filtering produced 2,092 parameter sets. Then, for these 2,092 parameter sets, multiple simulations were performed at different time points, as in Figure 3.7, due to the fact that random parameter values produce random phases. The peak values in the *mRNA* responses for each parameter set were averaged together and plotted against the amplitude of ultradian rhythms in homeostasis, shown in Figure 3.8. There is a positive correlation between ultradian amplitude and peak stress responsiveness at amplitude values greater than 1.5. High levels of responsiveness, such as that of the default model parameters in Table 3.1, are attainable almost exclusively through parameter values which lead to ultradian rhythms in homeostasis. These same general relationship between ultradian amplitude and responsiveness to acute stimuli was also observed when similar simulations were performed in a similar HPA axis model (Jelic, Cupic et al. 2005).

3.4: Discussion

The pulsatile dynamics of glucocorticoid secretion from the HPA axis are important in governing downstream responses. As summarized in Figure 3.2, even for the same total amount of glucocorticoid exposure, the presence of pulsatility exerts a suppressive effect on glucocorticoid responsive genes. The existence of such a difference in responses in this model is due to nonlinearities in glucocorticoid signal transduction, otherwise the aggregate output would not depend on the input pattern. This is evident in Figure 3.2, where *DR* is activated at a higher mean level in the constant glucocorticoid case, and the ultradian peaks in DR_1 do not even reach the level of its constitutive activation in the constant case. This behavior is driven by two properties of the system.

First, the nuclear GR complex concentration responds quickly to the level of systemic glucocorticoids (Stavreva, Wiench et al. 2009) and GR quickly associates and dissociates from its DNA targets (McNally, Muller et al. 2000). This is reflected in Figure 3.2 where ultradian oscillations propagate from their origin in the HPA axis through to the nuclear concentration of activated GR (DR_1). In the ultradian nadirs, the value of DR_1 rapidly declines. In the constant scenario, there is no such period of clearance, so the nuclear levels of activated GR remain constitutively elevated. This is similar to recent experimental results showing that the synthetic glucocorticoid dexamethasone does not to dissociate from the receptor on the timescale of physiological ultradian glucocorticoid rhythms, resulting in a flat level of nuclear GR in response to cyclic dexamethasone treatment (Stavreva, Wiench et al. 2009). The second property leading to a difference between ultradian and constant cases is the nonlinear binding relationship between glucocorticoids and GR. Eq. 3.2b represents a generic sigmoidal binding relationship between ligand (glucocorticoids) and receptor (glucocorticoid receptor), where the ligand rapidly binds to its receptor as a function of ligand concentration, until the concentration grows so high that the receptor is saturated. The nonlinear activation of DR depends on the level of glucocorticoids relative to the dissociation constant K_d. As the mean level of plasma glucocorticoids is higher than K_d, the high levels of glucocorticoids in ultradian bursts approach the saturation limit. Therefore, the very high peak levels of glucocorticoids reached during secretory bursts cannot drive proportionally large increases in DR. Thus, the specific properties of endogenous glucocorticoids, as represented in the pharmacodynamic model in Eq. 3.2, are critical in generating the differential response to glucocorticoid ultradian rhythms.

In recent years, systems biology has become sufficiently sophisticated that researchers often move beyond simply asking how a system functions to asking why it functions in a certain manner (Lander 2004). Along these lines, the association between ultradian rhythmicity and stress responsiveness shown in Figure 3.8 suggests that the presence of pulsatility in homeostatic HPA function confers the potential for increased acute stress responsiveness. This relationship between pulsatility and responsiveness has been previously hypothesized to exist based on studies showing rapid transcriptional responses to bursts of glucocorticoids (Desvergne and Heligon 2009; Lightman and Conway-Campbell 2010), and the modeling work here suggests that the magnitude of the response as well as the timing (Figure 3.7) may be of importance with respect to pulsatility. This is particularly interesting given that disruptions in HPA axis responsiveness have been implicated in a variety of diseases including rheumatoid arthritis, asthma, and chronic fatigue syndrome (Webster, Tonelli et al. 2002). The results presented here provide computational evidence that the loss of ultradian rhythms in homeostasis may reflect underlying HPA axis dysfunction (such as shown in Figure 3.3 and Figure 3.4) that is manifested in diminished stress responsiveness.

When the CRH stimulus was given in the rising phase, significantly larger responses were observed than in the falling phase, as shown in Figure 3.7. This is in agreement with experiments in rats showing that the response to noise stress is enhanced in the rising or interpulse corticosterone phase and diminished in the falling corticosterone phase (Windle, Wood et al. 1998; Windle, Wood et al. 2001). Therefore, based on this relationship between pulse phase and the magnitude of an acute stress response, altered pulsatile patterns should be expected to lead to altered stress responses.

The results in Figure 3.8 go further than just looking at rising and falling responses in one model. Based on the large number of random parameter sets tested, which lead to a wide range of ultradian amplitudes, Figure 3.8 shows that the peak responsiveness of the system generally increases with the amplitude of ultradian rhythms.

The relationship between peak responsiveness and amplitude in Figure 3.8 makes sense in light of the relationship between pulsatility and downstream transcriptional effects (*mRNA*) in Figure 3.2. The presence of oscillations, assuming a constant total amount of glucocorticoids, effectively suppresses homeostatic responses to glucocorticoids. Then, in a stress response where the system is responding to the magnitude rather than the homeostatic oscillations of glucocorticoids, *mRNA* has further to increase relative to its mean value in the oscillatory case.

In addition to the mechanisms for downstream ultradian regulation present in this model, other mechanisms to explain nonlinearities in glucocorticoid signal transduction have been proposed. However, the inclusion of further nonlinearities into the model would only serve to heighten the differences between pulsatile and constant glucocorticoid exposure. For instance, our model does not consider the behavior of corticosteroid-binding globulin (CBG), a plasma protein that binds to cortisol. At 400-500 nM of cortisol, plasma CBG is saturated (Ballard 1979), so increases in cortisol beyond this level are free to move into cells. As ultradian rhythms in cortisol move above and below this saturation threshold, one would expect this nonlinearity to have a significant effect on the behavior of glucocorticoid responsive genes (Lightman and Conway-Campbell 2010). However, it is known that the synthetic glucocorticoid dexamethasone has no affinity to CBG, and in a study on the pharmacodynamics of both

dexamethasone and corticosterone, it was found that a simple linear term relating plasma glucocorticoid concentration and cytoplasmic glucocorticoid concentration can sufficiently model the action of both glucocorticoids (Yao, DuBois et al. 2006). Therefore, we have not included CBG binding and saturation in our model and instead used the linear relationship in Eq. 3.2a. Similar linear approximations for the effect of cortisol at normal concentrations have been widely used in HPA axis models and glucocorticoid pharmacodynamic models (Mager, Pyszczynski et al. 2003; Jelic, Cupic et al. 2005; Savić and Jelić 2005; Yao, DuBois et al. 2006; Bairagi, Chatterjee et al. 2008; Vinther, Andersen et al. 2010; Walker, Terry et al. 2010), which allows for simpler models which do not explicitly account for cortisol binding proteins.

It has also been observed experimentally that different genes respond to differently to glucocorticoids. Dexamethasone activates glucocorticoid responsive genes in a concentration dependent manner, although the mechanism of activation of specific genes at lower doses than others is not yet understood (Reddy, Pauli et al. 2009). Rate-sensitive responses to glucocorticoids have also been observed on a nongenomic timescale (Dallman and Yates 1969; Atkinson, Wood et al. 2008; Russell, Henley et al. 2010), although this fast feedback mechanism has mainly been studied within the HPA axis and not in peripheral glucocorticoid regulated systems. Due to the importance of glucocorticoid signaling in a wide range of critical biological processes, it is plausible that multiple complimentary mechanisms govern downstream responses to ultradian rhythms.

The decrease in time delay shown in Figure 3.4 produces a similar loss of ultradian amplitude as the decrease in feedback strength shown in Figure 3.3. It is not

surprising that decreasing the time delay results in diminished oscillations, as the time delay was introduced specifically so that this model could account for ultradian rhythmicity (Walker, Terry et al. 2010). Intuitively, this result may be explained by thinking about the size of the time windows in which plasma glucocorticoid concentration is increasing and decreasing. As the frequency increases, both of these windows shrink: there is less time to reach a very high ultradian peak, and there is less time to clear to a very low ultradian nadir. This predicted relationship between the frequency and amplitude of ultradian rhythms is supported by *in vivo* human experimental evidence correlating the sizes of cortisol secretory bursts with the durations of postsecretory pauses (Veldhuis, Iranmanesh et al. 1989). Pathophysiological conditions involving chronic stress have also been linked to increases in glucocorticoid pulse frequency. In rats with adjuvant-induced arthritis, the frequency of corticosterone pulses is significantly increased, producing elevated resting hormone levels and more continuous GR activation, qualitatively matching to the results in Figure 3.4 (Harbuz, Windle et al. 1999; Windle, Wood et al. 2001). In severely depressed patients, HPA axis dysfunctions result in a similar increase in cortisol pulse frequency (Deuschle, Schweiger et al. 1997).

Approximately 30% of patients with major depression exhibit hypercortisolemia (Young, Carlson et al. 2001), and an elevated baseline level of plasma cortisol would diminish the suppressive effects of pulsatility and possibly lead to glucocorticoid resistance due to constitutive exposure to glucocorticoids (Desvergne and Heligon 2009). Glucocorticoid resistance has been hypothesized to arise due to several different mechanisms in the presence of chronic glucocorticoid exposure (Schaaf and Cidlowski

2002; Ito, Chung et al. 2006). The effect of high glucocorticoid levels is also important from a clinical perspective as glucocorticoid drugs are typically given without regard for pulsatility. Treatment of inflammatory diseases with high doses of glucocorticoids often results in deleterious side effects and no current glucocorticoid therapy attempts to mimic physiological pulsatility (Lightman, Wiles et al. 2008). The computational results presented here support the idea that pulsatility itself regulates the downstream effects of glucocorticoids and should be considered in the therapeutic delivery of glucocorticoids, rather than seeking more potent drugs which minimize the frequency of treatment (Lightman and Conway-Campbell 2010).

Although changes in pulsatility have been observed in chronically stressed rats (Windle, Wood et al. 2001), it is difficult to draw specific conclusions about the importance of pulsatility in chronic stress, particularly as different forms of chronic stress produce very different pathophysiological changes. For instance, it has been observed that chronic stress can facilitate increased HPA axis responsiveness through interactions between elevated glucocorticoid levels and insulin secretion (Dallman, Akana et al. 2004), yet decreased HPA axis responsiveness has also been observed in chronic stress (Raison and Miller 2003). As our model does not explicitly account for these and other interacting systems, as well as glucocorticoid tolerance, it is difficult to derive specific conclusions about the importance of glucocorticoid pulsatility in the context of chronically stress without a more refined and model of the specific pathophysiology.

In any model of a biological system, determining appropriate parameter values is a challenge. As much as possible, we used parameter values from the literature that were previously set in the original development of the HPA axis model (Walker, Terry et al.

2010) and the glucocorticoid pharmacodynamic model (Yao, DuBois et al. 2006). However, the experiments performed using large numbers of random parameter sets shows that the model's general function is not dependent on specific parameter values. The HPA axis model was originall developed to study pulsatile secretion of glucocorticoids, but not their downstream effects. The glucocorticoid pharmacodynamic model was developed in the context of understanding how endogenous circadian rhythms regulate glucocorticoid action. The fact that we used models and parameters designed without the applications in this chapter in mind supports the generality of our conclusions and helps overcome issues of overfitting that are common in systems biology (Gutenkunst, Waterfall et al. 2007). An issue with this approach of combining models from the literature is that the models may not have been designed to study the exact system at hand. For instance, in (Yao, DuBois et al. 2006), the glucocorticoid pharmacodynamic model is developed for rat skeletal muscle. Although the GR signaling pathway is conserved across tissues, the relation between plasma and intracellular steroid concentrations (α in Eq. 3.2a) is unlikely to be constant in different tissues. Tissues with high capillary permeability, such as the liver, have been shown to respond to total glucocorticoid concentration (free and bound) while tissues with less capillary permeability, such as the pancreas, respond only to free glucocorticoids (Keller, Richardson et al. 1969). A slightly higher value of α was estimated for the liver (Mager, Pyszczynski et al. 2003), and one would expect a significantly higher value for cells that are more directly exposed to plasma glucocorticoids, such as peripheral blood leukocytes. However, increasing the value of α in the simulations performed here does not alter any of the conclusions about the effects of glucocorticoid pulsatility. As increasing α is

effectively the same as exposing the system to a higher amplitude glucocorticoid ultradian rhythm, GR would be even more saturated at an equivalent constant dose, resulting in an even larger difference between pulsatile and constant glucocorticoid exposure. This implies that, even if the pharmacodynamics are identical in different tissues, pharmacokinetic effects may result in enhanced responses to pulsatility in certain tissues. Precise quantification of this effect is complicated by the experimental challenges in determining the cyotosolic concentrations of lipophilic molecules like glucocorticoids (Garnier-Suillerot 1995).

Studies of glucocorticoid ultradian rhythms are complicated by interpretation of prior experimental evidence: sampling frequencies lower than once every ~15 minutes do not sufficiently capture ultradian rhythms; pulses in cortisol are sometimes mislabeled as noise or as responses to a stimulus; and multiple replicates with unsynchronized ultradian rhythms produce an overly flat ensemble average. For these reasons, glucocorticoid pulsatility is often understated (Young, Abelson et al. 2004). Despite these limitations, a growing body of experimental evidence suggests that the properties of glucocorticoid ultradian rhythms dynamically change with seasonal (Ingram, Crockford et al. 1999), menstrual (Feldman, Mondon et al. 1979; Bao, Liu et al. 2003), and circadian (Veldhuis, Iranmanesh et al. 1989) rhythms. These longer-term rhythms, in addition to significant interindividual heterogeneity, illustrate the value of a model-based approach which can be used to assess the implications of a wide range of system dynamics on downstream effects of HPA pulsatility.

The impact of glucocorticoid pulsatility on the stress response is particularly of interest in the context of inflammation, given that glucocorticoids are powerful regulators

of many inflammatory genes. Although many inflammatory effects of glucocorticoids are mediated through protein-protein interactions, rather than direct transcriptional modulation as considered here, those effects still depend on the concentration activated nuclear GC-GR complex. For instance, it has been shown that cortisol infusion prior to an inflammatory challenge can modulate cytokine responses (Barber, Coyle et al. 1993). While it is not yet clear how ultradian rhythms impact this type of phenomenon, the results presented here suggest that some of this effect could be related to the disturbance of rhythmic cortisol levels. Integrating this ultradian model into our larger endotoxemia model described in Chapter 2 will allow us to further refine our understanding of the interplay between physiologic variability and the inflammatory response.

Chapter 4: Heart Rate Variability and Human Endotoxemia

This chapter contains two primary sections. First, section 4.1 discusses how the model of endotoxemia discussed in Appendix A and Chapter 2 can be linked to HRV through a semi-mechanistic model. Then, section 4.2 focuses on what this type of modeling can inform us about autonomic function in human endotoxemia.

4.1: Modeling Autonomic Regulation of Cardiac Function and Heart Rate Variability in Human Endotoxemia

4.1.1: Introduction

Heart rate variability (HRV) is generally defined as the quantification of the distribution of time intervals between successive heartbeats. Reduction in HRV, a manifestation of altered autonomic function under stress, is potentially a useful predictor of outcome in myocardial infarction (Kleiger, Miller et al. 1987), congestive heart failure (Ponikowski, Anker et al. 1997), diabetic neuropathy (Pagani 2000), and neonatal sepsis (Lake, Richman et al. 2002). Diminished HRV has also been observed in critically ill patients in intensive care units (Morris, Norris et al. 2007), which motivates interest in HRV as a critical variable in the recovery from critical illness (Lowry and Calvano 2008). Due to this clinical relevance, dynamic characteristics of HRV have been assessed by time domain, frequency domain (Task 1996), and nonlinear metrics (Peng, Havlin et al. 1995; Lake, Richman et al. 2002). The majority of HRV research has thus far focused on the interpretation of the patterns of HRV (Lahiri, Kannankeril et al. 2008) rather than linking cellular-level mechanisms to patterns (Buchman 2009). The realization that health may be characterized by a certain degree of variability of human heart signals motivates the hypothesis that appropriate physiologic variability is the manifestation of robust

dynamics of control signals whose fluctuations equip the host with the ability to anticipate external and internal disturbances. We hypothesize that these variable dynamics are driven by the convergence of rhythmic physiological signals on the heart via autonomic modulation.

Studying the effects of critical illness on HRV requires a clinical model that can be experimentally evaluated in great detail. Human endotoxemia, the injection of lipopolysaccharides (LPS or endotoxin, used interchangeable herein) into healthy human subjects, has been extensively used as a model of systemic inflammation due to qualitatively similar responses in systemic physiologic and metabolic processes, including changes in leukocyte abundance and behavior, hormonal secretion, and cardiac function (Lowry 2005). Responses observed in human endotoxemia experiments mimic observed responses in systemic inflammation in ICU patients, albeit over different timescales (Haimovich, Reddell et al. 2010), thus making the human endotoxemia model an excellent platform for exploring mechanistic underpinnings of the systemic inflammatory response. A key component in the response to endotoxemia is a decrease in HRV, concomitant with imbalances in autonomic activity reflected by perturbed autonomic oscillatory responses in HR (Godin, Fleisher et al. 1996; Rassias, Holzberger et al. 2005; Jan, Coyle et al. 2009; Jan, Coyle et al. 2010).

Despite an understanding of the importance of inflammation in a wide variety of disorders and a large number of experiments elucidating the details of the inflammatory response, novel treatments aimed at controlling inflammation remain elusive (Freeman and Natanson 2000). The complexity of the interacting, redundant pathways involved in the inflammatory response necessitate a systems-level understanding of inflammation

(Seely and Christou 2000; Vodovotz, Clermont et al. 2004), thus leading to interest in the inflammatory response from a systems biology perspective (Vodovotz 2010). The dynamic signals evoked in an inflammatory response are propagated to the sinoatrial (SA) node of the heart to assess how HRV is perturbed in endotoxemia. Previously, endotoxemia-induced changes in HR and HRV have been described by physicochemical relations which begin to elucidate the signals that give rise to altered phenotypes (Foteinou, Calvano et al. 2010; Foteinou, Calvano et al. 2011). However, this neglects that HR and HRV are both derived from the same physiological process, the beats of the heart, and that the contraction of the heart as initiated by firing neurons at the SA node is a noisy, discrete process. This motivates the development of a more mechanistic model to produce discrete heartbeat signals that can then be used to calculate HR and HRV, providing a basis for the development of autonomic dysfunction in endotoxemia. This chapter proposes a semi-mechanistic mathematical model linking endotoxemia to cardiac function through an integral pulse frequency modulation (IPFM) model (Bayly 1968) that produces discrete heartbeats as output based on autonomic modulation of the heart. Variability is considered both at high frequencies (autonomic oscillations) and much lower frequencies (circadian rhythms). Outputs of the model, namely HR and HRV, are shown to accurately capture experimentally-observed phenomena in human endotoxemia studies. Furthermore, the links between autonomic activity and cardiac function are explored, as well as how these communication links are affected by acute stress. Understanding the loss of variability of cardiac function in endotoxemia serves as a step towards gaining insight into similar changes in HRV observed clinically in response to stress (Haimovich, Reddell et al. 2010). It is important to consider how the

communication between the autonomic nervous system and the heart in endotoxemia (Sayk, Vietheer et al. 2008) will affect both measureable parameters of HRV and the mechanistic underpinnings that give rise to altered cardiac function. Thus, connections between processes at the cellular, molecular, and neural levels are quantitatively linked to HRV. This work builds towards translational applications of systems biology (Vodovotz, Csete et al. 2008; Foteinou, Calvano et al. 2009) by moving towards an understanding of the relationship between fundamental biological processes and clinical outcomes.

4.1.2: Methods

4.1.2.1: Human Endotoxemia Model

Bacterial endotoxin, a component of the outer cell membrane of gram-negative bacteria, is an important mediator in the pathophysiology of gram-negative bacterial sepsis (Opal, Scannon et al. 1999). This complex macromolecule induces its injurious effects by a non-cytotoxic interaction with CD14-bearing inflammatory cells, such as macrophage-monocytes, circulating neutrophils and lung epithelial cells. These effector cells are activated through a family of Toll-like receptors and subsequently release a network of inflammatory products. These host-derived mediators function in concert to induce the systemic inflammatory response syndrome (SIRS) (Parrillo 1993) leading to a variety of clinical disorders, including adult respiratory distress syndrome (ARDS) (Miyata and Torisu 1986; Bayston and Cohen 1990). Elective administration of endotoxin to otherwise healthy human volunteers has been used to study systemic inflammation and gain insight into behavior of inflammatory mediators encountered in acute, as well as chronic, inflammatory disease. Human endotoxemia precipitates signs and symptoms characteristic of clinical sepsis (Lowry 2005; Andreasen, Krabbe et al.

2008) and ARDS (Buttenschoen, Kornmann et al. 2008), inducing a reduction in HRV (Godin, Fleisher et al. 1996; Rassias, Holzberger et al. 2005). While we do not argue that the human endotoxin (lipopolysaccharide=LPS) challenge model precisely replicates an acute infectious or sepsis condition, human endotoxin challenge does serve as a useful model of toll-like receptor 4 (TLR4) agonist-induced systemic inflammation by providing a reproducible experimental platform tying systemic inflammation to physiological signal generation and alterations in HRV. As an example, it has recently been demonstrated that LPS challenge induces transient dynamic changes in leukocyte gene expression similar to day 1 trauma patients (Shanker, Coyle et al. 2010).

In an effort to establish quantitative relationships among the components involved in endotoxemia, we developed a mathematical model of human endotoxemia (Foteinou, Calvano et al. 2009; Foteinou, Calvano et al. 2009). A detailed description of the components of the mathematical model is given in Appendix A and Chapter 2 and the network structure is displayed in Figure 4.1. At the cellular level, recognition of LPS by TLR4 on immune cells leads to the activation of the NF-κB pathway and ultimately the production of both pro-inflammatory (*P*) and anti-inflammatory (*A*) cytokines, which are proximal mediators of the systemic inflammatory response (Opal and DePalo 2000) and antagonistically work towards the self-regulation and resolution of inflammation. At the neuroendocrine level, the hypothalamic-pituitary-adrenal (HPA) axis and the sympathetic nervous system (SNS) are the primary stress response pathways by which the central nervous system (CNS) regulates the immune response (Sternberg 2006). This was modeled by assuming that the production and release of counter-regulatory anti-inflammatory endogenous hormones cortisol (*F*) and epinephrine (*EPI*) respond to pro-

inflammatory cytokines, and then these hormones feed back to modulate the transcriptional response in leukocytes. In addition, circadian rhythms in model components, both at the level of immune cells and CNS activity, were considered by accounting for diurnal patterns in the release of the hormones cortisol and melatonin (*M*), which then propagate their circadian rhythmicity to other variables (Scheff, Calvano et al. 2010).

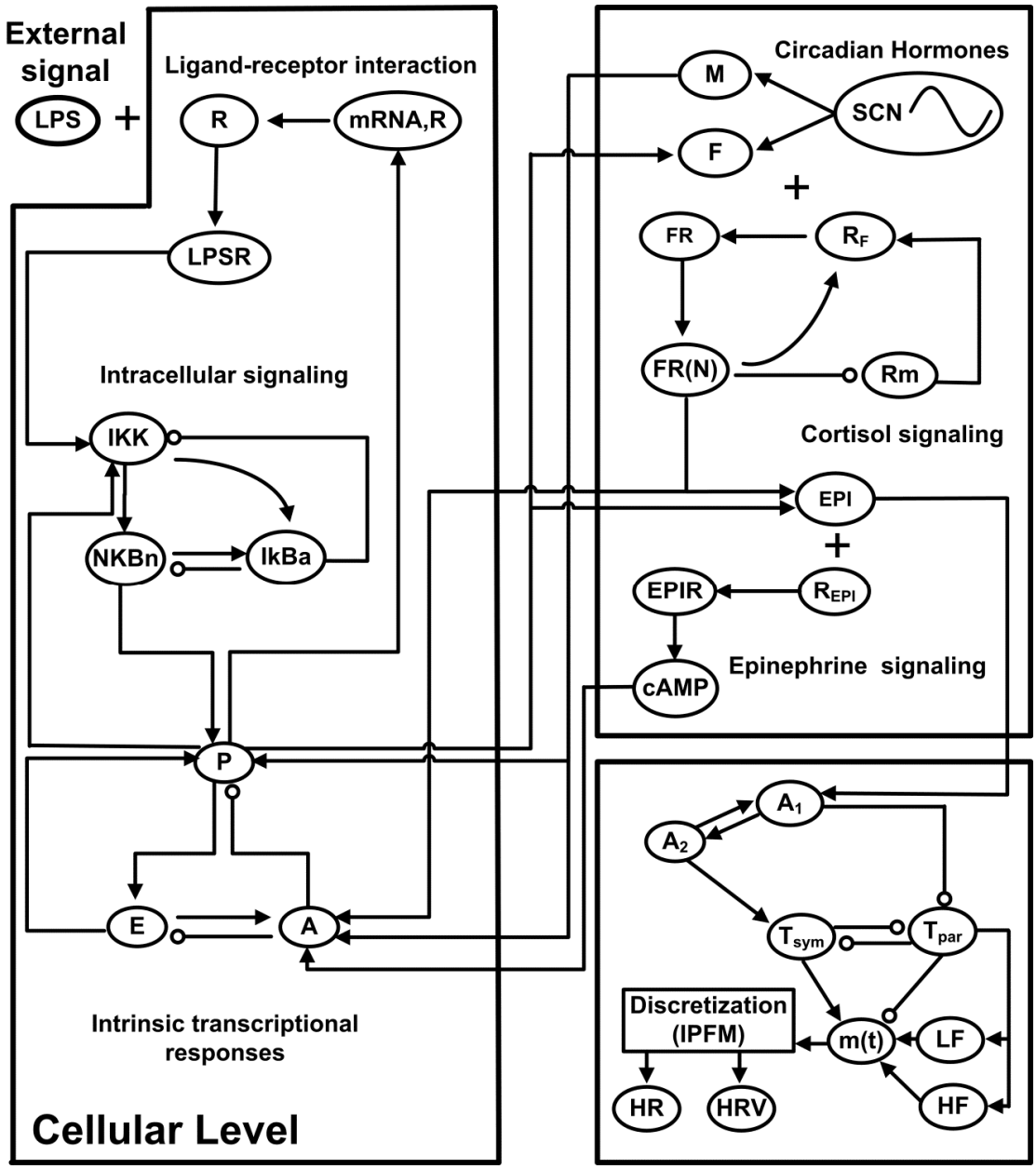

Figure 4.1: Network structure. At the cellular level, LPS is recognized by its receptor, activating the NF-κB signaling cascade that provokes a significant transcriptional response consisting primarily of pro-inflammatory (P) and anti-inflammatory (A) signaling as well as a decrease in cellular bioenergetic processes (E). Neuroendocrine-immune crosstalk results in the secretion of stress hormones cortisol (F) and epinephrine (EPI), which serve as immunoregulatory branches of the central nervous system. They are also centrally regulated to obey circadian dynamics. Finally, these signals propagate to the heart, where HR and HRV are modulated in a systemic inflammatory response.

We previously explored the principles of the Warner model (Warner and Cox 1962) to describe the influences of the antagonistic relationship between the sympathetic and parasympathetic branches of the autonomic nervous system on the firing at the SA node of the heart (Foteinou, Calvano et al. 2011). Autonomic activity at the SA node of the heart can be inferred based on blood epinephrine concentration (Foteinou, Calvano et al. 2011), which has a circadian pattern with a peak during the middle of the day, slightly lagging the diurnal behavior of cortisol (Kronfol, Nair et al. 1997; Dimitrov, Benedict et al. 2009; Scheff, Calvano et al. 2010). A_1 (Eq. 4.1a) represents the neurotransmitter concentration at the SNS nerve ending, which is associated with blood norepinephrine concentration and is assumed to be similarly responsive to endotoxemia as epinephrine (Schaller, Waeber et al. 1985). Plasma norepinephrine ultimately influences the local concentration at the SA node as described by A_2 (Eq. 4.1b). This produces antagonistic changes in effective local sympathetic (Eq. 4.1c) and parasympathetic (Eq. 4.1d) activity. These relationships were used to develop a physicochemical model of the effect of endotoxemia on HR (Foteinou, Calvano et al. 2011), with parameters given in Table 4.1.

$$\frac{dA_1}{dt} = K_{a1} \cdot \left(EPI - A_1 \right) - K_{a2} \cdot \left(A_2 - A_1 \right) \tag{4.1a}$$

$$\frac{dA_2}{dt} = K_{a2} \cdot \left(A_1 - A_2 \right) \tag{4.1b}$$

$$\frac{dT_{sym}}{dt} = \frac{K_{a3} \cdot A_2 \cdot (K_C - T_{sym})}{\left(1 + k_{T_{sym},T_{T_{par}}} \cdot T_{par} \right)} - K_{a4} \cdot T_{sym} \tag{4.1c}$$

$$\frac{dT_{par}}{dt} = \frac{K_{in,T_{par}}}{\left(1 + k_{T_{par},T_{sym}} \cdot T_{sym} \right) \cdot A_1} - K_{out,T_{par}} \cdot T_{par} \tag{4.1d}$$

Parameter	Value	Parameter	Value	Parameter	Value
K_{a1}	3.654	K_C	11.286	$K_{in,Tpar}$	45.181
K_{a2}	0.055	$k_{Tsym,Tpar}$	7.764	$k_{Tpar,Tsym}$	9.756
K_{a3}	2.927	K_{a4}	3.435	$K_{out,Tpar}$	4.201

Table 4.1: Parameters used in Eq. 4.1, as defined in (Foteinou, Calvano et al. 2011).

When combining Eq. 4.1 with our circadian model (Scheff, Calvano et al. 2010), described above and in Appendix A, we now observe that the effective sympathetic (T_{sym}) and parasympathetic (T_{par}) modulation of HR and HRV exhibit diurnal patterns as imposed by central circadian regulation. Experiments measuring muscle sympathetic nerve activity show that it is responsive to light (Saito, Shimizu et al. 1996) and that during sleep, sympathetic activity decreases (Gherghel, Hosking et al. 2004). Based on experimental evidence that parasympathetic activity can be estimated by respiratory sinus arrhythmia measured by the spectral analysis of heart rate, it has been shown that parasympathetic activity also follows circadian dynamics (Burgess, Trinder et al. 1997), as measured by both time domain (pNN50) and frequency domain metrics (Burger, Charlamb et al. 1999). These oscillatory dynamics, leading to short-term HRV and long-term circadian rhythms in HR and HRV, have not yet been studied in a model that links autonomic activity to the beating of the heart within the context of an integrated model of inflammation. Below, variability in HR is studied in terms of these rhythmic signals through the development of a model linking the inflammatory response with alterations in the pattern of discrete heart beats.

4.1.2.2: Modeling Autonomic Influence on Cardiac Dynamics

To describe how internal signals representing cellular and molecular processes responsive to endotoxemia are propagated to the heart, the oscillatory signals giving rise to variability in HR must first be accounted for. We hypothesize that the convergence of these variable autonomic signals, representing both circadian rhythms and higher frequency oscillations, gives rise to the characteristic patterns of variability in HR. Thus, the first step towards developing a more mechanistic model of cardiac function in

endotoxemia is describing the nature of autonomic regulation at the SA node of the heart. Three sources of oscillations are considered: sympathetic and parasympathetic oscillations and circadian rhythms.

HRV is typically calculated based on a series of RR intervals, which are generated from ECG signals by measuring the time interval between successive R waves. In the frequency domain of RR intervals, the power spectrum is typically divided into two frequency bands: low frequency (LF, 0.04-0.15 Hz) and high frequency (HF, 0.15-0.4 Hz). While the precise autonomic underpinnings of HF and LF power are unclear and likely indirect (Karemaker 1999), HF is related to vagal activity and LF responds to changes in both vagal and sympathetic tone; thus, the ratio LF/HF may give some insight into the relative autonomic control of HR. Incorporating higher-frequency oscillations in autonomic modulation of HR allows for the production of a more biologically realistic heartbeat signal.

Long-term circadian oscillations in autonomic activity at the SA node influence the diurnal pattern of heartbeats. Sympathetic activity increases HR, while parasympathetic activity decreases HR; therefore, combining models that represent autonomic activity in inflammation (Foteinou, Calvano et al. 2011) and circadian rhythms in inflammation (Scheff, Calvano et al. 2010) generates variables reflecting circadian rhythms in sympathetic and parasympathetic activity at the SA node. These circadian autonomic activities lead to diurnal patterns in both HR and HRV (Huikuri, Niemela et al. 1994; Korpelainen, Sotaniemi et al. 1997; Nakagawa, Iwao et al. 1998). Circadian rhythms are hypothesized to express sympathetic activity as proportional to autonomic modulation and parasympathetic activity as inversely proportional. Circadian

rhythms are included to represent autonomic influences on the SA node, specifically slowly evolving circadian rhythms.

The inclusion of autonomic activity through a modified Warner-type model (Eq. 4.1), stimulated by central hormonal circadian rhythms allow for the assessment of changes in autonomic control of heart rate variability (Chiu and Kao 2001). When sympathetic activity increases, the SA autonomic modulation is expected to increase, corresponding to more frequent firing and thus higher HR. When parasympathetic activity increases, the opposite occurs and HR decreases. Our model aims to introduce circadian variability in the autonomic modulation of the SA node, through the connections to our endotoxemia model via T_{sym} (Eq. 4.1c) and T_{par} (Eq. 4.1d), which are ultimately linked to circadian rhythms in HR that match well with experimental data showing that HR peaks during the day and is lower at night (Nakagawa, Iwao et al. 1998).

HF and LF power have been observed to exhibit circadian rhythms under normal conditions (Huikuri, Niemela et al. 1994; Korpelainen, Sotaniemi et al. 1997; Nakagawa, Iwao et al. 1998). In human endotoxemia, HF and LF power both decrease acutely before recovering (Godin, Fleisher et al. 1996; Jan, Coyle et al. 2009; Jan, Coyle et al. 2010). Both circadian and acute responses may be explained by the link between vagal activity and HF and LF oscillations. Suppressing vagal activity leads to decreases in both HF and LF power, contrary to the outdated view that HF reflects only vagal activity and LF reflects only sympathetic activity (Task 1996). Experimental data of circadian rhythms in HF and LF are in phase with the predicted circadian oscillations in T_{par} in Figure 4.2. Further, in human endotoxemia, T_{par} decreases to reflect diminished parasympathetic

activity during the acute systemic inflammatory response (Foteinou, Calvano et al. 2011). Thus, we hypothesize that the variable amplitudes of HF and LF oscillations are governed by parasympathetic activity.

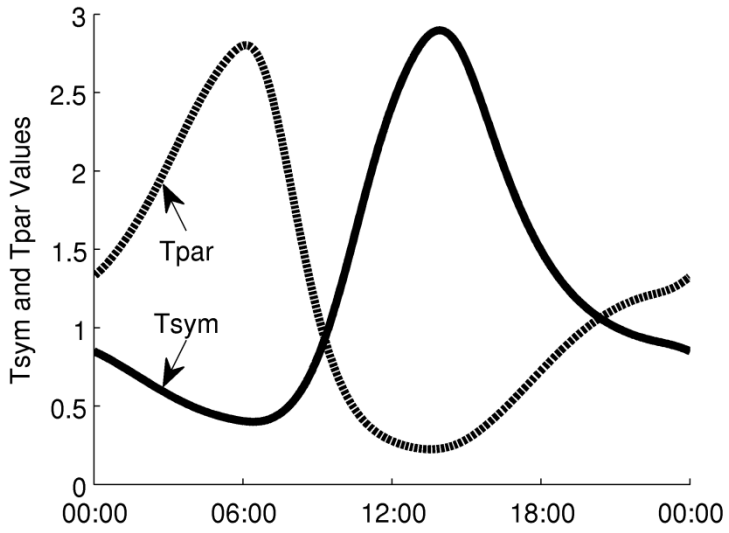

Figure 4.2: Circadian rhythms in the effective sympathetic and parasympathetic activity (Tsym and Tpar) at the sinus node of the heart. Diurnal rhythms from the circadian release of cortisol propagate through epinephrine, ultimately influencing Tsym and Tpar, which oscillate out of phase in homeostasis.

HF and LF oscillations are assumed to contribute in an additive manner to SA node autonomic modulation as two sinusoids. In (Brennan, Palaniswami et al. 2002), HF and LF oscillations are similarly modeled as sinusoids with frequencies 0.334 Hz and 0.025 Hz, respectively. The LF frequency is set so low (below the LF range) because it is meant to also allow for realistic changes in very low frequency (VLF, <0.05 Hz) activity. However, this impedes the direct calculation of LF and HF powers because the peak in the power spectrum is so narrow that it hardly influences the power in the LF frequency band. Therefore, in Eq. 4.2, the mean values of the frequencies in the HF and LF bands were used. Then, the peaks in the power spectrum fall directly within the HF and LF bands, facilitating the use of standard methods of calculating HF and LF power to study

model output. The amplitudes of the HF and LF sinusoids depend on T_{par}, which produces homeostatic circadian rhythms in HRV (Huikuri, Niemela et al. 1994; Korpelainen, Sotaniemi et al. 1997; Nakagawa, Iwao et al. 1998) as well as acute suppression of HRV in endotoxemia (Godin, Fleisher et al. 1996; Jan, Coyle et al. 2009; Jan, Coyle et al. 2010).

The aforementioned assumptions are succinctly summarized in the model of Eq. 4.2 and Table 4.2. The effective autonomic modulation at the SA node depends on contributions including circadian and higher frequency modulation of the heart as well as a constant activity level which gives rise to the mean resting HR.

$$m(t) = \underbrace{\underline{HR}}_{\substack{\text{constant}\\ \text{activity}\\ \text{level}}} + \underbrace{k_{circ}\left(T_{sym} + \frac{1}{T_{par}}\right)}_{\substack{\text{circadian}\\ \text{variability}}} + \underbrace{k_{osc}\left(1 + k_{par,LF}T_{par}\right)\sin\left(f_{LF}t\right)}_{\text{LF/sympathetic oscillations}} + \underbrace{k_{osc}\left(1 + k_{par,HF}T_{par}\right)\sin\left(f_{HF}t\right)}_{\text{HF/sympathetic oscillations}} \tag{4.2}$$

Parameter	Value	Parameter	Value
HR	1	$k_{par,HF}$	1
k_{osc}	0.05	f_{HF}	0.275
$k_{par,LF}$	0.5	k_{circ}	0.04
f_{LF}	0.105		

Table 4.2: Parameter values used in Eq. 4.2. Frequencies for the HF and LF bands are set to the mean value of the standard limits of those bands. The other parameters are set manually. In practice, the parameters in the IPFM model would need to be tuned to an individual subject due to significant person-to-person variability in cardiac dynamics, such as the mean heart rate and the amplitude of circadian rhythms.

4.1.2.3: Generation of Discrete Heartbeats

Autonomic activity influences the heart by modulating the pattern of discrete heartbeats by altering the concentration of neurotransmitters at the SA node. An idealized

neuron functions by sensing local neurotransmitter concentration and, when that concentration crosses a threshold, the postsynaptic neuron fires. This type of neural-based discretization process occurs at the sinoatrial (SA) node of the heart, which normally initiates the electrical impulses that trigger contraction of cardiac tissue. As the SA node is innervated by both sympathetic and parasympathetic branches of the autonomic nervous system and the imbalance between these branches is critical to the loss of HRV, an ideal model would be one that dynamically controls the time interval of integration between successive firings based on autonomic activity as defined in Eq. 4.2.

A continuous signal can be converted to discrete events via an integrate-and-fire model in which the signal is repeatedly integrated until it reaches a threshold, thus signifying an event. One realization of an integrate-and-fire model which can discretize a continuous signal is an integral pulse frequency modulation (IPFM) model. IPFM models allow for the translation of a continuous signal into a discrete series of events, conceptually similar to the behavior of a neuron (Bayly 1968). A continuous input signal *m(t)* represents modulation of neural firing, such as is defined in Eq. 4.2 to represent modulation at the SA node. Then, the times of firings are found by repeatedly integrating *m(t)* until a threshold Δ has been reached: $\int_{t_k}^{t_{k+1}} m(t)dt = \Delta$. Δ is set to 1 in all simulations performed here.

This produces a vector t with elements t_k to represent the kth discrete event. In our model of heartbeat generation, *m(t)* represents autonomic modulation of the heart and the discrete events produced through the IPFM model represent heartbeats initiated by the SA node (Chiu and Kao 2001; Brennan, Palaniswami et al. 2002). HR is modulated by

shifting the mean value of *m(t)* up (increased HR) or down (decreased HR). And because of variations in autonomic activity, the output of the IPFM model (heartbeats) will contain some variability. There are two primary mechanisms by which HRV is modulated through this model. Most directly, changes in HRV are driven by variable amplitudes of the HF and LF oscillators in Eq. 4.2. When the amplitude of these oscillators decreases, *m(t)* becomes more and more flat until there is very little beat-to-beat variability. However, even with constant amplitudes for HF and LF, HRV can still change because RR intervals become shorter as the mean value of *m(t)* shifts up due to circadian influences from T_{sym} and T_{par},. Thus, the observed decrease in variability as assessed by HRV metrics is partially reflecting the changing mean value of heart rate (Niklasson, Wiklund et al. 1993). This initially may seem analogous to what is observed when sympathetic activity increases, such as in exercise where there seems to be an inverse relationship between HR and HRV (Javorka, Zila et al. 2002). However, looking at the raw HR data in these cases makes it clear that the amplitude of oscillations in HR is lost in concert with increased mean HR. Therefore, if the amplitude of these oscillations, and thus HRV, is to be dynamic, it must be represented with a model that has the ability to alter the amplitude of oscillatory components, as in Eq. 4.2.

4.1.2.4: Calculation of HRV

A variety of HRV parameters are assessed, spanning the time domain (SDNN, the standard deviation of normal-to-normal heartbeat intervals), frequency domain (HF, LF, and associated measures), and nonlinear analysis (sample entropy). All parameters are calculated over epochs that are 5 minutes in length, as is typical in the analysis of HR data (Task 1996). Each of the *i* epochs of RR intervals is denoted by RR_i. The time

domain measure, SDNN, is simply the standard deviation of interbeat intervals generated by the IPFM model, defined in Eq. 4.3.

$$SDNN_i = \text{stdev}(RR_i) \tag{4.3}$$

The frequency domain statistics are calculated from mean-subtracted RR interval sequences based on the output of MATLAB's `pyulear` function with an order of 12, which implements an autoregressive model using the Yule-Walker algorithm to estimate the power spectral density. Then, HF and LF values represent the area under the curve in linear units over the appropriate frequency ranges of 0.15-0.4 Hz and 0.04-0.15 Hz respectively. HF_n and LF_n are normalized values, defined as $HF_n=HF/(HF+LF)$ and $LF_n=LF/(HF+LF)$. The *LF/HF* ratio is also computed.

Sample entropy (*SampEn*) (Richman and Moorman 2000) is calculated using the implementation available on PhysioNet (http://www.physionet.org/physiotools/sampen/). *SampEn* is defined as the negative natural logarithm of the estimated conditional probability that two subseries of *m* points that have all matched within a tolerance *r* continue to match within that tolerance at the next point. Therefore, a low value of *SampEn* means that the input series has a very regular structure, and high values correspond with high entropy, irregular signals.

4.1.2.5: Generation of Poincaré Plots and their Geometric Properties

Poincaré plots of RR intervals are generated for the scenarios described above. These plots are derived from a time series of RR intervals by plotting each value RR(i) on the x-axis versus its successive value RR(i+1) on the y-axis. Thus, if the system generated two consecutive RR intervals that were identical, that point would lie directly on the 45° diagonal. Variability in the Poincaré plot can be quantified by calculating the

standard deviation along this diagonal line and perpendicular to the diagonal line. These values, called *SD1* and *SD2*, are visualized by plotting an ellipse whose axes are equal to *SD1* and *SD2*. *SD1* and *SD2* have been used to roughly represent short-term and long-term variability in HR due to their intuitive, geometric interpretations (Brennan, Palaniswami et al. 2001).

4.1.3: Results

Circadian and higher-frequency variability in autonomic modulation at the SA node is taken into account in Eq. 4.2, allowing for simulation of homeostasis and the biologically rhythms present in homeostasis. Based on this, Figure 4.3 shows the homeostatic model output. *m(t)* has a clear circadian pattern in Figure 4.3A and also exhibits higher-frequency variability in Figure 4.3B. Both the mean value and the amplitude of variability of *m(t)* are under diurnal regulation. Circadian rhythms in HR (Figure 4.3C) and HRV as assessed by SampEn and SDNN (Figure 4.3D) are present in model output. HF and LF power, visualized on the power spectra in Figure 4.3E-F representing 00:00 and 12:00 respectively, also contain significant diurnal variability.

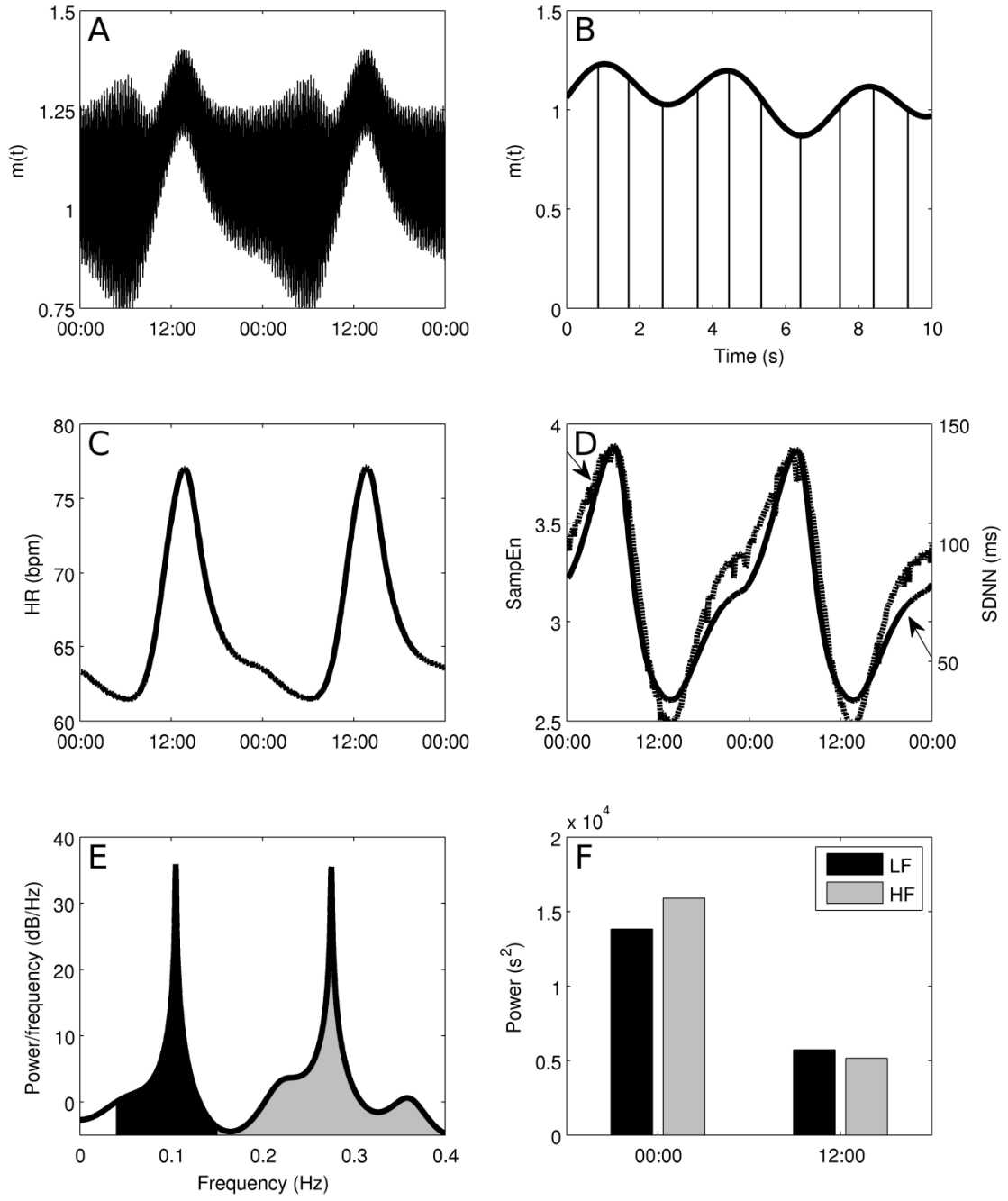

Figure 4.3: Autonomic modulation at the SA node of the heart, shown at two scales (A and B), leading to circadian rhythms in smoothed HR (C) and HRV (D), as assessed by time domain (SDNN, solid line) and nonlinear (SampEn, dashed line) metrics. E shows a power spectrum calculated from a 5 minute window of RR intervals at 12am. Two peaks, representing LF and HF oscillations, are present. LF and HF values are calculated as the area under this curve, 0.04-0.15 Hz for LF and 0.15-0.4 Hz for HF. F shows how that these HF and LF values undergo significant changes throughout the daily circadian cycle.

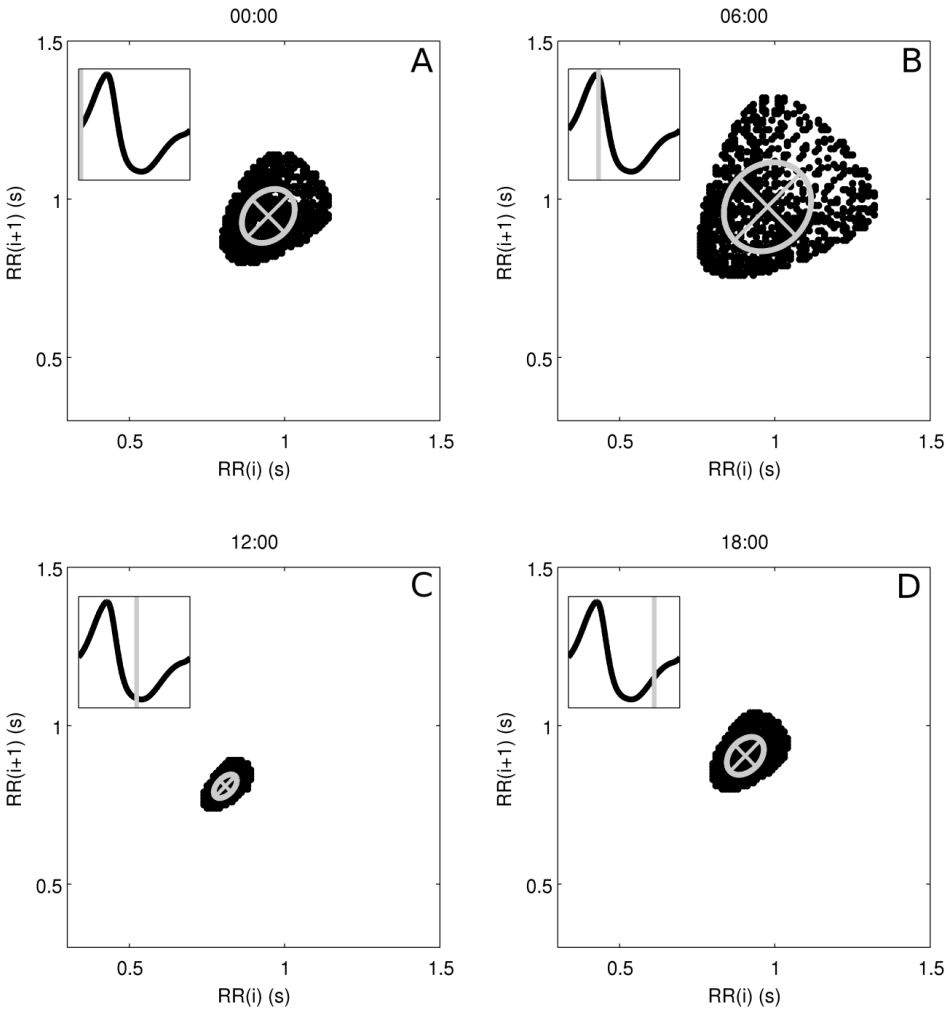

Figure 4.4: Poincaré plots of RR intervals in homeostasis, at 00:00 (A), 06:00 (B), 12:00 (C), and 18:00 (D). Inset in each figure is the circadian pattern of T_{par} and the region that was used to generate the Poincaré plot. The ellipses represent the dispersion of points as the axes are equal to the standard deviation of points on each axis. The major and minor axes of the ellipses are drawn on the figure, representing the standard deviations along the y=x diagonal (SD1) and the y=-x diagonal (SD2). A large circadian pattern in the geometry of the Poincaré plots is observed, ranging from a maximum of (SD1, SD2) = (0.13, 0.15) in B to a minimum of (0.027, 0.046) in C.

The addition of beat-to-beat variability in RR intervals permits the visualization of the RR interval time series via the Poincaré plots in Figure 4.4. Four maps are shown, evenly spaced throughout the day: 00:00, 06:00, 12:00, and 18:00. Inset in each figure is

the state of T_{par} at the time when the map is generated. The ellipses have axes equal to the standard deviations of the points along the diagonal and perpendicular to the diagonal (Brennan, Palaniswami et al. 2001). The mean value of the RR interval (roughly the center of the mass of points) moves, illustrating long term variability due to circadian changes in the mean value of *m(t)*. Local variability (roughly the spread of points) also undergoes significant changes throughout the day in Figure 4.5 where the HF and LF values are plotted over time, exhibiting clear circadian patterns.

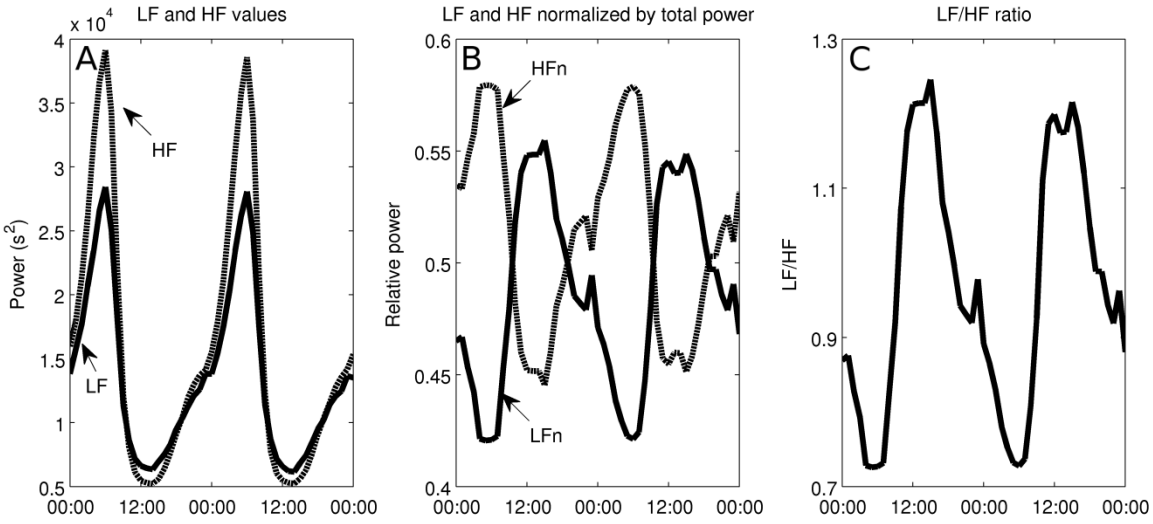

Figure 4.5: LF and HF values are calculated, as shown in Figure 4.3E, at many points throughout the simulation, and these values are plotted as functions of time. A: Circadian rhythms in LF and HF; B: normalized LF and HF (LFn=LF/(LF+HF), HFn=HF/(LF+HF)); and C: the LF/HF ratio. LF and HF are in phase, but their normalized values are out of phase.

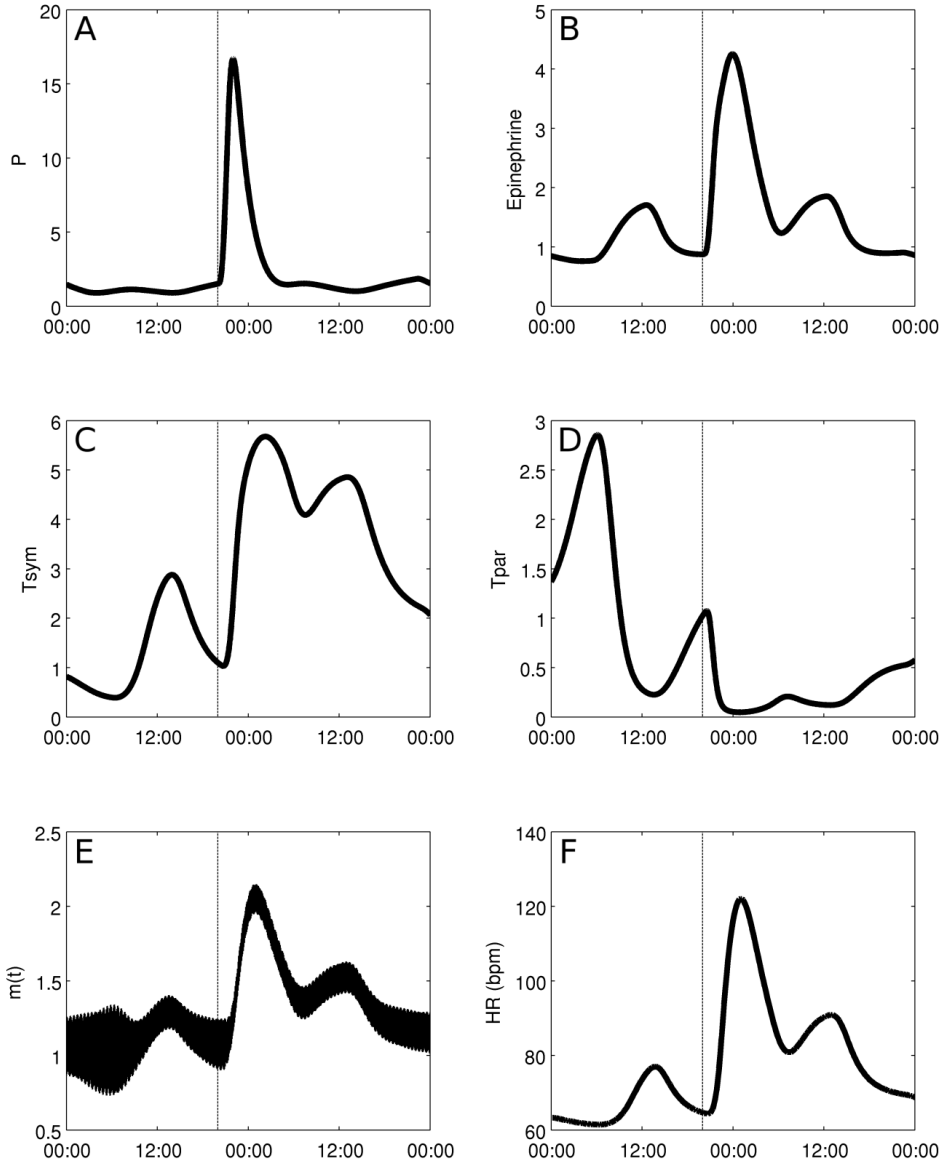

Figure 4.6: Response to a dose of LPS given at 20:00. Changes propagate through proinflammatory cytokines secreted by immune cells (A) to neuroendocrine-mediated effects (epinephrine release in B; autonomic activation in C and D) to the activity of the heart, reflected by changes in effective autonomic modulation (E) and HR (F).

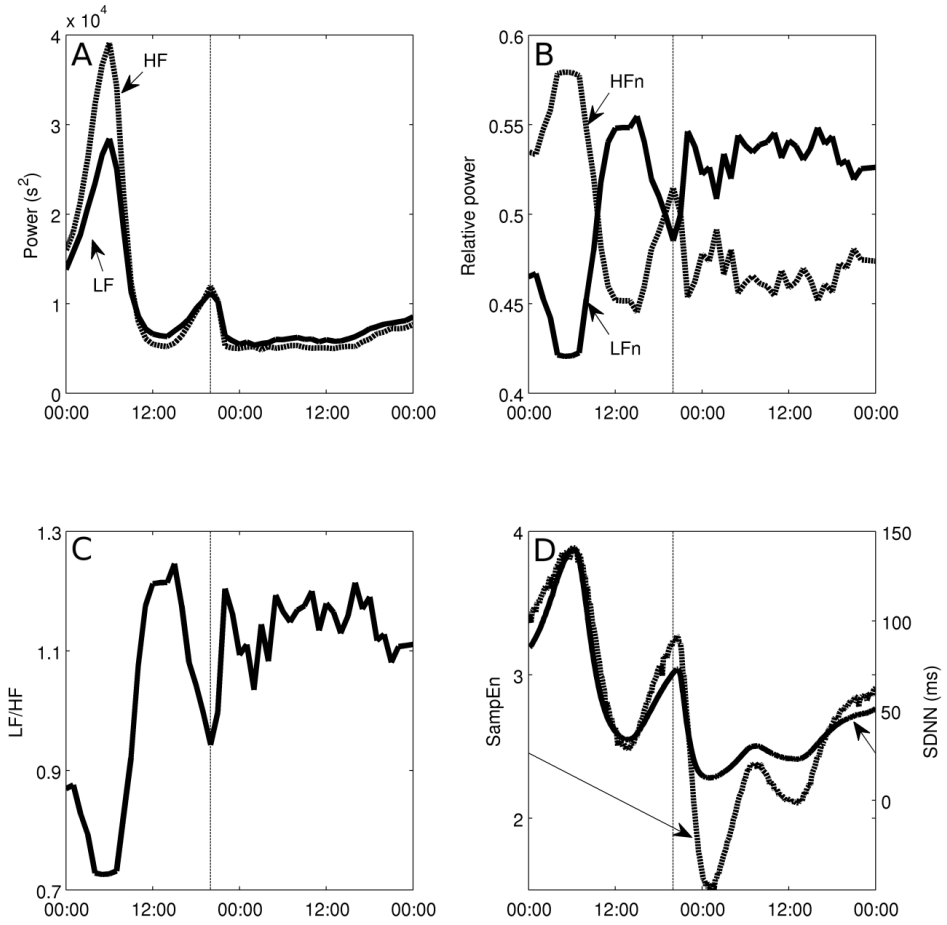

Figure 4.7: Changes in HRV in response to a dose of LPS given at 20:00. Both LF and HF are suppressed (A), but relative values (B) and the LF/HF ratio (C) show that HF is more strongly suppressed than LF. SampEn (dashed line) and SDNN (solid line) both decrease in response to LPS, but SampEn decreases more relative to the amplitude of its normal circadian rhythm.

An acute dose of LPS is given at 20:00, thus provoking a simulated systemic inflammatory response. As described in detail in Appendex A, LPS is recognized by TLR4 on immune cells and instigates a wide range of transcriptional responses, including those that lead to the release of pro-inflammatory cytokines. These cytokines serve as mediators in neuroendocrine-immune communication, leading to the central release of stress hormones such as cortisol and catecholamines. Figure 4.6 shows how this acute disturbance propagates through the system, from pro-inflammatory mediators to anti-

inflammatory hormones, finally leading to an increase in T_{sym} and a decrease in T_{par}, which then provoke changes in cardiac dynamics in response to acute stress. In response to changes in T_{sym} and T_{par}, the autonomic modulation of the SA node, *m(t)* as given in Eq. 4.2, is shifted up and the amplitudes of its higher-frequency oscillatory components are diminished in Figure 4.6E. Figure 4.7 shows how LF and HF both decrease while the LF/HF ratio increases, in agreement with experimental data (Godin, Fleisher et al. 1996; Jan, Coyle et al. 2009; Jan, Coyle et al. 2010). The Poincaré plots displayed in Figure 4.8 show a significant tightening that begins directly after LPS injection and reaches maximal tightening several hours later. Figure 4.7D shows the output of two HRV parameters, SDNN and SampEn. Both parameters capture the circadian pattern prior to LPS and both show an acute decrease after LPS treatment, but the decrease in SampEn is much larger than the decrease in SDNN relative to the normal circadian rhythms observed in each parameter. The above results concerning LPS all study the system response to a dose of LPS at the same time point. The computational model presented here allows for a more broad exploration of the circadian influence on the endotoxemia response, shown in Figure 4.9 where LPS is given at 5:00 and 12:00, illustrating the maximum differences in responses as quantified by HRV.

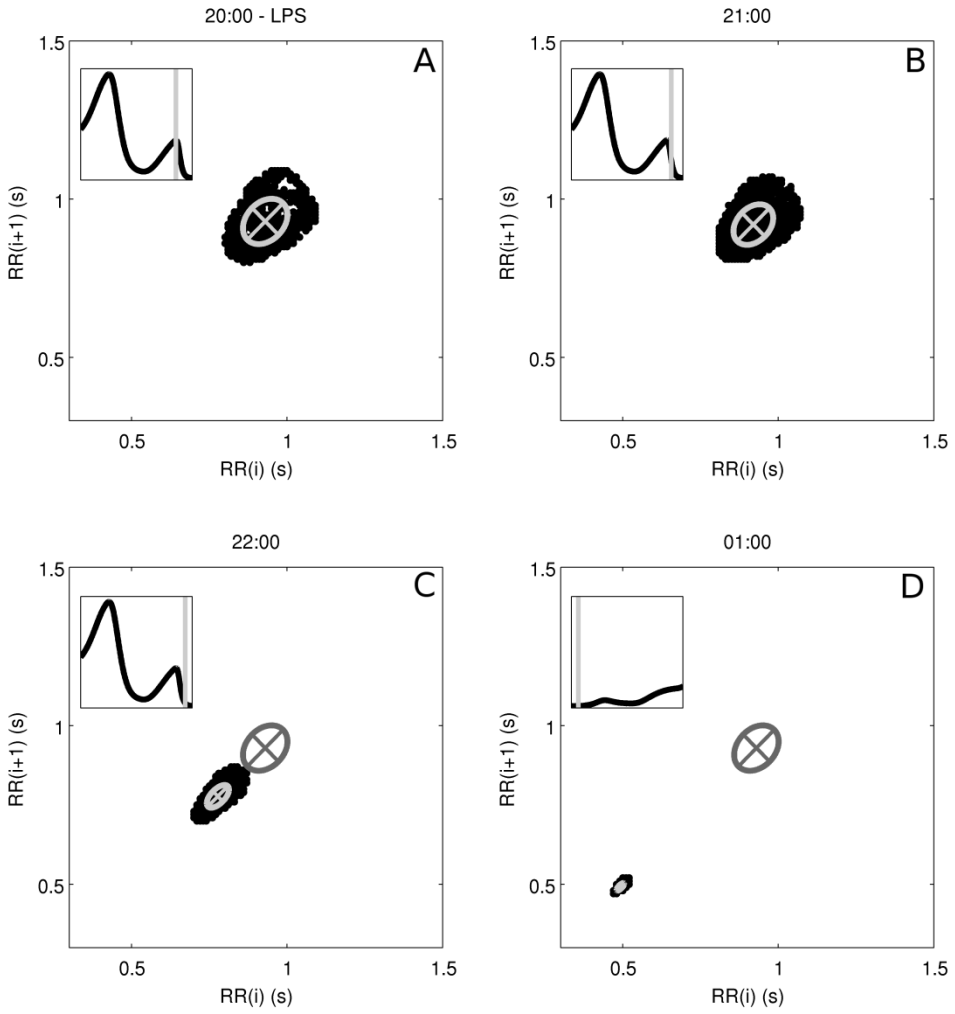

Figure 4.8: Poincaré plots showing the response to a dose of LPS at 20:00, showing maps at 20:00 (A), 21:00 (B), 22:00 (C), and 01:00 (D). Inset in each figure is the circadian pattern of T_{par} and the region that was used to generate the Poincaré plot; in D, the next 24 hours are shown. After injection, the points on the map shift down and to the left, reflecting decreased RR intervals and decreased HR. The points also become more tightly distributed, illustrating the loss of HRV in endotoxemia. D shows the Poincaré plot at 01:00, which is when HRV is most suppressed. The ellipses represent the dispersion of points as the axes are equal to the standard deviation of points on each axis. A change in the geometry of the Poincaré plots is observed, ranging from a maximum of (SD1, SD2) = (0.060, 0.082) at the time of injection in B to a minimum of (0.0060, 0.017) in C. The pre-LPS fitted ellipse from A is shown in C and D to illustrate the difference in both the mean and the distribution of points during the acute response.

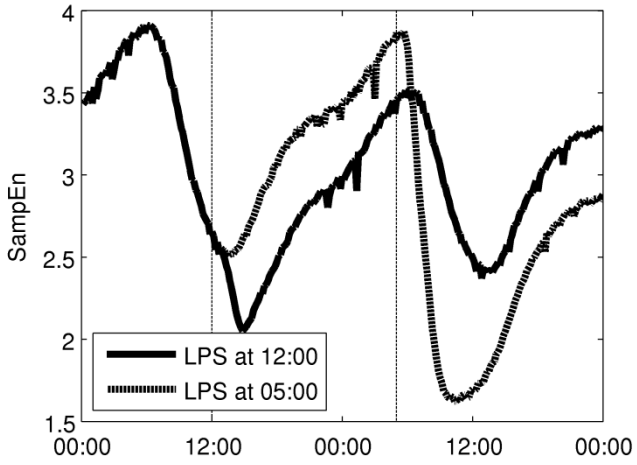

Figure 4.9: There is a circadian dependence on the response of the model to a dose of LPS. The maximum difference is observed between LPS given at 5:00 and 12:00; HRV is quantified by SampEn.

To determine the model response to decoupling between the heart and the autonomic nervous system, the amplitude of HF and LF oscillations, k_{osc} in Eq. 4.2, is halved. Figure 4.10 shows how SDNN changes under these conditions by showing a 24-hour period of diminished k_{osc} in between one day on each side of normal conditions. The amplitude of circadian rhythms in SDNN and the magnitude of SDNN are both diminished in the decreased coupling region.

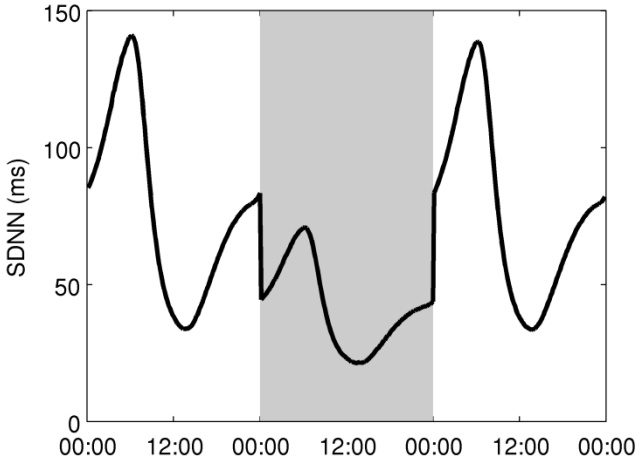

Figure 4.10: Decoupling between the autonomic nervous system and the heart is simulated by decreasing coupling by 50% during the shaded area in the figure. Both the amplitude of circadian rhythms and the magnitude of HRV (assessed by SDNN) are diminished.

4.1.4: Discussion

The components required to link neuroendocrine-immune interactions with circadian and higher-frequency autonomic variability in HR are combined through our proposed model (Eq. 4.2), which incorporates circadian control of cardiac function via autonomic activity along with HF and LF oscillations. While hormonal circadian rhythms alone produce circadian rhythms in model output, some higher frequency oscillations are required to produce the local variability that is observed in real heartbeat signals. HF and LF power is dependent on vagal signaling, and more specifically it is known that HF and LF are diminished under human endotoxemia (Godin, Fleisher et al. 1996; Jan, Coyle et al. 2009). Thus, Eq. 4.2 represents the dependence of HF and LF oscillatory amplitudes on T_{par}. Figure 4.3A displays a clear change in the shape of $m(t)$ as the local oscillations have very different amplitudes depending on the position in the circadian cycle. Power spectra, taken at 00:00 and 12:00 respectively which are close to times at which T_{par} is at its maximum and minimum values, processed to calculate the HF and LF values shown in

Figure 4.3F show a significant drop in the area under the curve of the power spectrum over those frequency ranges throughout the normal diurnal cycle. These HF and LF powers, calculated more frequently, are shown in Figure 4.5. Though raw LF and HF are in phase, HF is suppressed more strongly so that the normalized values LFn and HFn are actually out of phase (Godin, Fleisher et al. 1996; Jan, Coyle et al. 2009). A similar pattern is seen in Figure 4.7A-C after an acute dose of LPS. Both LF and HF decrease, but the decrease in HF is more profound, so that the LFn increases relative to HFn. Thus, the LF/HF ratio remains elevated throughout the recovery phase, illustrating continued imbalance between sympathetic and parasympathetic modulation at the SA node (Godin, Fleisher et al. 1996; Jan, Coyle et al. 2009).

In Figure 4.6 and Figure 4.7, changes in T_{sym}, T_{par}, and the HRV parameters are persistent for over 24 hours after an LPS injection while all other variables in the model recover to their baseline conditions within 24 hours. Run for a longer period of time, these model variables recover within a couple days. Despite this, HRV parameters do recover to within the normal range of circadian variability within 24 hours. In studies where LPS is given to humans and ECGs are recorded for 24 hours as the inflammatory response is initiated and then resolves in a self-limited response, HRV has generally been observed to recover within 24 hours post-injection (Alvarez, Katsamanis Karavidas et al. 2007).

The HF and LF sinusoids in Eq. 4.2 are assumed to mechanistically arise somewhere outside of the model. Biologically, LF and HF oscillations arise largely from vasomotor activity and respiration under control conditions, respectively (Lombardi, Malliani et al. 1996). As *m(t)* represents only the autonomic modulation specifically at

the SA node of the heart, the transduction of the signals producing HF and LF oscillations to the heart must be considered. So, the terms that modulate the amplitude of these sinusoids based on the level of T_{par} represent the ability of the oscillatory signals to be reflected in neurotransmitter concentrations at the SA node, based on the observed relationship between vagal signaling and HF and LF components of HR. Vagal activity modulates LF and HF oscillations in HR and without this vagal activity, LF and HF responses are blunted (Karemaker 1999). In other words, the HF and LF peaks that appear in the power spectrum of HR depend on the autonomic nervous system to communicate these signals to the SA node. Thus, LF and HF give some indication as to the coupling between the heart and the autonomic nervous system, which is of particular interest as HR is relatively easy to assess noninvasively. Indeed, in endotoxemia, an increase in regularity is observed in HR, neutrophil function, and plasma cortisol levels (Rassias, Holzberger et al. 2005), in line with theoretical expectations of the response of decoupled biological systems (Pincus 1994) and the results shown in Figure 4.10 where variability is lost under decoupling. Although these results show an instant decoupling rather than a gradual process as likely occurs *in vivo*, decoupling may be important in adverse conditions such as endotoxemia when interorgan communication is diminished (Godin and Buchman 1996; Godin, Fleisher et al. 1996). Clinically, assessing the interorgan communication by means such as evaluating HF and LF is critical to understanding and assessing the extent of injury in multiple organ dysfunction syndrome (MODS) and sepsis (Schmidt, Müller-Werdan et al. 2007). HF and LF most directly measure cardiac-autonomic coupling, but they can also be used as accessible proxies for measuring general interorgan communication (Schmidt, Müller-Werdan et al. 2007). In

addition, drugs that normally alter heart rate by autonomic modulation fail to have an effect in endotoxemia (Sayk, Vietheer et al. 2008). Thus, the effect of endotoxemia on the heart can be viewed as a decoupling between the autonomic nervous system and the SA node. This decoupling represents a potential mechanism for the observed decreased complexity and increased regularity in physiological signals (Pincus 1994; Buchman 1996). The recovery of HRV following injury can then be viewed as a recoupling of autonomic and cardiac systems, and more generally a recoupling of organ systems in the recovery phase. The model presented here begins to decipher the nature of this relationship through the variable *m(t)* which represents the communication link between the autonomic nervous system and the heart.

One of the fundamental contributions of the described modeling work is the incorporation of circadian rhythms in both HR and HRV parameters. This is of particular interest due to the loss of circadian rhythms observed in inflammation (Lowry 2009) and the interplay between inflammatory mediators and molecular circadian machinery both centrally in the suprachiasmatic nucleus (SCN) and in peripheral tissues (Haimovich, Calvano et al. 2010; Scheff, Calvano et al. 2010). The circadian dependence of this model is shown in Figure 4.9 where identical doses of LPS are given at two different times, 0:500 and 12:00. These two times produce a maximal difference in responses, as the diurnal peak in cortisol occurs between these time points, and this primes the system for a robust anti-inflammatory response. Thus, before this hormonal priming occurs, a significantly larger decrease in HRV (quantified by SampEn) is observed. However, in both cases, the overall dynamics of the system (an acute response and recovery to baseline) are similar. These computational results match with clinical observations that

sepsis patients are at elevated risk of mortality from 02:00 to 06:00, before the circadian peak in cortisol secretion (Hrushesky, Langevin et al. 1994). Considering this type of circadian dependence on responses to pathogens, and also to therapies, is important in optimizing treatment of inflammatory disease (Hrushesky and Wood 1997). In Figure 4.6, circadian rhythms in cardiac function are blunted in response to a dose of LPS as the LPS-induced acute increase in T_{sym} and acute decrease in T_{par} overwhelm the normal diurnal pattern of those variables. In Figure 4.7A, the decrease in both LF and HF in response to endotoxemia is only slightly larger than the physiologic changes in LF and HF due to circadian rhythms. This is because, in the model, T_{par} is predicted to pass relatively close to zero in its diurnal cycle, so in endotoxemia, there is not much further for it to fall. While this result may seem unintuitive, it matches with experimental results showing that the drop from maximum to minimum values during circadian rhythms in HF and LF (Huikuri, Niemela et al. 1994; Korpelainen, Sotaniemi et al. 1997; Nakagawa, Iwao et al. 1998) and the depression in HF and LF due to endotoxemia (Godin, Fleisher et al. 1996; Jan, Coyle et al. 2009; Jan, Coyle et al. 2010) can both be anywhere from 50% to 90% depending on experimental protocol. However, by looking at Poincaré plots (compare Figure 4.4 and Figure 4.8) or by assessing HRV by other metrics such as SDNN and SampEn as in Figure 4.7D, it is clear that there is a significant increase in regularity in response to LPS that is fundamentally different than what is observed in normal circadian patterns. This illustrates the importance of assessing multiple variability/regularity metrics to tease out subtle patterns in HR data.

An advantage of the model presented here, relative to a continuous physicochemical model of either HR or HRV, is that it produces discrete beats as output.

This allows both HR and HRV to be derived from a single variable signal, as they are experimentally, and it allows for comparison of the performance of HRV metrics. Figure 4.7D is provocative in this regard as it shows SDNN and SampEn, two common HRV parameters, both are able to capture normal circadian dynamics as well as the acute response to LPS; however, when their axes are aligned such as in Figure 4.7D so that the amplitude of circadian rhythms is equal for both parameters, it is clear that SampEn is much more significantly suppressed in endotoxemia. Thus, by taking a more mechanistic approach that models heartbeats rather than attempting to directly estimate changes in HRV, these types of quantitative differences can be discovered.

The representation of neurotransmitter concentration at the SA node (Foteinou, Calvano et al. 2011) is conceptually based on the Warner model (Warner and Cox 1962) of sympathetic and vagal influences of HR. A similar idea is explored in the work of Chiu and Kao (Chiu and Kao 2001) in which an IPFM model is modulated by the vagal and sympathetic outputs of the Warner model. The work presented in this chapter goes a step further by ultimately linking the model of autonomic modulation at the SA node with a larger, well-established model of human endotoxemia to explore changes in cardiac output specifically within this context. This introduces some additional complexity into $m(t)$ since the amplitude of HF and LF oscillations depend on a nonlinear model, and also circadian influences are directly incorporated through T_{sym} and T_{par}. In general, one cannot assume that this type of multimodal input signal will be effectively transduced through an IPFM model without the addition of significant distortion (Nakao, Norimatsu et al. 1997). However, the power spectra in Figure 4.3 clearly show that the HF and LF

frequency components are strongly present in the short-term variability of IPFM-generated HR.

By linking cardiac dynamics with a detailed model of the inflammatory response, we have begun to explore the mechanistic underpinnings that may underlie the relationship between autonomic dysfunction and modulated HR and HRV in endotoxemia, and by extension, possible decoupling among other organ systems. The mechanism-based approach (Vodovotz, Constantine et al. 2009) of the endotoxemia model allows for the future investigation of the relationship between neuroendocrine-immune state and cardiac function. This linking of processes at the molecular and cellular level with outcomes at the systemic level (namely clinically accessible variables such as HR and HRV) is an important step towards developing translational applications of systems biology.

4.2: On Heart Rate Variability and Autonomic Activity, in Homeostasis and in Systemic Inflammation

4.2.1: Introduction

A marker of a healthy functioning heart is variability in the time intervals between successive heart beats, known as heart rate variability (HRV). There are a wide range of analytical techniques to quantify HRV from heart rate (HR) measurements (Bravi, Longtin et al. 2011), including power spectral analysis which has traditionally been viewed as a way to quantify the states of the sympathetic and parasympathetic branches of the autonomic nervous system (ANS), since both branches of the ANS converge at the sinoatrial (SA) node and convey oscillatory signals to the heart (Malliani, Lombardi et al. 1994). This type of mechanistic interpretation of HRV data has long been a contentious

issue (Eckberg 1997); however, broad inferences about autonomic activity are still commonly made from HRV data, due in large part to the difficulty of more directly measuring autonomic activity (Scheff, Mavroudis et al. in press). Analysis of HRV data aimed at diagnostic and prognostic applications is appealing because of the noninvasive nature of HRV assessment and the apparent correlation between HRV depression, *i.e.*, loss of HR variability, with disease severity and poor clinical outcomes (Garrard, Kontoyannis et al. 1993; Piepoli, Garrard et al. 1995; Annane, Trabold et al. 1999; Korach, Sharshar et al. 2001; Barnaby, Ferrick et al. 2002; Tateishi, Oda et al. 2007). In particular, dysregulation of autonomic signaling is seen as a critical component in the progression of inflammation-linked disorders like sepsis (Annane, Trabold et al. 1999; Schmidt, Werdan et al. 2001), which has motivated research on inflammation and HRV. However, there is still a limited understanding of the precise mechanistic links between inflammation and HRV, which limits the clinical uses of HRV metrics and the potential knowledge gained from HRV analysis (Dick, Molkov et al. 2012; Scheff, Mavroudis et al. 2012).

Due to the significant challenges remaining in understanding the underlying mechanistic basis of the inflammatory response in general, there has been extensive work on experimental models of systemic inflammation such as the human endotoxemia model (Lowry 2005). Elective administration of bacterial endotoxin (LPS) to otherwise healthy human volunteers serves as a useful model of TLR4 agonist-induced systemic inflammation, providing a reproducible experimental platform tying systemic inflammation to physiological signal generation (Lowry 2005; Lowry 2009). Low doses of LPS given to humans elicit neuroendocrine, hemodynamic, and leukocyte

transcriptional responses that reproduce, in part, those seen after acute injury and systemic inflammation (Lowry 2005; Andreasen, Krabbe et al. 2008; Lowry 2009; Shanker, Coyle et al. 2010), including a reduction in HRV (Godin, Fleisher et al. 1996; Lowry 2005; Rassias, Holzberger et al. 2005; Alvarez, Katsamanis Karavidas et al. 2007; Jan, Coyle et al. 2009; Haimovich, Calvano et al. 2010; Jan, Coyle et al. 2010). Thus, human endotoxemia experiments represent a platform for the analysis of relationships between inflammation, autonomic dysfunction, and changes in HRV(Scheff, Mavroudis et al. 2012) . While a number of studies have explored the effect of endotoxemia on HRV as well as other metrics of autonomic function (Godin, Fleisher et al. 1996; Rassias, Holzberger et al. 2005; Alvarez, Katsamanis Karavidas et al. 2007; Sayk, Vietheer et al. 2008; Jan, Coyle et al. 2009; Jan, Coyle et al. 2010; Lehrer, Karavidas et al. 2010; Kox, Ramakers et al. 2011; Rassias, Guyre et al. 2011; Scheff, Mavroudis et al. 2011), careful experimental design and analysis is required to interpret results and coherently build a conceptual framework linking inflammation with autonomic dysfunction (Scheff, Mavroudis et al. 2012; Scheff, Mavroudis et al. 2012). It is important to extract the maximal amount of information from experiments while understanding their limitations and the scope of remaining unknowns. For instance, while changes in HRV metrics are often cited as evidence for changes autonomic function, the underlying physiological complexity makes such conclusions difficult (Eckberg 1997). If alternative hypotheses can equally plausibly explain experimental observations, then further investigations are required for a more complete understanding; but if this is not appreciated, then scientific progress will be impeded. In this respect, a mathematical model can serve as a framework

allowing for the rationalization of experimental results and the elucidation of deeper meaning (Ottesen 2011).

In this section, we study models describing the relationship between the autonomic nervous system and patterns of heart beats. These models incorporate mechanisms that govern the relationship between autonomic activity and HRV, such as high frequency autonomic oscillations, binding kinetics of neurotransmitters to receptors at the SA node, changes in mean levels of autonomic activity, and inflammation-induced uncoupling between the heart and the autonomic nervous system. We analyzed these models first to illustrate the complexity inherent in inferring autonomic function from HR and HRV data alone and how even simple assumptions about cardiac autonomic modulation can lead to unintuitive results. We then investigated the human endotoxemia response in particular by leveraging our models to explain and rationalize experimental observations. The unintuitive relationships between autonomic signaling and HRV play a role in explaining the effect of the cholinergic anti-inflammatory pathway on the inflammatory response. Furthermore, by combining experimental data with model analysis, we concluded that significant uncertainty remains in the general function of the autonomic nervous system, even in a very controlled experimental model like human endotoxemia. Multiple plausible patterns of autonomic changes could be leading to the observed responses (increased HR, decreased HRV, uncoupling between the autonomic nervous system and the heart) and it is important to properly interpret what is learned from experiments measuring HRV.

4.2.2: Methods

HRV arises largely due to oscillations in autonomic activity which are apparent in the power spectrum of RR intervals primarily in two frequency bands termed low frequency (LF, 0.04-0.15 Hz) and high frequency (HF, 0.15-0.4 Hz) (Task 1996). A model to evaluate the relationship between the autonomic nervous system and the beating of the heart requires, at a minimum, four components, as shown in Figure 4.11: (1) a representation of sympathetic activity; (2) a representation of parasympathetic activity; (3) a combination of sympathetic and parasympathetic activities, representing autonomic modulation of the SA node; (4) a method to convert this autonomic modulation into heart beats, which can then be analyzed through the application of HRV metrics, as we have previously demonstrated in (Scheff, Mavroudis et al. 2011).

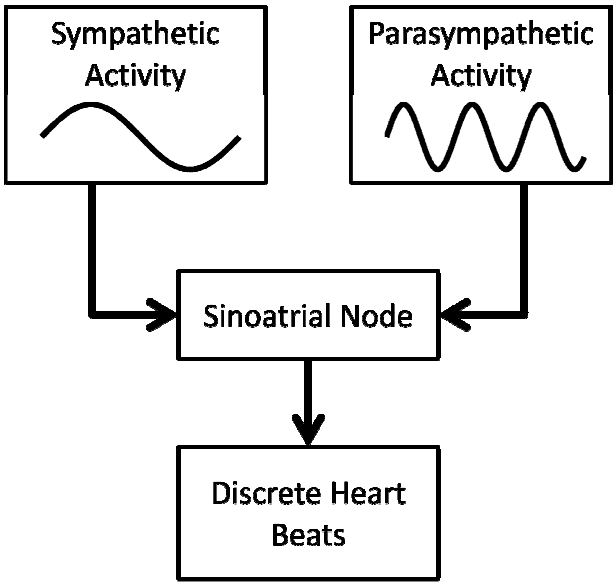

Figure 4.11: Components of the models linking autonomic activity with heart beats shown in Eq. 4.4 and Eq. 4.5. Sympathetic and parasympathetic nerves impose oscillatory activation of the sinoatrial (SA) node, leading to variability in discrete heart beats.

A simple model including these four components was earlier investigated by Brennan *et al*. in an attempt to gain insight into the relationship between autonomic

signaling and Poincaré plots of RR intervals (Brennan, Palaniswami et al. 2002). Chiu *et al*. analyzed a slightly more complex model that accounts for some of the signal transduction steps between the release of autonomic neruotransmitters and the regulation of SA node activity (Chiu and Kao 2001; Chiu, Wang et al. 2003). The goal was to investigate the relationship between autonomic inputs, such as oscillating frequency and mean levels of autonomic outputs, and the beating of the heart. Eq. 4.4 shows a general example of this type of model structure.

$$nor = m_{nor} + a_{nor} \cdot sin(\omega_{nor} \cdot t) \tag{4.4a}$$

$$ach = m_{ach} + a_{ach} \cdot sin(\omega_{ach} \cdot t) \tag{4.4b}$$

$$m(t) = k_{icpm} + k_{nor} \cdot nor - k_{ach} \cdot ach \tag{4.4c}$$

$$I = \int_{t_k}^{t_{k+1}} m(t)dt \tag{4.4d}$$

The variables *nor* and *ach* represent norepinephrine and acetylcholine, neurotransmitters released by the sympathetic and parasympathetic nerves respectively which modulate the beating of the heart. Each of these variables has a mean level m_k as well as an oscillatory component with amplitude a_k and frequency ω_k. These sinusoids represent the underlying LF and HF signals apparent in HRV data. In reality, oscillations at other time scales are also present, such as circadian rhythms, but the analysis presented here focuses only on a short time scale so these much higher frequency rhythms are not included. The two autonomic variables are linearly combined to produce *m(t)*, the autonomic modulation of the SA node. This equation also includes the parameter k_{icpm} to account for the intrinsic cardiac pacemaker function in the absence of autonomic signaling. Sympathetic activity increases *m(t)* and parasympathetic activity decreases *m(t)*. Then, Eq. 4.4d defines an integral pulse frequency modulation (IPFM) model,

which consists of the repeated integration of *m(t)* up to a threshold *I*. Whenever this threshold is reached, it represents a heartbeat. Thus, the differences between successive firings of the IPFM model constitute RR intervals. It is important to note that, while Eq. 4.4d models the SA node as a single cell when in reality it is a cluster of cells, this assumption matches well with experimental data on the high-level function of the SA node (Dexter, Levy et al. 1989; Pyetan and Akselrod 2003).

However, there is an obvious drawback to these kinds of linear models: they do not account for nonlinearity in the effects of autonomic activity on the heart. Although there are clearly myriad complexities of physiology not embodied by Eq. 4.4, possibly the most significant issue is that any change in the autonomic inputs proportionally produces a change in *m(t)* regardless of the state of the system; for instance, repeatedly increasing *nor* will lead to faster and faster HRs with no upper bound. Of course, autonomic modulation of the heart does not simply linearly reflect autonomic signaling; as is typical in physiology, saturation introduces an upper bound on the response of the heart (Saul 1990; Goldberger, Challapalli et al. 2001). Considering the model in Eq. 4.4, increases in mean sympathetic activity (*i.e.* increases in m_{nor}) will produce corresponding increases in HR, even going well beyond what is physiologically possible. Furthermore, oscillations in autonomic activity will always be equally transduced to the SA node, regardless of the mean levels of oscillations. Saturation of autonomic modulation of the SA node destroys the linearity that facilitates those behaviors in the model. An expanded version of Eq. 4.4, including saturation effects, is shown in Eq. 4.5.

$$nor = m_{nor} + a_{nor} \cdot sin(\omega_{nor} \cdot t) \quad (4.5a)$$

$$ach = m_{ach} + a_{ach} \cdot sin(\omega_{ach} \cdot t) \quad (4.5b)$$

$$adr = \frac{nor}{k_{nor,1} + k_{nor,2} \cdot nor} \tag{4.5c}$$

$$cho = \frac{ach}{k_{ach,1} + k_{ach,2} \cdot ach} \tag{4.5d}$$

$$m(t) = k_{icpm} + k_{adr} \cdot adr - k_{cho} \cdot cho \tag{4.5e}$$

$$I = \int_{t_k}^{t_{k+1}} m(t)dt \tag{4.5f}$$

Eq. 4.5 is largely the same as Eq. 4.4, except that a saturation function appears between each neurotransmitter and the SA node, representing binding of norepinephrine to adrenergic receptors (*adr*, Eq. 4.5c) and acetylcholine to cholinergic receptors (*cho*, Eq. 4.5d). Although autonomic neurotransmitters do act primarily through binding to receptors and a finite number of receptors does imply that saturation will occur at some point, conceptually the model structure would be the same for any type of similar saturation occurring upstream of the SA node. These saturation functions limit the range of potential HR responses to autonomic signaling.

Eq. 4.4 contains 9 parameters and Eq. 4.5 contains 13 parameters. Given that these parameters are generally not known and that the majority of insights derived from these theoretical models are qualitative and independent of specific parametrizations, the simulations below were performed with all parameters set to 1, with the following exceptions: the frequencies of autonomic oscillations were set to the mean values of the standard LF and HF ranges, 0.095 Hz and 0.275 Hz respectively; and the amplitudes of oscillations a_{nor} and a_{ach} were both set to 0.25, as if they were 1 then some simulations would result in $m(t)$ becoming negative. Scenarios where specific parametrizations of the model may become important are discussed in more detail in subsequent sections.

Frequency domain HRV metrics were calculated by estimating the power spectrum of RR intervals with MATLAB's `fft` function and finding the area under the curve over the LF (0.04-0.15 Hz) and HF (0.15-0.4 Hz) frequency bands.

4.2.3: Results

4.2.3.1: HRV as a Function of Autonomic Activity

Two features of the models in Eq. 4.4-4.5 contribute to a relationship between mean levels of autonomic activity and HRV. First, there is an effect related to the magnitude of the inputs to an IPFM model, as illustrated in Figure 4.12. As $m(t)$ increases and thus heart beats become faster, variability decreases because successive intervals are more similar due to their closeness relative to the frequency of oscillations in $m(t)$. This means that perturbations that tend to increase $m(t)$, such as increased sympathetic activity or decreased parasympathetic activity, suppress HRV while changes in the opposite direction lead to more variability. Second, the inclusion of saturation, which only appears in the nonlinear model in Eq. 4.5, plays an important role in evaluating the relationship between mean autonomic activity and transduction of oscillatory signals through an IPFM model, as shown in Figure 4.13. Increased mean values of sympathetic or parasympathetic activities leads to blunted oscillations in their corresponding neurotransmitters downstream due to saturation, thus leading to lower HRV.

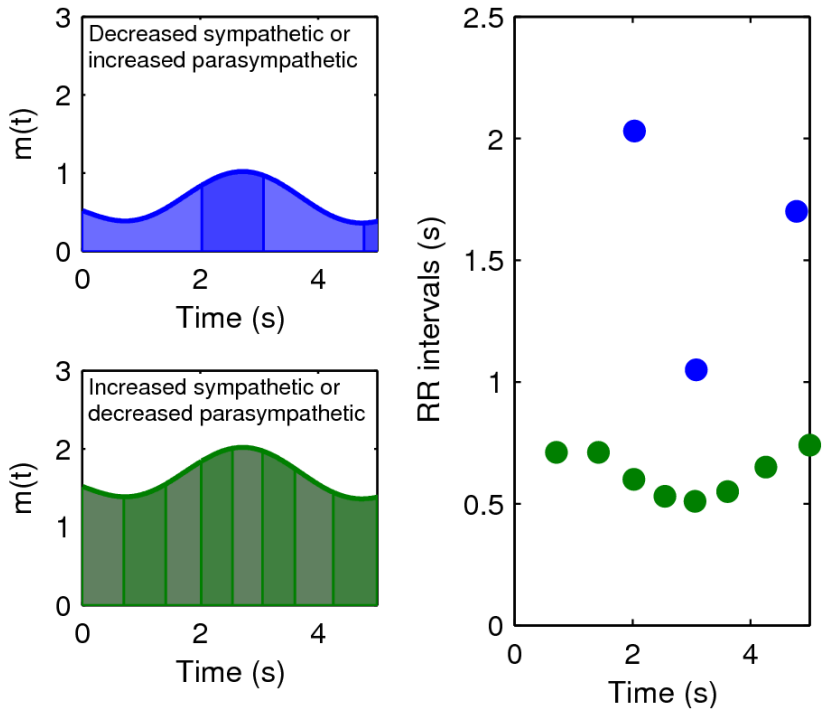

Figure 4.12: Relationship between mean HR and HRV. Holding all parameters in Eq. 4.4 constant except the mean sympathetic activity m_{nor} produces the blue (m_{nor} = 0.5) and green (m_{nor} = 1.5) curves on the left, with the gray curve having higher values of $m(t)$. Because sympathetic and parasympathetic are combined additively in the linear model, these are equivalent to setting m_{ach} to 1.5 and m_{ach} to 0.5, respectively. Increasing the mean of $m(t)$ produces higher HR (shorter RR intervals) as well as decreased variability, as all of the integrals (highlighted areas under the curves on the left) are over more similar time ranges.

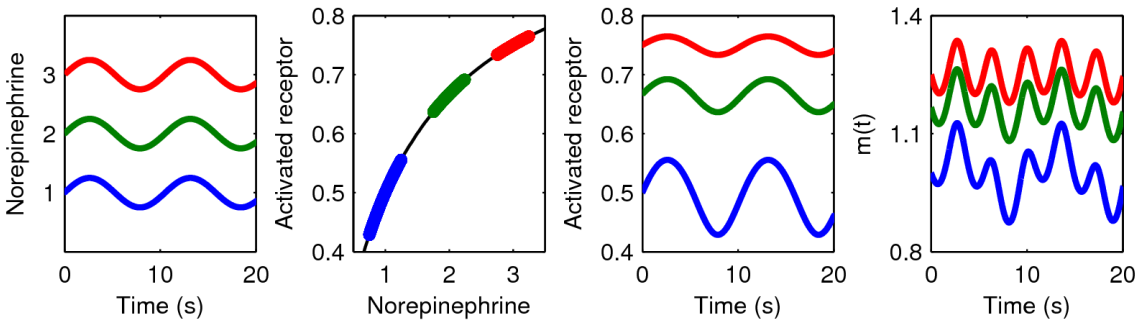

Figure 4.13: Three sinuosoids with identical amplitudes and different means representing different norepinephrine profiles (Eq. 4.5a) pass through a saturation function representing the binding of norepinephrine to a finite number of adrenergic receptors (Eq. 4.5c), producing significantly different oscillatory amplitudes. The higher values experience more of the saturation effect, blunting oscillations in the output. This ultimately leads to differences in the variability of autonomic stimulation of the SA node, $m(t)$ (Eq. 4.5e). In the linear model of Eq. 4.4, there is no saturation function and thus the inputs and outputs would have the same amplitudes.

For the linear model (Eq. 4.4), only the first mechanism plays a role, and thus Table 4.3 and Figure 4.14 show a direct relationship between the mean value of $m(t)$ and HRV. For the nonlinear model, both mechanisms are active, and under different regimes of autonomic signaling these two effects can be either cooperative or competitive, as shown in Table 4.3 and Figure 4.14. In the case of changing mean sympathetic activity, the two effects are cooperative. Increased mean sympathetic activity leads to smaller RR intervals as well as saturation-blunted amplitudes, which both decrease variability in IPFM output; the reverse is true for decreased mean sympathetic activity. However, the two effects are in opposition for parasympathetic activity. As mean parasympathetic activity increases, RR intervals grow longer and variability increases, but the saturation effect blunts parasympathetic oscillations and variability decreases. Thus, in the nonlinear model, HF power can either increase or decrease as parasympathetic activity increases,

depending on which effect predominates due to the particular parametrization of the model.

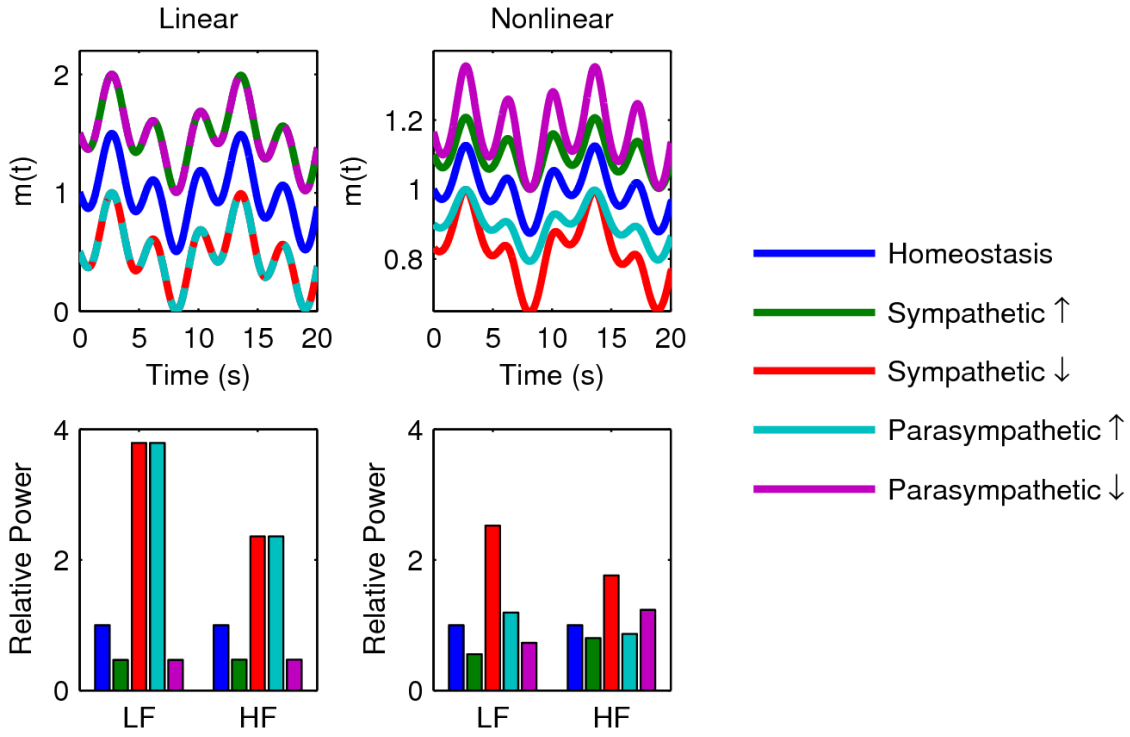

Figure 4.14: Relationship between changes in mean autonomic activity and changes in LF power and HF power for both the linear (Eq. 4.4) and nonlinear (Eq. 4.5) models. The LF and HF values show the changes produced by 50% increases/decreases in mean sympathetic/parasympathetic activities, scaled relative to homeostasis. For the linear model, increased sympathetic activity and decreased parasympathetic activity both decrease LF and HF, while decreased sympathetic activity and increased parasympathetic activity both increase LF and HF; the magnitude of these changes in *m(t)* is identical, which is reflected by the overlapping dashed lines. For the nonlinear model, the same directional relationships hold of LF, although changes in sympathetic activity produce larger magnitude changes in LF. These relationships also hold for the response of LF to changes in parasympathetic activity. However, depending on the parametrization of the model, a change in parasympathetic activity can either increase or decrease HF. These differences between the two models are due to the competing effects of the two mechanisms driving changes in LF and HF as mean autonomic levels change.

	Linear model	**Nonlinear model**

Perturbation	ΔHR	ΔLF	ΔHF	ΔLF	ΔHF
Increase mean sympathetic activity	↑	↓	↓	↓↓	↓
Decrease mean sympathetic activity	↓	↑	↑	↑↑	↑
Increase mean parasympathetic activity	↓	↑	↑	↑	?
Decrease mean parasympathetic activity	↑	↓	↓	↓	?

Table 4.3: Relationship between changes in mean autonomic activity and changes in mean HR size, LF power, and HF power. Results are shown for both the linear (Equation 1) and nonlinear (Equation 2) models (ΔHR is the same for both models). Up and down arrows represent increases and decreases. Two arrows represent a larger magnitude change, due to the cooperativity of both mechanisms for amplitude changes in the nonlinear model. A question mark represents an uncertain change, due to the two mechanisms working in opposite directions and thus leading to either and increase or decrease depending on the parametrization of the model.

While these results only consider the effect of changing mean sympathetic or parasympathetic activities while holding oscillatory amplitudes constant, Appendix B considers the case where mean value and amplitude are proportional.

4.2.3.2: Autonomic Function in Human Endotoxemia

In human endotoxemia, consistent patterns in HR and HRV have been observed across several different experiments. HR increases while metrics of HRV, including LF and HF powers, decrease (Godin, Fleisher et al. 1996; Rassias, Holzberger et al. 2005; Alvarez, Katsamanis Karavidas et al. 2007; Sayk, Vietheer et al. 2008; Jan, Coyle et al. 2009; Jan, Coyle et al. 2010; Lehrer, Karavidas et al. 2010; Kox, Ramakers et al. 2011; Rassias, Guyre et al. 2011; Scheff, Mavroudis et al. 2011). Considering the results in Table 4.3, this is in line with what would be expected to occur from stimuli leading to increased HR, such as increased sympathetic activity and/or decreased parasympathetic activity (Scheff, Mavroudis et al. 2011). This type of unbalanced autonomic response, leading to sympathetic predomination and thus increased HR and LF/HF ratio, represents a conventional wisdom that pervades the literature. Another key feature observed in

human endotoxemia is uncoupling between the autonomic nervous system and the heart, such that induced changes in autonomic activity during endotoxemia fail to produce corresponding changes in the output of the heart (Sayk, Vietheer et al. 2008).

Three hypothetical scenarios for autonomic function giving rise to these observed patterns of HR, HRV, and uncoupling in human endotoxemia are shown in Figure 4.15, along with a homeostatic case for comparison. These scenarios represent different levels of autonomic activity (by altering m_{nor} and m_{ach}), receptor-level regulation and coupling between the autonomic nervous system and the heart (by altering k_{adr} and k_{cho}), and non-autonomic influences on HR (by altering k_{icpm}), all producing similar outputs in terms of HR and HRV:

1. **Homeostasis**. The nominal parameter values given in the Methods section were used to create a reference simulation.
2. **Endotoxemia mechanism 1**. Sympathetic and parasympathetic activities increase (m_{nor} = 10 and m_{ach} = 5) leading to blunted oscillations due to saturation as in Figure 4.13. Sympathetic activity predominates ($k_{ach,2}$ = 1.5) resulting in increased HR.
3. **Endotoxemia mechanism 2**. Sympathetic activity increases (m_{nor} = 10), resulting in increased HR and decreased LF rhythms. Diminished autonomic sensitivity at the SA node (k_{adr} = 0.5 and k_{cho} = 0.5) further reduces both LF and HF. In this scenario, parasympathetic activity can either increase or decrease, but the results shown in Figure 4.15 are for decreased parasympathetic activity (m_{ach} = 0.5).

4. **Endotoxemia mechanism 3**. Autonomic activity is largely uncoupled from the SA node (k_{adr} = 0.5 and k_{cho} = 0.5), resulting in decreased HRV. HR increases due to non-autonomic factors (k_{icpm} = 1.4). In this scenario, autonomic activities can change in either direction, but the results shown in Figure 4.15 are for decreased sympathetic activity (m_{nor} = 0.5) and increased parasympathetic activity (m_{ach} = 5).

Furthermore, Appendix B illustrates how, even after significantly changing the assumptions that give rise to Eq. 4.5, these three scenarios depicted in Figure 4.15 continue to reproduce changes in HR, HRV, and uncoupling similar to what has been observed in human endotoxemia experiments.

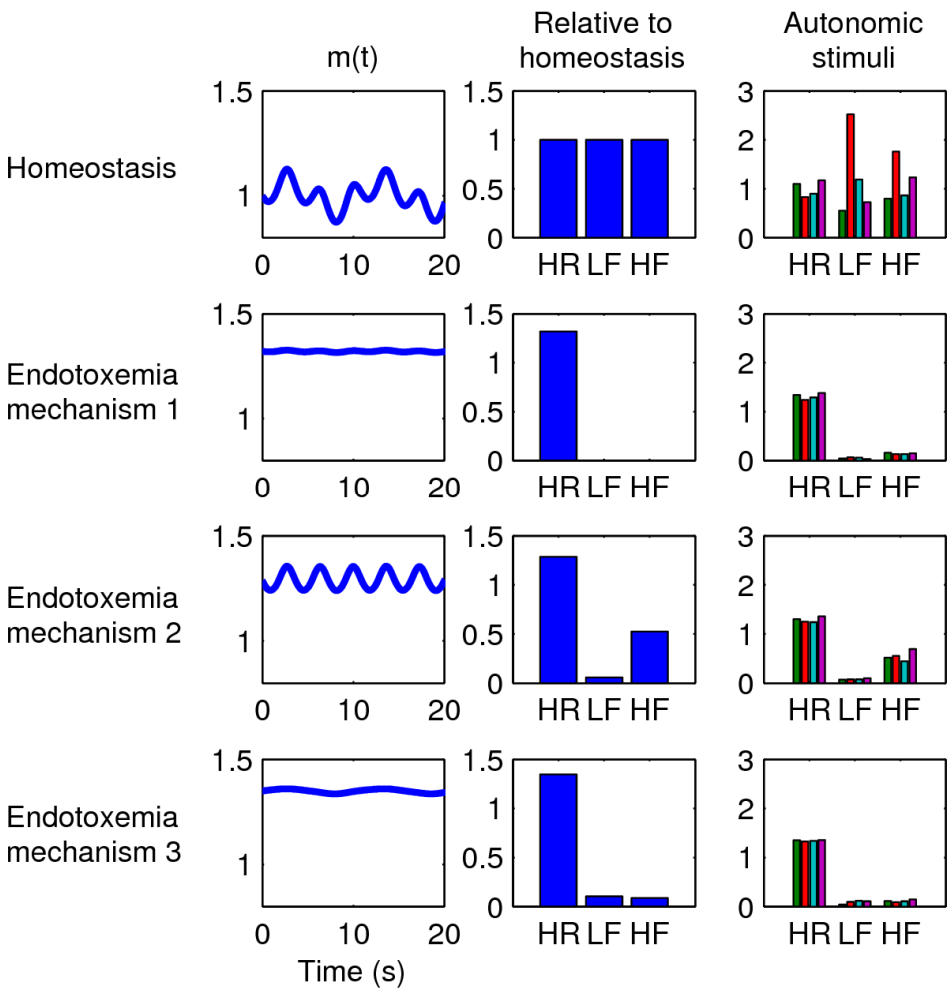

Figure 4.15: Mechanisms for HR/HRV changes in endotoxemia. Each row represents a different simulation. The $m(t)$ column shows the autonomic modulation of the heart as defined in Eq. 4.5e based on the oscillations shown in the first two columns. The "Relative to homeostasis" column shows how HR, LF, and HF changed relative to homeostatic values in the first row. In all cases relative to homeostasis, HR increases while LF and HF decrease; the specific magnitudes of these changes (*i.e.* how much HR increases, etc.) can be tuned by the parameters of the model. The "Autonomic stimuli" column shows how HR, LF, and HF respond to 4 perturbations (as in Figure 4.14: increased sympathetic activity 50%, decreased sympathetic activity 50%, increased parasympathetic activity 50%, and decreased parasympathetic activity 50%, respectively) to quantify the level of uncoupling between the autonomic nervous system and the heart, again shown relative to homeostatic values. Uncoupling is indicated by relative insensitivity to autonomic stimuli. **First row**: homeostasis. **Second row**: endotoxemia mechanism

1, where sympathetic and parasympathetic activities increase and saturation of receptors leads to uncoupling. **Third row**: endotoxemia mechanism 2, where sympathetic activity increases, parasympathetic activity decreases (or increases), and uncoupling is due to a loss of sensitivity of the heart to autonomic stimuli. **Fourth row**: endotoxemia mechanism 3, where autonomic activities are uncoupled from the heart due to a loss of sensitivity but non-autonomic factors still increase HR.

4.2.4: Discussion

Although traditionally LF oscillations were seen as reflecting sympathetic activity and HF oscillations representing parasympathetic activity, spectral analysis truly quantifies the amplitudes of oscillations at certain frequencies, not their mean values (Saul 1990; Akselrod 1995; Eckberg 1997). In other words, LF and HF powers most closely reflect a_{nor} and a_{ach} in Eq. 4.5a-b rather than m_{nor} and m_{ach}. This is a critical point, as LF and HF powers do not directly represent mean autonomic activities; instead they reflect the amount of oscillations on top of these mean levels. Furthermore, it is generally the mean values that are of interest, rather than the oscillatory amplitudes, but there is not a one-to-one correspondence between the amplitude of oscillations in inputs to the IPFM model and variability in generated heart beat intervals. Niklasson *et al*. found that HRV analysis based on RR intervals reveals a negative correlation between HR and HRV in both homeostatic experimental data as well as in a theoretical IPFM model (Niklasson, Wiklund et al. 1993), as is described in Figure 4.12. This was more thoroughly investigated by Chiu *et al*., revealing that autonomic perturbations that increase HR (increased sympathetic activity or decreased parasympathetic activity) tend to decrease both LF and HF powers, while perturbations that decrease HR (decreased sympathetic activity or increased parasympathetic activity) have the opposite effect (Chiu and Kao 2001; Chiu, Wang et al. 2003). The results of Niklasson *et al*. and Chiu *et al.* roughly

correspond to the results for the linear model (Eq. 4.4) shown here in Table 4.3 and Figure 4.14. These results clearly illustrate how conventional wisdom about the physiological interpretation of frequency domain HRV metrics does not necessarily correspond with the basic mechanisms by which the ANS regulates the heart, as even under the very simplistic assumptions of the linear model, the relationship between autonomic activity and LF and HF powers is contrary to conventional wisdom.

The nonlinear model (Eq. 4.5) is still fairly simple, yet adds even more complexity to the relationship between autonomic activity and HRV. Pyetan *et al*. studied this issue specifically for the parasympathetic branch alone (Pyetan, Zoran et al. 2001; Pyetan and Akselrod 2003; Pyetan and Akselrod 2004) and also found complex relationships between autonomic inputs and HRV. In total, what we learn from these simple modeling studies in isolation is that changes in HRV can be difficult to interpret, as changes in even basic assumption can have significant impacts on the results (see the differences between the linear and nonlinear models in Table 4.3 and Figure 4.14).

These challenges in interpretation are important in experimental settings such as human endotoxemia, where HRV analysis is applied in attempts to gain insight into autonomic dysfunction in systemic inflammation. For instance, consider the cholinergic anti-inflammatory pathway, a key link between the ANS and the immune system (Pavlov, Wang et al. 2003; Huston and Tracey 2011). Parasympathetic afferent sensory fibers are activated in response to inflammation, leading to not only the central release of hormones, but also efferent parasympathetic activity which exerts an anti-inflammatory effect through acetylcholine signaling. Based on the view that HF power reflects parasympathetic activity, some have deemed it paradoxical that HF power and other

correlated HRV metrics are so significantly suppressed in endotoxemia (Fairchild, Srinivasan et al. 2011; Gholami, Mazaheri et al. 2012). Fairchild *et al*. addressed this issue at least in part by identifying transient increases in HRV mediated by parasympathetic signaling in response to a variety of different bacterial infections in mice (Fairchild, Srinivasan et al. 2011). However, this does not necessarily explain scenarios like human endotoxemia where no such transient increase in HRV is observed, and instead there is only a decrease in HRV until homeostasis is restored.

Thinking in terms of the nonlinear model presented in Eq. 4.5 presents an alternative explanation as to the effect of the cholinergic anti-inflammatory pathway on HRV. An increase in parasympathetic signaling can lead to either increased or decreased HF power depending on the particular situation, as illustrated in Table 4.3 and Figure 4.14. Therefore, there is no theoretical disconnect between heightened parasympathetic signaling and decreased HF power and HRV in general. This is fundamentally due to HF power reflecting the oscillatory amplitude rather than the mean level of parasympathetic activity, thus making the cholinergic anti-inflammatory response only indirectly linked to HRV, such as through the model shown in Eq. 4.5. And in reality, physiology is much more complex than Eq. 4.5, thus presenting even more opportunities for deviation from the normally-assumed relationship between HF and parasympathetic activity.

The concept of uncoupling, the loss of interorgan communication, is also important in the context of systemic inflammation, as it has long been hypothesized to play a critical role in disease progression (Godin and Buchman 1996) and changes in variability metrics such as HRV have been proposed as metrics for uncoupling (Pincus 1994; Godin, Fleisher et al. 1996). Clinically, similar quantification of uncoupling has

been shown to be a marker of disease severity in patients with multiple organ dysfunction syndrome (Schmidt, Muller-Werdan et al. 2004). The most thorough investigation of the autonomic nervous system in human endotoxemia was performed by Sayk *et al*. through two novel experimental techniques: 1.) measuring muscle sympathetic nerve activity (MSNA) to directly quantify sympathetic activity in endotoxemia; and 2.) modulating blood pressure (BP) to quantify how BP-induced autonomic signaling is coupled to the heart in endotoxemia (Sayk, Vietheer et al. 2008). This produced two novel insights. They found that MSNA in the peroneal nerve is suppressed in endotoxemia, which is the opposite of what would have been expected based on changes in HR, and that the autonomic nervous system and the heart were effectively uncoupled in endotoxemia, as autonomic perturbations induced by changes in BP produced no significant effect on HR or HRV even as they significantly altered MSNA.

The fact that sympathetic output of the peroneal nerve is diminished in endotoxemia does not necessarily mean that sympathetic activity at the heart behaves similarly, as different parts of the sympathetic nervous system may respond differently. Thus, the conventional wisdom of increased sympathetic activity in endotoxemia discussed above could very well still be true. However, the striking uncoupling found between changes in BP and HR requires closer examination. One can imagine that saturation at some point in autonomic signaling pathways, such as defined in Eq. 4.5c-d, could explain a kind of uncoupling in that if the system was responding to very high levels of autonomic activity, such that further changes in autonomic activity were be blunted by the time they reached the SA node and thus were not reflected in the output of the heart. For the model in Eq. 4.5, this would only be possible to rationalize with

observations of increased HR and decreased HRV in endotoxemia if mean sympathetic and parasympathetic activities were either 1.) significantly elevated in endotoxemia (*e.g.* by increasing m_{nor} and m_{ach} in Eq. 4.5a-b) or if 2.) sensitivity to autonomic signaling was significantly decreased (*e.g.* by increasing the parameters in the denominators of Eq. 4.5c-d). The former is possible, particularly in light of the cholinergic anti-inflammatory response as discussed above. The latter is possible as well, as non-autonomic inflammatory mediators exert regulatory effects on the beating of the heart (Takayama, Yuhki et al. 2005; Zorn-Pauly, Pelzmann et al. 2007; Gholami, Mazaheri et al. 2012) and crosstalk between the sympathetic and parasympathetic activities can result in altered sensitivities to autonomic neurotransmitters (Pyetan and Akselrod 2003).

Additionally it is possible that 3.) the decrease in peroneal MSNA (Sayk, Vietheer et al. 2008) is matched by a decrease in sympathetic activity at the heart. Experiments in rats found that endotoxemia led to increased acetylcholine concentration and decreased norepinephrine concentration in the liver, lending further support to the hypothesis that sympathetic activity is diminished in endotoxemia (Huang, Wang et al. 2010). In this hypothetical regime, uncoupling between the autonomic nervous system and the heart (Sayk, Vietheer et al. 2008) would mask the effects of diminished sympathetic activity on HR, and the endotoxemia-induced increase in HR could be due to non-autonomic pathways (Takayama, Yuhki et al. 2005; Zorn-Pauly, Pelzmann et al. 2007; Gholami, Mazaheri et al. 2012). In terms of Eq. 4.5, this scenario would be equivalent to decreasing m_{nor} to simulate decreased sympathetic activity, decreasing k_{icpm} to simulate a non-autonomic increase in HR, and decreasing both k_{adr} and k_{cho} to represent uncoupling.

Distinguishing between these three mechanisms, as shown in Figure 4.15, requires novel experimental work to look more closely at the autonomic nervous system in human endotoxemia (Sayk, Vietheer et al. 2008). It is important that these issues are approached with an accurate mindset of what the analysis of heart beats can and cannot provide. Signal transduction from the autonomic nervous system to the heart is complex, nonlinear, unintuitive, and often misinterpreted. Simple mathematical models, as discussed here and elsewhere (Niklasson, Wiklund et al. 1993; Chiu and Kao 2001; Brennan, Palaniswami et al. 2002; Pyetan and Akselrod 2003), can elucidate issues related to the interpretation of HR and HRV data. Specifically in the literature related to human endotoxemia, overzealous interpretation of HR and HRV signals is common and may be impeding more fundamental understanding of autonomic function in systemic inflammation. All three hypothetical mechanisms discussed above also allow for the possibility that autonomic modulation of the heart may be substantially different than autonomic activity elsewhere in the body. While quantification of HR and HRV can provide valuable insight into a system, the extent of this insight depends on how well the specific underlying mechanisms in a specific scenario are known, so that physiologically important signals can be accurately identified and isolated.

Even the simple models discussed here illustrate some of the challenges in interpreting HRV data, despite the lack of such physiological elements as crosstalk between branches of the autonomic nervous system, redundant/complementary pathways, and closed loop autonomic control, to name just a few of the simplifications made here. Incorporating these further complexities into the conceptual picture makes the relationship between HRV and autonomic signaling even less clear. However, in a well-

characterized system where relationships between autonomic activity and HRV have been established experimentally within a specific context, changes in HF and LF powers may still be meaningful and may predictably reflect changes in autonomic signaling. Lacking that, it is difficult to draw mechanistic conclusions from HRV data, as exemplified by the competing mechanisms shown in Figure 4.15 that can all equally rationalize HRV changes in human endotoxemia. Proper understanding of the information content and interpretation of HRV data is important in accurately assessing experimental data; thus, these issues also influences the perceived state of knowledge about autonomic function in systemic inflammation. Therefore, it is important to keep this in mind in experimental design and interpretation as progress is made towards the goal of deciphering the function of the autonomic nervous system in systemic inflammation.

Chapter 5: Predicting Critical Transitions in a Model of Systemic Inflammation

5.1: Introduction

Clinical data can be viewed in the context of the physiological state space, where each physiological parameter represents a dimension and common conditions appear clustered together due to their shared physiological underpinnings (Buchman 1996). These clusters represent steady states, regions where physiological parameters tend to stay constant in the absence of some perturbation to push the system towards another steady state. From this perspective, there is great value in determining to which steady state a patient belongs and if they are likely to move to another steady state as time progresses and their condition evolves (Buchman 2010; Cohen 2012). In terms of a dynamical system, this is equivalent to identifying a forthcoming bifurcation that will lead to a transition from the current steady state to a new steady state. In general, the earlier the diagnosis, the better the outcome, and thus it is important to detect warning signals of deterioration as early as possible. For example, there are approximately 750,000 cases of sepsis leading to 200,000 deaths annually in the US (Angus, Linde-Zwirble et al. 2001) and earlier detection of sepsis leads to more effective treatment and improved clinical outcomes, including lower mortality (Ridley 2005)..

Identifying transitions between steady states of gradually changing dynamical systems is a problem with broad applications in many fields. For this reason, many prior studies have attempted to find markers of a system approaching a critical transition (Scheffer, Bascompte et al. 2009; Dakos, Carpenter et al. 2012). The general concept behind techniques for identifying critical transitions is that, as a dynamical system

approaches a bifurcation, characteristic patterns emerge in the output of the system due to the underlying mathematical structures. For instance, the responses of a system to random deviations from its steady state may become slower as the loss of stability is approached, a phenomenon known as “critical slowing down”. Statistically identifying hallmarks of deteriorating stability has yielded impressive results in some instances (Carpenter, Cole et al. 2011), but applications in physiology and medicine have been rare (Venegas, Winkler et al. 2005; Mormann, Andrzejak et al. 2007; Chen, Liu et al. 2012) likely due to most clinical measurements being relatively low frequency and noisy while the statistical identification of critical transitions traditionally relies on large amounts of data. This has been somewhat assuaged by the advent of modern clinical and experimental techniques, including such technologies as microfluidics and high-throughput transcriptional screening, but the large-scale collection of most physiological data remains invasive and expensive, and thus researchers and clinicians typically remain data-limited. With this in mind, techniques to identify transitions based on limited data are required for physiological applications.

Lade and Gross recently proposed a novel technique for the identifications of critical transitions (Lade and Gross 2012). Rather than taking a purely statistical approach, they considered the possibility of improving performance by leveraging additional information about the system in question, namely knowledge of its network structure. While detailed models with perfectly identified parameter values are rare, often some very general principles are well established. By using data to numerically estimate the stability of a simple high-level model of a system, Lade and Gross tracked changes in stability over time as new data streamed in. This model-based approach produced

intriguing results suggesting that it allows for the robust prediction of forthcoming transitions based on sparser data than prior statistical approaches, making it an ideal candidate for evaluating physiological systems. However, application of Lade and Gross's approach still requires significant assumptions about the measurability of internal components of the system (such as production and degradation rates), the structure of the system, or both, which may not be feasible in practice.

In this chapter, we propose an approach for identifying critical transitions and apply it to a model of systemic inflammation that moves between steady states due to a progressing bacterial infection. Based on a combination of data and some high-level knowledge of the system's network structure, a metric was derived to serve as a warning signal of abrupt transitions between steady states before the state variables begin their trajectories to the new steady state. Intervention to remove the inflammatory instigator proved successful in restoring homeostasis when performed after the warning signal became elevated, but was unsuccessful in this task when initiated later, after the system was already visibly on its trajectory towards a heightened inflammatory state. Critically, this approach requires a minimal amount of assumptions about the availability of data and the structure of the system while still retaining predictive power. Successful translation of the identification of transitions to clinical practice could have a transformational impact on healthcare, and this work represents a step towards that goal.

5.2: Methods

5.2.1: Generalized Modeling

The study of physiological systems is hindered by both limited data and limited mechanistic knowledge. These practical limitations necessitate the use of analytical

methods designed to function in the presence of significant uncertainty. One such approach is generalized modeling (Gross and Feudel 2006; Kuehn, Siegmund et al. 2012). A generalized model is a system of equations representing interactions between variables based only on *placeholder functions*, which represent the connectivity between equations without making any assumptions about specific functional forms or parametrizations that all correspond to the same network structures.

Although generalized models cannot simply be simulated forward to study a system because the placeholder functions are not explicitly defined mathematical functions, insights can still be drawn from the analysis of generalized models. For example, stability of a steady state can be quantified by calculating the eigenvalues of the Jacobian matrix, a local linearization of the system (Gross and Feudel 2006; Kuehn, Siegmund et al. 2012). The Jacobian matrix of a generalized model can be estimated in terms of partial derivatives of placeholder functions. If sufficient data is available, then those partial derivatives can be numerically estimated, and then stability of a system can be assessed without ever assuming any further properties of the system, such as the specific functional forms of the placeholder functions. In a system that is gradually approaching a critical transition, characteristic patterns often arise in the eigenvalues of the Jacobian matrix when a bifurcation occurs. This type of analysis can produce warning signals of an impending critical transition because changes in these eigenvalues often occur before the transition would be otherwise apparent from monitoring the state variables alone (Kuehn 2011; Lade and Gross 2012). Thus, if the dynamics of the system are reflected in the generalized model, then stability analysis of the generalized model may produce a quantifiable warning signal of critical transitions (Lade and Gross 2012).

5.2.2: Human Endotoxemia as a Model of Systemic Inflammation

As in the preceding chapters, we consider human endotoxemia as a model of systemic inflammation. The underlying model used here is as defined in Appendix A, except that we studied this system in the presence of a gradually-increasing inflammatory load, mimicking a growing bacterial infection, by assuming linear growth with time in the production rate of LPS. Due to a positive feedback loop in the pro-inflammatory response (P), this model is bistable, with one steady state representing healthy homeostasis with low levels of inflammatory mediators, and the other steady state exhibiting heightened levels of inflammatory mediators that persist even when LPS is completely removed. As the bacterial load gradually increases, the system enters a slowly changing intermediate state followed by an abrupt transition to the heightened inflammatory state, as shown in Figure 5.1. If it were possible to perfectly model the inflammatory response and identify all model parameters, then that ideal model could be used to reliably predict future transitions. Instead, we use this model as a source of data and evaluate the ability of generalized models of systemic inflammation to predict critical transitions.

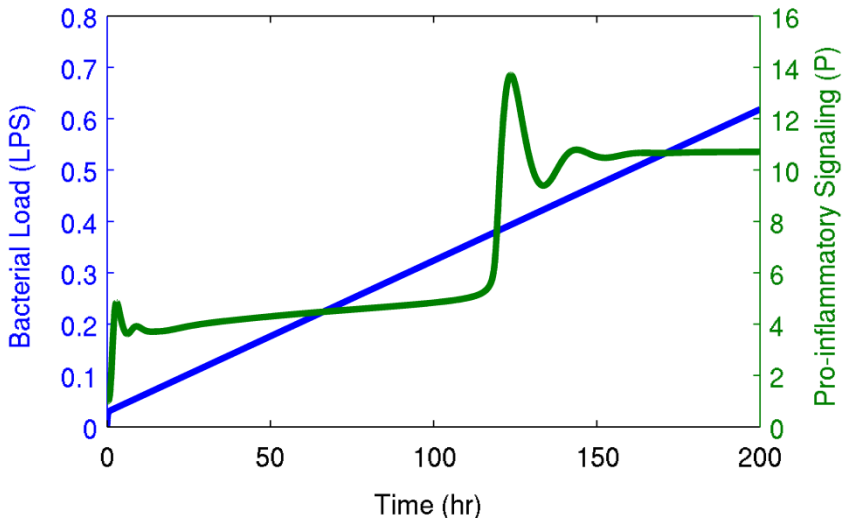

Figure 5.1: Transition between steady states in chronic inflammation. A gradually increasing bacterial load (LPS) produces an abrupt transition from a gradually-changing intermediate state to a heightened persistent inflammatory state. This transition is shown in the pro-inflammatory signaling variable (P), but it is equally apparent in other components of the system.

5.2.3: Generalized Modeling of Systemic Inflammation

In many respects, a generalized model can be considered to be a mathematical representation of a network diagram, encoding only the components of a system, connections between components, and the directionalities of connections. However, in the context of stability analysis, this network must be relatively simple; otherwise, the number of partial derivative estimates will grow to require an unreasonable volume of data. Therefore, a complex system must be reduced to a limited number of motifs to be represented in a generalized model. In systemic inflammation, key motifs include an injury or pathogen stimulating a pro-inflammatory response; the antagonistic relationship between pro- and anti-inflammatory mediators; and the positive feedback between tissue damage and pro-inflammatory signaling (Vodovotz, Constantine et al. 2009). These motifs are all represented in the model shown in Figure 5.2. Lipopolysaccharides (LPS) stimulate the pro-inflammatory transcriptional response (P), which then activates both

central immunomodulatory mechanisms (such as the release of cortisol, F) and peripheral transcriptional responses (A), which both serve to suppress pro-inflammatory activity. Generalized models, listed in Figure 5.2B, were constructed as high-level representations of systemic inflammation based on these critical motifs present in the systemic inflammatory response. A variety of models were constructed to more broadly assess performance, as the reduction of a large network to represent a limited number of motifs includes some degree of qualitative analysis. The generalized models evaluated here are those made up of anti- and pro-inflammatory signaling (A-P), cortisol and pro-inflammatory signaling (F-P), either of those models plus LPS (A-LPS-P and F-LPS-P), and all four variables together (A-F-LPS-P). These five models represent every combination of A, F, LPS, and P that include both negative feedback (between P and either A or F) and positive feedback (in the equation for P).

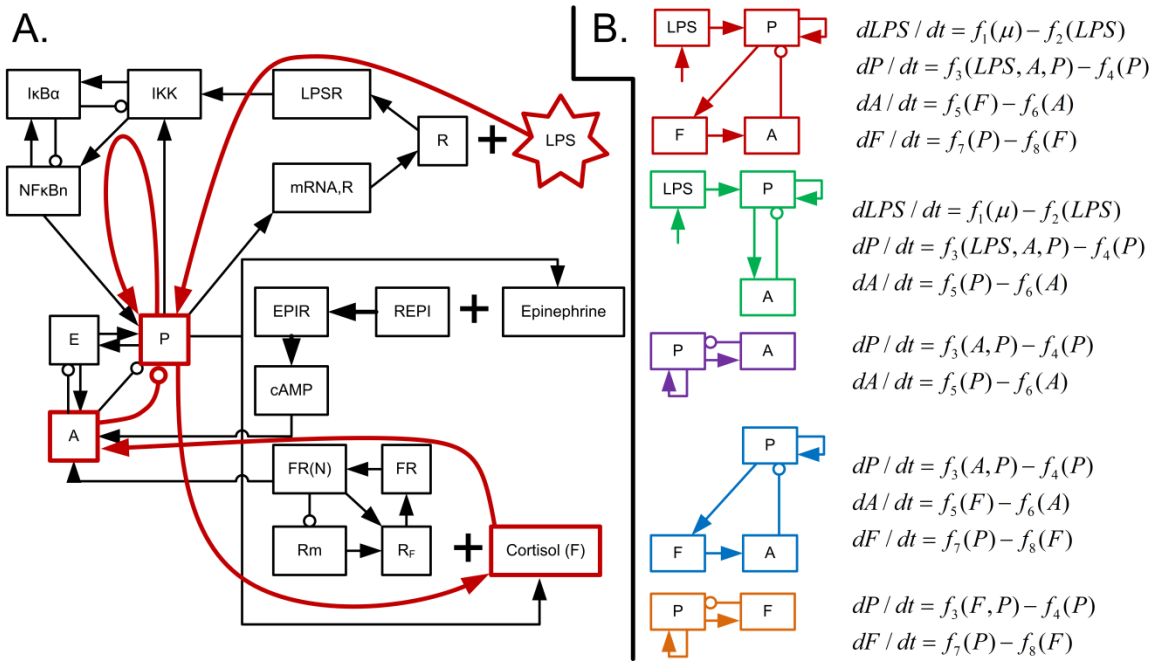

Figure 5.2: Network structures of the underlying detailed model and the generalized models. A: network structure of the model of human endotoxemia used to generate data (Foteinou, Calvano et al. 2010). The red overlaid lines represent a high level simplification of this network structure, which corresponds to the first generalized model in B. B: network structures and equations for all five generalized models considered in this work. The systems are all comprised of, at most, four variables: bacterial load (LPS), pro-inflammatory signaling (P), anti-inflammatory signaling (A), and cortisol (F). The generalized model equations are mathematical formalizations of the network structures.

However, even making broad assumptions to significantly reduce the complexity of a generalized model is not necessarily sufficient to allow for the data-driven estimation of stability. If an equation in a generalized model depends on more than one variable, then its partial derivatives cannot be directly calculated based on measurements of the state variables alone unless some partial derivatives can be measured (*e.g.* the degradation rate of a variable) and/or some information can be gleaned from other equations (*e.g.* if the production rate of one variable equals the degradation rate of another) (Lade and Gross 2012). For a physiological response like systemic

inflammation, neither of these options is generally feasible. Instead, we estimated all partial derivatives from measurements of the state variables alone. From the output of the *in silico* model of systemic inflammation, we sub-sampled only the limited set of state variables used in the generalized models in Figure 5.2B to use as input data for the prediction of critical transitions. Using this data to estimate the stability of generalized models requires the estimation of partial derivatives of every generalized model equation. These partial derivatives were estimated by assuming the placeholder functions are linear over a relatively small time window and minimizing the least squared error of the data fit to these equations. Then, these estimated partial derivatives were used to find the eigenvalues of the Jacobian matrix of the generalized model. Repeated application of this process allows for tracking the estimated stability of the generalized model over time. This algorithm is described in more detail in Appendix C.

A unique feature of this procedure is that the dimensionality of the underlying system (20 equations) is substantially larger than the dimensionality of the generalized models (2-4 equations), whereas previous applications of generalized models for predicting critical transitions used synthetic data from models with the same dimensionality as the generalized models (Lade and Gross 2012). Therefore, we are testing the hypothesis that only a subset of a system needs to be included in a generalized model to predict critical transitions. A complete formulation of the detailed model as well as the procedures for generating data and evaluating stability are found in the Appendix C.

5.3: Results

The existence of a critical transition for the detailed model of systemic inflammation in the presence of a gradually increasing bacterial load is shown in Figure 5.1. The critical transition that occurs at around 120 hours is abrupt and is preceded only by very gradually changing state variables. Thus, taking a traditional approach and deriving a warning signal based on a cutoff in the state variables would not provide a significant amount of time before the system was already well on its way to its new steady state. Thus, we derived an earlier warning signal of this transition with a minimal amount of assumptions through generalized modeling.

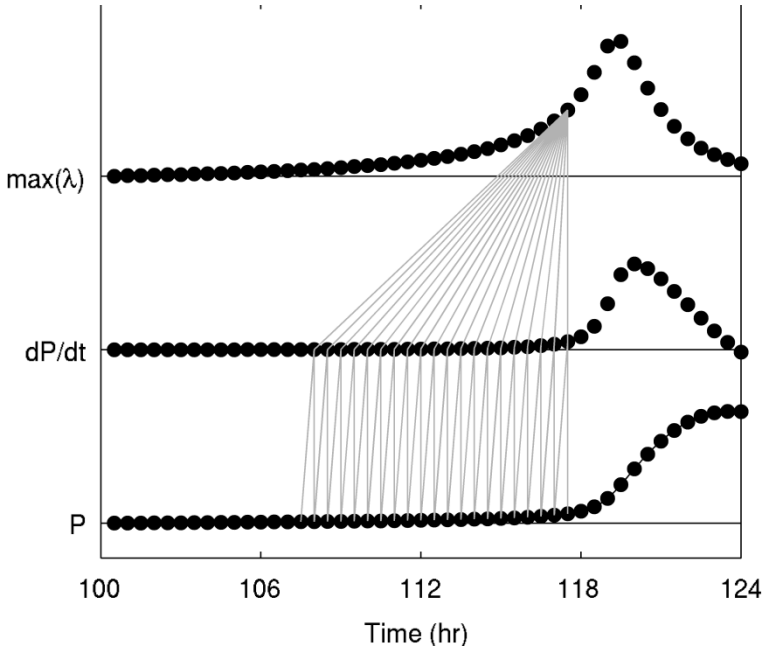

Figure 5.3: Translation from data to a warning signal. From bottom to top, the three plots show: (1) pro-inflammatory signaling (P), with the line representing the detailed model output and the dots representing discrete samples every half hour; (2) the numerical derivative of P calculated with the backwards difference method; and (3) the maximum eigenvalue of the generalized model. Vertical lines between P and dP/dt indicate that the backwards difference method was used to estimate each derivative, taking into account the current time point and the previous time point only. Then, all of these values over a 10 hour window are used to estimate a single warning signal for the current time point. Thus, all of the vertical lines show all of the data that is used to produce the warning signal at a particular time point.

Figure 5.3 displays an overview of how the output of the detailed model was translated into a warning signal. First, the state variables of the system were sampled at a constant rate, every 30 minutes in this example. This was done not for every variable in the model, but only for the variables that are included in the generalized model, in this case just pro-inflammatory signaling (*P*) and anti-inflammatory signaling (*A*). Then, derivatives of these state variables with respect to time were estimated at every point by using the backwards difference method, so that each estimate contains the most recent information possible. This also provided the opportunity to assess the predictive value of

quantifying the time derivatives of state variables. As can be seen in Figure 5.3, visible movement in both *P* and *dP/dt* occurred at approximately the same time. To evaluate the stability of the generalized model, a time window of 10 hours was used, combining the discretized state variables with the numerical derivatives to estimate partial derivatives of the system and thus estimate the eigenvalues of the two-variable generalized model. This produced two eigenvalues at each time point, of which only the larger eigenvalue is shown, as it dominates the response of the system. Conceivably, the other eigenvalues could provide information about changes in the dynamics of a system, but in all of the scenarios evaluated here, the maximum eigenvalue moved first. Each new estimate at a given time point was calculated based on the data from up to that time point, producing a warning signal updated in real time as data streamed in. The eigenvalue warning signal increased above its homeostatic value substantially earlier than either *P* or *dP/dt*, illustrating that generalized modeling can be leveraged as described here to develop a warning signal of critical transitions in the context of systemic inflammation. This validates the novel methodology for the estimation of stability based only on measurements of some state variables of a larger system without making any other assumptions about data availability or model structure. Furthermore, this shows that generalized models can provide warning signals even when they are fit to data generated by much more complex and higher dimensional systems.

In addition to the simplest two-variable generalized model including only pro- and anti-inflammatory signaling, several different generalized models were evaluated, all containing the common motifs of negative feedback between pro- and anti-inflammatory signaling and a self-stimulatory positive feedback loop in pro-inflammatory signaling. In

all of the evaluated models, the patterns of increases in the eigenvalues were largely similar, as shown in Figure 5.4. This illustrates that the results presented here are not dependent on even a specific generalized model structure, as long as they contain the relevant motifs. The generalized model eigenvalues were also compared in Figure 5.4 to the eigenvalues of the detailed model. This confirms that the patterns of changes in the estimated eigenvalues begin at roughly the same time as is observed in the eigenvalues of the underlying system.

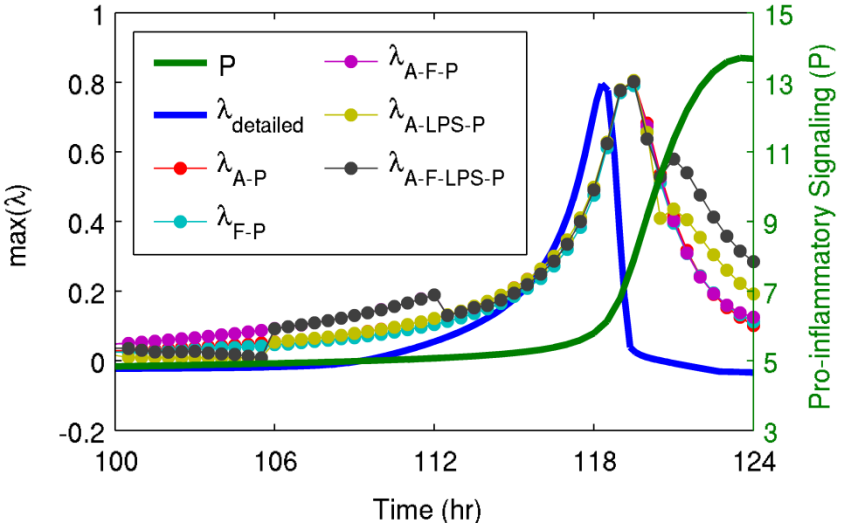

Figure 5.4: Comparison of eigenvalues from generalized models and from the underlying model. Shown here are eigenvalues estimated from all of the different generalized models (λ_i where i is the variables contained in the generalized model, as shown in Figure 5.2), the eigenvalue calculated directly from the detailed model ($\lambda_{detailed}$), and a state variable of the system (pro-inflammatory signaling, P). The estimated eigenvalues track the real eigenvalue, and they all clearly move before pro-inflammatory signaling enters its abrupt transition towards the persistent heightened inflammatory state.

The results discussed above all used data sampled every 30 minutes from the detailed model. Figure 5.5 illustrates that even lower frequency data can still be transformed into a predictive warning signal through the methods applied here. Although as the sampling rate decreases there was clearly a decrease in performance, in terms of

deviation of the eigenvalue from baseline prior to the transition, there were still clear patterns in the trajectories of the eigenvalues up to a sampling period of approximately 4 hours.

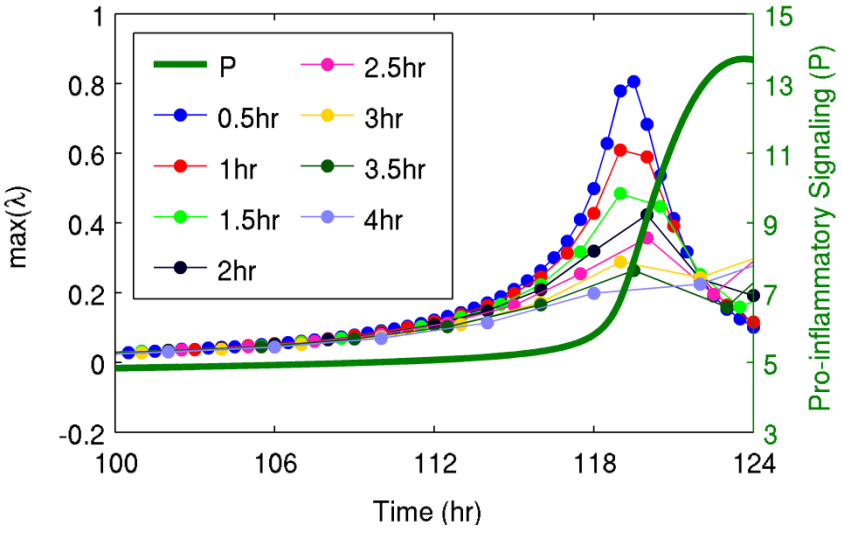

Figure 5.5: Effect of sampling frequency on predictions. Warning signals were calculated from data sampled at periods ranging from 0.5 hr to 4 hr based on the generalized model containing only pro-inflammatory signaling (P) and anti-inflammatory signaling (A). Predictive value is maximized as sampling frequency increases.

To study the implications of early detection of a critical transition, we investigated an intervention applied when signs of a transition are apparent either in the eigenvalue warning signal or directly in the state variables of the model. Figure 5.6 shows the effects of removing the inflammatory instigator at these two time points. The earlier intervention driven by the early warning signal restored homeostasis, but the later intervention after the system had already begun to move to the heightened inflammatory state was not sufficient to avert the transition, ultimately leaving the system in a persistent inflammatory state even in the absence of an inflammatory instigator. The presence of a critical time window between the time when markers of an impending

transition are apparent and the "point of no return" where intervention does not successfully restore homeostasis underscores the importance of identifying warning signals as early as possible.

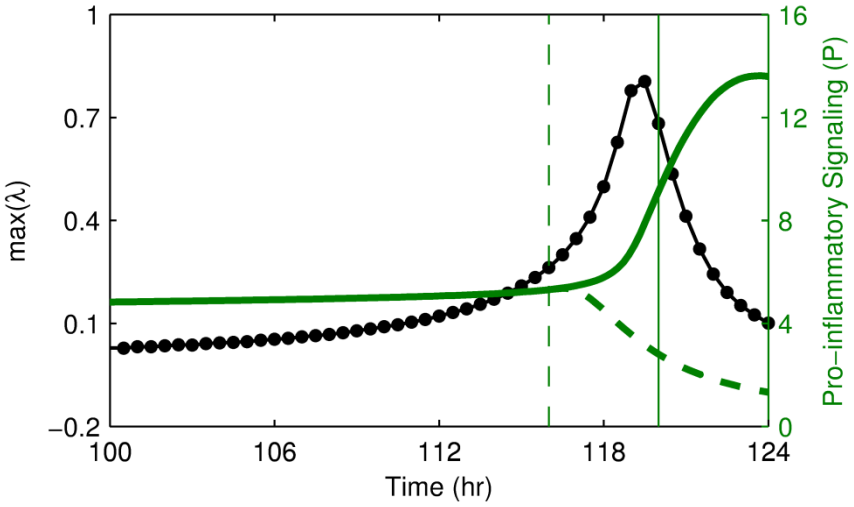

Figure 5.6: Intervention performed based on the warning signal or the magnitude of state variables. Intervention to remove the bacterial load is performed either at 116 hr when the warning signal is clearly elevated (dashed lines) or at 120 hr after the state variables of the system have clearly begun to transition (solid lines). The earlier intervention is able to restore homeostasis, but the later intervention after the transition has already begun is not sufficient to restore homeostasis.

5.4: Discussion

A key innovation here lies at the intersection of data and modeling. If very high resolution and low noise data was available, no model would be necessary to predict transitions as traditional statistical and signal processing approaches could be utilized (Scheffer, Bascompte et al. 2009). Conversely, if a perfect computational model was available, then it could simply be simulated forward to predict the future even without any data. As shown by Lade and Gross, combining relatively limited data with a simple model based on high-level network structure can result in informative predictions of

forthcoming transitions (Lade and Gross 2012). In addition to investigating a novel application in systemic inflammation, we extended this technique in two important ways. First, we established that the dimensionality of the underlying system (a detailed model of systemic inflammation) does not need to be the same as the dimensionality of the generalized model derived from the high-level network structure. This is important because it shows that the high-level network structure of a significantly more complex system is sufficient to predict transitions, which is critical in any application to real data generated by a much more complex biological system. Second, we derived predictive estimates of the stability of the system based only on data from the state variables, rather than assuming knowledge or measurability of internal production and degradation rates.

In our underlying model of systemic inflammation, bacterial load (*LPS*) drives the inflammatory response, and transitions were provoked by gradually increasing this variable. Yet even generalized models that do not include *LPS* still captured the loss of stability and movement between steady states driven by the self-stimulatory pro-inflammatory feedback loop, which is shown in Figure 5.4 by the similar results produced regardless of whether *LPS* was included or excluded. This highlights that appropriate analysis of internal components of the inflammatory response can reveal a universal dynamics-based marker of the risk of transition, independent of the specific cue. This is an important conclusion because in a clinical setting the ultimate source of inflammation might not be known, or it might be difficult to quantify, or there could be multiple inflammatory instigators such as an injury and a subsequent infection. Because internal dynamics of the inflammatory response on its own contain sufficient information

to predict transitions, similar dynamics would be expected in any gradually deteriorating inflammatory condition.

A high-level overview of the process for translating data into a warning signal is shown in Figure 5.3. In this example, the generalized model contained only variables representing pro- and anti-inflammatory signaling. Of course, there is no single biomarker that precisely corresponds to these terms. Thus, a significant challenge remains in determining how to reconcile data from a much higher dimensional system with a simple generalized model. One approach is through high-dimensional data analysis. Clusters of gene expression values could be used to define the state variables of a generalized model, similar to how we previously leveraged microarray data from peripheral blood leukocytes to infer levels of pro- and anti-inflammatory signaling (Foteinou, Calvano et al. 2009). Similarly, principal components analysis (PCA) has been applied to cytokine data, which can be used to identify key aggregate drivers of inflammation in a reduced dimensional space (Nieman, Brown et al. 2012). Based on these types of approaches, one can imagine the inputs to a generalized model being high-level markers of system function rather than raw data of individual biomarkers.

Another important issue in terms of the data input into a generalized model is sampling frequency. Other than through noninvasive metrics like ECG and EEG, which would not be sufficient to assess the inflammatory state of a patient to the extent necessary for the proposed computational methods, high frequency data is generally not available. As shown in Figure 5.5, performance increases as the sampling frequency decreases, but even with a relatively large sampling frequency, there is still predictive value in the eigenvalues. Depending on the speed of transition from one state to another,

the required sampling frequency would likely change, and factors such as biological or experimental noise could alter requirements. However, the salient point is that sampling at reasonable rates has the potential to provide predictive information when evaluated in the context of a generalized model.

The concept of making predictions based on fairly simple models calibrated based on limited data is particularly important from a translational perspective. Systems biology represents an especially challenging field in terms of data availability. In general, complex systems biology models (including the detailed model of systemic inflammation discussed here) are not uniquely identifiable from available experimental data (Gutenkunst, Waterfall et al. 2007). The implication of this is that there may be multiple formulations of a model, in terms of both structure and parametrization, which can equally well fit a dataset, thus presenting a challenge in predictive applications of models. However, even this realization understates the true scope of the problem. A systems biology model may be fit to experimental data generated from multiple subjects under multiple different conditions, which is typically quite difficult as described above. A translational model must be fit to data generated from a single subject in a single condition, which is a far more difficult problem. Dynamics-based analysis of limited data in the context of a simple model has the potential to overcome these challenges by minimizing data required to predict transitions.

The identification of early warning signals preceding a transition is particularly useful if it provides sufficient time for intervention to potentially avert an undesirable regime shift (Biggs, Carpenter et al. 2009). For instance, if a warning signal for the onset of a disease was identified, but earlier treatment did not improve clinical outcomes, it

would be of minor importance. The ultimate goal is not to simply detect a transition so that a patient could be more closely monitored and more rapidly treated, it is to detect a transition in sufficient time that the transition can be entirely averted through an appropriate intervention. In this regard, the results in Figure 5.6 are interesting as they show the potential for precisely this type of prediction by the presence of a critical time window between the identification of an early warning signal and the "point of no return". This presents the opportunity for earlier intervention to restore homeostasis, whereas an identical intervention would be unsuccessful at a later time point after the state variables of the system have begun to visibly move towards the unhealthy steady state.

The broad goal of data-driven prediction of the future state of patients is not new; ICU scoring systems have been designed and widely applied for this purpose. We draw a distinction between these traditional metrics, typically derived from simple combinations of commonly available clinical and demographic information, and newer dynamics-based methods that leverage advances in data collection towards more fine-grained predictions of imminent events. One class of approaches is based on the information content provided by very high dimensional measurements such as microarrays. Cobb *et al*. used microarrays to identify the onset of ventilator-associated pneumonia in trauma patients by identifying a subset of informative genes and using principal component analysis (PCA) to evaluate the movement of these genes from a normal recovering state to a pathological state representing pneumonia (Cobb, Moore et al. 2009). The identification of patients moving to different states in principal component space is similar to the concept of identifying transitions in physiological state space. This relationship is made more

explicit in the work by Chen *et al*. which attempts to identify "dynamical network biomarkers" (small clusters of genes representing components that change early in the transition between steady states) driven by a theoretical foundation based on statistical approaches towards identifying bifurcations in systems with multiple steady states (Chen, Liu et al. 2012). These microarray-based approaches are significantly different than the method proposed here in that they require high-dimensional measurements and they do not assume any *a priori* network structures to inform their predictions. High throughput measurements have also shown the potential to allow for the identification of changes in dynamics preceding transitions in other domains; for instance, high-resolution imaging revealed spatial patterns in ventilation driven by bistability and competition between short-range and long-range interactions (Venegas, Winkler et al. 2005).

In addition to techniques applying dynamical analysis of high throughput data to predicting physiological transitions, data that can be feasibly acquired in a very high frequency manner has also been found to be useful. One useful type of analysis in this regard is heart rate variability (HRV) derived from ECG data, which has been shown to be predictive of the onset of neonatal sepsis (Moorman, Carlo et al. 2011) and potentially also sepsis in adults (Ahmad, Ramsay et al. 2009). Although the precise mechanistic origins of HRV are uncertain, it has been hypothesized that the characteristic patterns in HRV preceding the onset of sepsis may be the outcome of a dynamical system undergoing a bifurcation (Flower, Moorman et al. 2010). If this is true, it lends credence to the hypothesis that stability analysis has a role in predicting this type of bifurcation in patient state. There has also been progress in the analysis of EEG data for predicting the onset of epileptic seizures. Despite challenges in validating preliminary studies and

translating seizure prediction to clinical practice, appropriate analyses of this high-frequency data have shown the ability to reveal predictive information (Mormann, Andrzejak et al. 2007). In total, experimental techniques that allow for either more frequent sampling or simultaneous measurements of large numbers of features enable dynamics-based approaches towards predicting future developments in patients' states.

Significant challenges remain in model-based prediction of critical transitions between physiological steady states. Homeostasis, in reality, is not simply a single fixed point. There are both random and deterministic patterns in homeostasis. Circadian rhythms are a prominent source of homeostatic variability. Although circadian rhythms are often suppressed in critically ill patients (Mundigler, Delle-Karth et al. 2002; Lowry 2009), there is still a need to very accurately distinguish between movement that is part of a healthy circadian rhythm and a pathological transition between steady states. Generalized models of periodic systems have been studied (Kuehn and Gross 2011), but not yet applied in the prediction of critical transitions. Random noise is another confounding factor which makes the estimation of partial derivatives from limited data more difficult, although appropriate smoothing of the data may be sufficient to retain predictive power (Lade and Gross 2012).

Current scientific literature contains examples of improved mathematical techniques for identifying critical transitions from limited data as well as novel experimental techniques to generate more and better physiological data. This convergence between theory and experimentation makes the prospect of predicting transitions between physiological steady states more and more plausible as time goes on, with potential applications in a wide range of systems. The work presented here

represents a step forward towards achieving these translational goals in conditions related to systemic inflammation.

Chapter 6: Conclusions and Future Outlook

In recent years, systems biology has shown the potential to produce impactful results from both scientific and translational perspectives. Systems biology facilitates approaching questions about complex and nonlinear systems that otherwise appear intractable (Lander 2004). It also allows for the opportunity to leverage these insights in a translational setting (Foteinou, Calvano et al. 2009). From this perspective, there are a number of potentially useful outputs of systems biology models: quantitative representations of existing hypotheses, novel hypotheses to guide future research, predictions of a system's behaviors in different conditions, rationalization of differences between competing experimental results and theoretical frameworks, and insight into the properties and abilities conferred by a particular network structure. The novel results presented here contribute towards all of these areas.

By evaluating the implications of circadian rhythms in human endotoxemia in Chapter 2, we tested the ability of a network structure based on central entrainment of peripheral inflammatory activity to reproduce experimental results and make predictions of network function throughout the circadian cycle. The model of ultradian rhythms in cortisol in Chapter 3 illustrates how modeling can give insight into the functional advantages of system-level properties by identifying a correlation between homeostatic ultradian rhythms and responsiveness to subsequent stress. Chapter 4 discusses how a quantitative model linking endotoxemia and HRV through autonomic activity can be used to evaluate the range of plausible mechanisms justified by experimental data. And Chapter 5 studies how model-based analysis can identify a warning signal of transitions between steady states in chronic inflammation.

In terms of the model linking circadian rhythms with human endotoxemia presented in Chapter 2, there are several factors not yet incorporated into the model that may be of significant importance. First, although our model considers circadian rhythms in components of the inflammatory response as driven by the central regulation of hormone secretion, in reality peripheralcircadian rhythms are driven by networks of clock genes in individual cells that are synchronized by central entraining signals. In the context of human endotoxemia, this distinction may be of significant importance because it has been shown experimentally that human endotoxemia results in altered expression of clock genes in peripheral immune cells (Haimovich, Calvano et al. 2010). Additionally, it is known that there is crosstalk between circadian and inflammatory systems, for instance clock genes respond to inflammatory mediators such as cortisol and various cytokines while cytokines production is also regulated by clock gene expression (Mavroudis, Scheff et al. 2012). Furthermore, while our model is of human endotoxemia and only acute LPS doses are considered in Chapter 2, the relationship between chronic inflammation and circadian rhythms is an important topic. While alterations in circadian rhythmicity have been observed in many different types of stress, deciphering the specific mechanisms (which may very well be different for different stressors) is an area of active research (Sriram, Rodriguez-Fernandez et al. 2012).

Chapter 3 presented a model linking ultradian cortisol production with downstream pharmacodynamic effects. An obvious next step would be to integrate this within the larger model of human endotoxemia discussed in the other chapters to evaluate the implications of ultradian rhythmicity in a systems-level context. A significant challenge in this regard lies in the availability of high-frequency cortisol measurements in

human endotoxemia experiments to understand how endotoxemia alters the dynamics of the HPA axis. More generally, studies attempting linking characteristics of cortisol's homeostatic ultradian rhythms with stress responsiveness would be of great interest, analogous to the Monte Carlo experiments in Chapter 3.

The relationship between human endotoxemia, the autonomic nervous system, and HRV was explored in Chapter 4. The conclusions of this chapter directly lead to one important area of future work: further human endotoxemia experiments with two primary goals. First, to study the autonomic nervous system through metrics besides HRV (such as chemoreflex sensitivity (Schmidt, Muller-Werdan et al. 2004)) so to gain a better understanding of how HRV relates to changes in autonomic activity in endotoxemia. Second, to study perturbations of autonomic activity during endotoxemia to evaluate coupling between the autonomic nervous system and the heart (Sayk, Vietheer et al. 2008). Additionally, from the modeling domain, one key issue is closing the feedback loop between inflammation, autonomic activity, and the heart. In the current model structure, the function of the heart is an output of the model and does not modulate any upstream components. In reality, altered HR leads to many physiological changes, for instance in blood pressure and autonomic activity (deBoer, Karemaker et al. 1987). Given the known relationships between autonomic activity and inflammation, it seems plausible that these physiological responses to changes in HR could modulate the progression of the inflammatory response.

In Chapter 5, the potential for model-based prediction of transitions between steady states was explored in the context of chronic systemic inflammation. This work was done in the absence of circadian rhythms. Although circadian rhythms are often

suppressed in critically ill patients (Mundigler, Delle-Karth et al. 2002; Lowry 2009), there is still a need to very accurately distinguish between movement that is part of a healthy circadian rhythm and a pathological transition between steady states. Generalized models of periodic systems have been studied (Kuehn and Gross 2011), but not yet applied in the prediction of critical transitions. Random noise is another confounding factor which makes the estimation of partial derivatives from limited data more difficult, although appropriate smoothing of the data may be sufficient to retain predictive power (Lade and Gross 2012). Taking a broader perspective, there are also other approaches towards the identification of critical transitions that should also be explored. For instance, rather than relying on high frequency data, it could also be possible to leverage high dimensional transcriptomic/proteomic data towards similar ends (Chen, Liu et al. 2012).

In total, each component of this dissertation has laid the groundwork for future research, both experimental and computational. Continued work along these lines would likely be fruitful in gaining further insight into the inflammatory response and guiding future investigations.

Appendix A: Multiscale Model of Human Endotoxemia

The model of human endotoxemia presented in this appendix was iteratively developed over several publications prior to this dissertation (Foteinou, Calvano et al. 2009; Foteinou, Calvano et al. 2009; Foteinou, Calvano et al. 2010; Foteinou, Calvano et al. 2011) and is used in Chapters 2, 4, and 5.

In vivo human endotoxin challenge is a commonly-used model for studying acute inflammation because it evokes signs and symptoms of systemic inflammation along with significant transcriptional and neuroendocrine responses (Lowry 2005). Lipopolysaccharides (LPS, endotoxin), found in the outer membrane of gram-negative bacteria are pathogen-associated molecular patterns (PAMPs) that are recognized by innate immune system pattern recognition receptors (PRRs), most notably Toll-like receptor 4 (TLR4), thus eliciting an inflammatory response.

Through the analysis of leukocyte gene expression data, the essential responses characterizing the leukocyte transcriptional dynamics were identified. Specifically, these responses, in the case of transient human endotoxemia, include (1) an early increase in pro-inflammatory signaling molecule production; (2) an anti-inflammatory response to counter pro-inflammatory signaling; and (3) an energetic response representing diminished cellular bio-energetic processes. These transcriptional responses are triggered by the activation of critical signaling cascades as a result of the recognition of the extracellular LPS signal. In the endotoxin injury model, the focus has been on NF-κB as the archetypical signaling module that regulates the expression of pro-inflammatory genes, as provoked by the binding of LPS to its receptor TLR4 (R) (Eq. A.1a-A.1d) leading to the activation of the NF-κB, which initiates the transcriptional response to

inflammation. NF-κB is normally bound to IκB molecules which inhibit its translocation to the nucleus, thus inactivating its role as a transcription factor. LPS via TLR4 and adapter molecules stimulates the activation of IKK, which phosphorylates IκBα leading, in turn, to ubiquitination and degradation of IκBα in the proteasome. Then, the free NF-κB can move into the nucleus and stimulate the transcription of a number of genes, including its inhibitor IκBα, thus creating a negative feedback loop. The NF-κB module is based on a reduced model of NF-κB dynamics that includes IKK (Eq. A.1e), nuclear (activated) NF-κB (Eq. A.1f), and IκBα (Eq. A.1g, A.1h) (Ihekwaba, Broomhead et al. 2004) which allows the model to broadly capture the negative feedback regulatory behavior of NF-κB . The fundamental transcriptional processes found in the gene expression data are the pro-inflammatory (Eq. A.1i), anti-inflammatory (Eq. A.1j), and energetic (Eq. A.1k) responses.

$$\frac{dLPS}{dt} = k_{lps,1} \cdot LPS \cdot (1 - LPS) - k_{lps,2} \cdot LPS \tag{A.1a}$$

$$\frac{dR}{dt} = k_{syn} \cdot mRNA, R + k_2 \cdot (LPSR) - k_1 \cdot LPS \cdot R - k_{syn} \cdot R \tag{A.1b}$$

$$\frac{d(LPSR)}{dt} = k_1 \cdot LPS \cdot R - k_3 \cdot (LPSR) - k_2 \cdot (LPSR) \tag{A.1c}$$

$$\frac{d(mRNA, R)}{dt} = k_{in,mRNA,R} \cdot (1 + H_{mRNA,R,P}) - k_{out,mRNA,R} \cdot mRNA, R \tag{A.1d}$$

$$\frac{dIKK}{dt} = k_3 \cdot (LPSR) / (1 + IkBa) - k_4 \cdot IKK + P \cdot \left(\frac{IKK^2}{1 + IKK^2} \right) \tag{A.1e}$$

$$\frac{dNFkBn}{dt} = \frac{k_{NFkB,1} \cdot IKK \cdot (1 - NFkBn)}{(1 + IkBa)} - k_{NFkB,2} \cdot NFkBn \cdot IkBa \tag{A.1f}$$

$$\frac{dmRNA_{IkBa}}{dt} = k_{in,IkBa} \cdot (1 + k_{IkBa,1} \cdot NFkBn) - k_{out,IkBa} \cdot mRNA_{IkBa} \tag{A.1g}$$

$$\frac{dIkBa}{dt} = k_{I,1} \cdot mRNA_{IkBa} - k_{I,2} \cdot (1 + IKK) \cdot (1 - NFkBn) \cdot IkBa - k_{I,1} \tag{A.1h}$$

$$\frac{dP}{dt} = k_{in,P} \cdot (1 + H_{P,NFkBn}) \cdot (1 + H_{P,E}) / A - k_{out,P} \cdot P \tag{A.1i}$$

$$\frac{dA}{dt} = k_{in,A} \cdot \left(1 + H_{A,cAMP}\right) \cdot \left(1 + k_{A,FRN} FR(N)\right) \cdot \left(1 + H_{A,E}\right) - k_{out,A} \cdot A \quad \text{(A.1j)}$$

$$\frac{dE}{dt} = k_{in,E} \cdot (1 + H_{E,P}) / A - k_{out,E} \cdot E \quad \text{(A.1k)}$$

$$H_{i,j} = k_{i,j} \cdot J$$

The interplay between the NF-κB pathway and the pro- and anti-inflammatory responses normally leads to a self-limited inflammatory response that resolves after LPS has been cleared, but high doses of LPS can lead to a state of persistent inflammation. Additionally, corticosteroids (both endogenous and exogenous) play a critical role in modulating the progression of inflammation and significant prior research has elucidated the mechanisms driving corticosteroid activity (Jusko 1994; DuBois, Xu et al. 1995; Xu, Sun et al. 1995; Sun, DuBois et al. 1998; Almon, DuBois et al. 2002; Almon, Dubois et al. 2005; Almon, Lai et al. 2005; Almon, DuBois et al. 2007). Such studies simulate the pharmacodynamic action of glucocorticoids at the cellular level and the pharmacogenomic effect of glucocorticoids at the transcriptional level (Ramakrishnan, DuBois et al. 2002; Jin, Almon et al. 2003; Jusko, DuBois et al. 2005). Corticosteroid pharmacodynamics include: (i) the binding of the corticosteroid to its cytosolic receptor; (ii) the subsequent formation of the corticosteroid-receptor complex; and (iii) the translocation of the cytosolic complex to the nucleus that alters the transcriptional machinery, activating or repressing numerous genes. This is modeled by equations governing the inflammation-induced production of cortisol (Eq. A.1l), transcription and translation of cytosolic glucocorticoid receptor (Eq. A.1m, A.1n), and the intracellular dynamics as the signal is transduced from the cytoplasm (Eq. A.1o) to the nucleus (Eq. A.1p).

$$\frac{dF}{dt} = k_{in,F_{en}} \cdot \left(1 + H_{F_{en},P}\right) - k_{out,F} \cdot F \tag{A.1l}$$

$$\frac{dR_m}{dt} = k_{syn\_Rm} \cdot \left(1 - \frac{FR(N)}{IC_{50\_Rm} + FR(N)}\right) - k_{\deg} \cdot R_m \tag{A.1m}$$

$$\frac{dR_F}{dt} = k_{syn\_R} \cdot R_m + r_f \cdot k_{re} \cdot FR(N) - k_{on} \cdot \left(F - 1\right) \cdot R_F - k_{dgr\_R} \cdot R_F \tag{A.1n}$$

$$\frac{dFR}{dt} = k_{on} \cdot (F - 1) \cdot R_F - k_T \cdot FR \tag{A.1o}$$

$$\frac{dFR(N)}{dt} = k_T \cdot FR - k_{re} \cdot FR(N) \tag{A.1p}$$

Pro-inflammatory cytokines interact with neural-based pathways that modulate the progression of the immune response. As a result of the activation of neuroendocrine axis, anti-inflammatory hormones are secreted and recognized by immune cells. In the case of catecholamines, the secretion of catecholamines from SNS and adrenal medulla attenuates the pro-inflammatory manifestations of human endotoxemia, as evidenced by reduced TNF levels (van der Poll, Coyle et al. 1996). The anti-inflammatory influence is mediated by intracellular cAMP signaling potentiating anti-inflammatory (IL-10) signaling (van der Poll, Coyle et al. 1996; van der Poll 2001). Epinephrine is modeled as being secreted in response to stimulation by the pro-inflammatory response (Elenkov, Wilder et al. 2000), and ultimately leads to increased anti-inflammatory signaling, as shown in Eq. A.1q-A.1t).

$$\frac{dEPI}{dt} = k_{in,EPI} \cdot \left(1 + H_{EPI,P}\right) - k_{out,EPI} \cdot EPI \tag{A.1q}$$

$$\frac{dR_{EPI}}{dt} = k^0_{R_{EPI}} - \left[k_{1,R_{EPI}} \cdot \left(1 + H_{R_{EPI},EPI}\right) + k_{2,R_{EPI}}\right] \cdot R_{EPI} \tag{A.1r}$$

$$\frac{dEPIR}{dt} = k_{1,R_{EPI}} \cdot \left(1 + H_{R_{EPI},EPI}\right) \cdot R_{EPI} - k_{3,EPIR} \cdot \left(EPIR + 1\right) \tag{A.1s}$$

$$\frac{dcAMP}{dt} = \frac{1}{\tau} \cdot \left((1 + EPIR)^n - cAMP\right) \tag{A.1t}$$

Taken together, these elements in Eq. A.1 and the corresponding parameters in Table A.1 comprise a semi-mechanistic model of human endotoxemia. Further detail is available in previous publications (Foteinou, Calvano et al. 2009; Foteinou, Calvano et al. 2009; Foteinou, Calvano et al. 2010; Foteinou, Calvano et al. 2011).

Parameter	Value	Parameter	Value	Parameter	Value
$k_{lps,1}$	4.5	$k_{in,P}$	0.03	k_{deg}	0.112
$k_{lps,2}$	6.79	$k_{out,P}$	0.33	k_{syn_R}	1.2
k_{syn}	0.5	$k_{P,NFkBn}$	29.74	r_f	0.49
k_1	3	$k_{P,E}$	9.05	k_{re}	0.57
k_2	0.04	$k_{in,A}$	0.461	k_{on}	0.00329
k_3	5	$k_{out,A}$	0.811	k_{dgr_R}	0.0572
k_4	2.24	$k_{A,cAMP}$	0.145	k_T	0.63
$k_{in,mRNA,R}$	0.09	$k_{A,E}$	0.534	$k_{in,EPI}$	5.921
$k_{out,mRNA,R}$	0.32	$k_{A,FRN}$	0.401	$k_{out,EPI}$	7.286
$k_{mRNA,R,P}$	1.74	$k_{in,E}$	0.08	$k_{EPI,P}$	0.231
$k_{NFkB,1}$	16.29	$k_{out,E}$	0.26	k^0_{REPI}	11.01
$k_{NFkB,2}$	1.18	$k_{E,P}$	2.21	$k_{1,REPI}$	3.01
$k_{in,IKBa}$	0.46	$k_{in,F}$	0.842	$k_{REPI,EPI}$	0.85
$k_{IkBa,1}$	13.27	$k_{out,F}$	1.058	$k_{2,REPI}$	5.46
$k_{out,IkBa}$	0.46	$k_{F,P}$	0.256	$k_{3,REPI}$	5.55
$k_{I,1}$	1.4	k_{syn_Rm}	2.9	τ	0.053
$k_{I,2}$	0.87	IC_{50_Rm}	26.2	n	5.509

Table A.1: Parameters for the human endotoxemia model equations given in Eq. A.1.

Appendix B: Alternative Assumptions in Autonomic Regulation of the Heart

The analysis presented in section 4.2 of Chapter 4 relies on a number of assumptions with regards to the analysis techniques used to investigate HRV and the structure of the models in Eq. 4.4-4.5. In the results presented in this appendix, we evaluated the implications of altering or relaxing these assumptions on the conclusions drawn about the relationship between the autonomic nervous system and the heart, particularly in human endotoxemia.

B.1: Alternative Method for Calculating LF and HF Powers

LF and HF powers are typically calculated by estimating the power spectrum of RR intervals (Task 1996), which is what was done for the results shown in the main text. However, it is known that calculating LF and HF powers based on RR intervals introduces dependencies on mean values of autonomic inputs, as was originally discussed by Niklasson *et al*. (Niklasson, Wiklund et al. 1993). This effect contributes to the dependency of LF and HF powers on mean autonomic activities illustrated in Figure 4.14 and Table 4.3. By estimating the power spectrum based on instantaneous HR rather than RR intervals, this relationship would be expected to change (Niklasson, Wiklund et al. 1993) and therefore could also impact the theoretical human endotoxemia results in Figure 4.15.

Using HR rather than RR to calculate LF and HF powers produced the results shown in Figure B.1. The linear case is similar to the model considered by Niklasson *et al*. where they also found that using HR eliminates the relationship between mean autonomic inputs and spectral powers (Niklasson, Wiklund et al. 1993). For the nonlinear

model, LF and HF powers do continue to change as the input changes, but the pattern is different than in Figure 4.14; this is because these changes are all driven purely by the saturation mechanism. For instance, increased sympathetic activity leads to blunted oscillations in norepinephrine, ultimately resulting in decreased LF power.

However, when this technique is applied for the endotoxemia scenarios in Figure B.2, it does not significantly impact the level of uncoupling present in the various hypothetical scenarios in Figure 4.15.

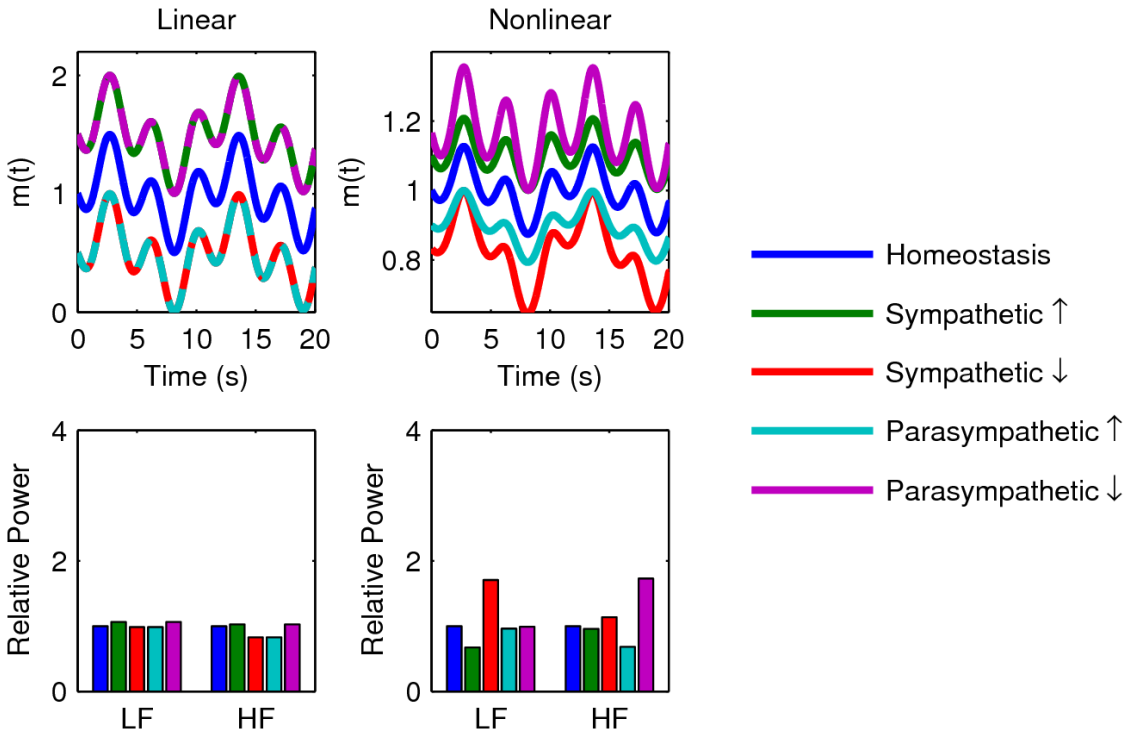

Figure B.1: Relationship between changes in mean autonomic activity and changes in LF power and HF power for both the linear (Eq. 4.4) and nonlinear (Eq. 4.5) models. This is the equivalent of Figure 4.14 but with HR used instead of RR intervals for HRV calculation.

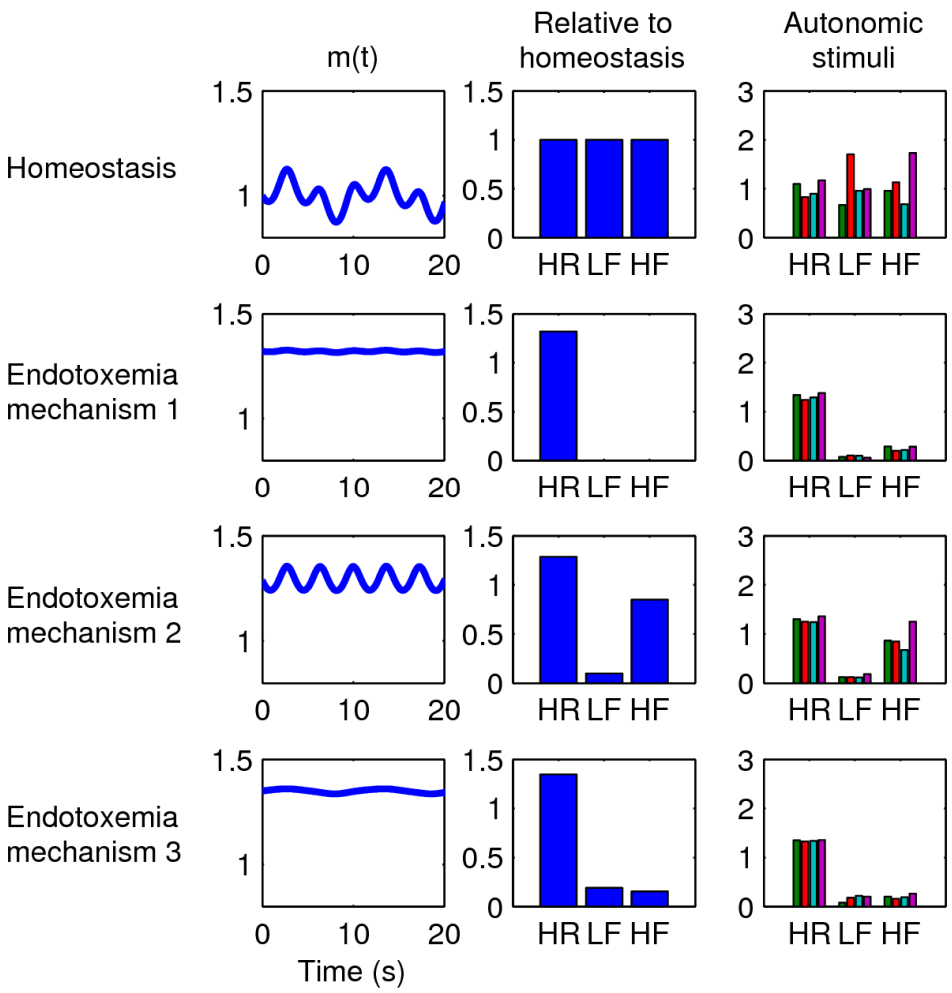

Figure B.2: Mechanisms for HR/HRV changes in endotoxemia. This is the equivalent of Figure 4.15 but with HR used instead of RR intervals for HRV calculation. The last two columns show that there is still significant uncoupling.

B.2: Proportional Changes in Mean Value and Amplitude

To interpret LF and HF powers, it is often implicitly (and sometimes explicitly) assumed that the amplitude of oscillations is proportional to the mean value, even though it is not clear if such a relationship generally holds (Saul 1990; Akselrod 1995; Eckberg 1997). In Eq. 4.4-4.5, the opposite assumption is made: mean value and amplitude are independent.

In both the linear (Eq. 4.4) and nonlinear (Eq. 4.5) models in Chapter 4, neurotransmitter concentrations are defined as:

$$nor = m_{nor} + a_{nor} \cdot sin(\omega_{nor} \cdot t) \quad \text{(B.1a)}$$

$$ach = m_{ach} + a_{ach} \cdot sin(\omega_{ach} \cdot t) \quad \text{(B.1b)}$$

The mean values *m* and the amplitudes *a* are independent in Eq. B.1. An alternative formulation is shown in Eq. B.2, where the amplitude is directly proportional to the mean value.

$$nor = m_{nor} \cdot (1 + a_{nor} \cdot sin(\omega_{nor} \cdot t)) \quad \text{(B.2a)}$$

$$ach = m_{ach} \cdot (1 + a_{ach} \cdot sin(\omega_{ach} \cdot t)) \quad \text{(B.2b)}$$

The effect of Eq. B.2 is to counter the saturation mechanism. Saturation causes high values of neurotransmitters to produce blunted oscillations downstream. However, if the amplitudes of oscillations are proportional to mean values, they oppose the saturation-induced decreases in oscillations.

The result of applying Eq. B.2 within the linear and nonlinear models is shown in Figure B.3. For the linear case, as there is no saturation, the relative powers change with the amplitudes of the relevant neurotransmitters, relative to Figure B.4. However, in the nonlinear case, since the changes in Eq. B.2 oppose the saturation in the nonlinear model, differences in relative powers are blunted.

As in the previous section, the differences shown in Figure A3 do not substantially affect the uncoupling in the hypothetical endotoxemia scenarios in Figure A4.

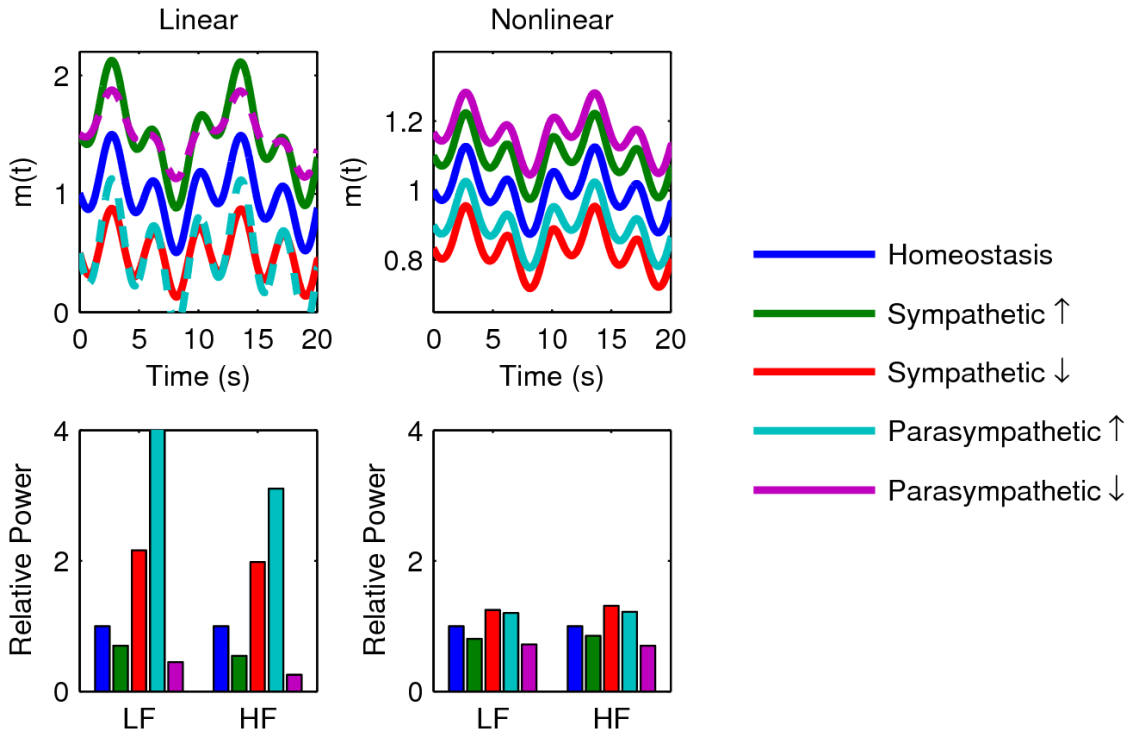

Figure B.3: Relationship between changes in mean autonomic activity and changes in LF power and HF power for both the linear (Eq. 4.4) and nonlinear (Eq. 4.5) models. This is the equivalent of Figure 4.14 but with neurotransmitter oscillatory amplitudes proportional to mean values.

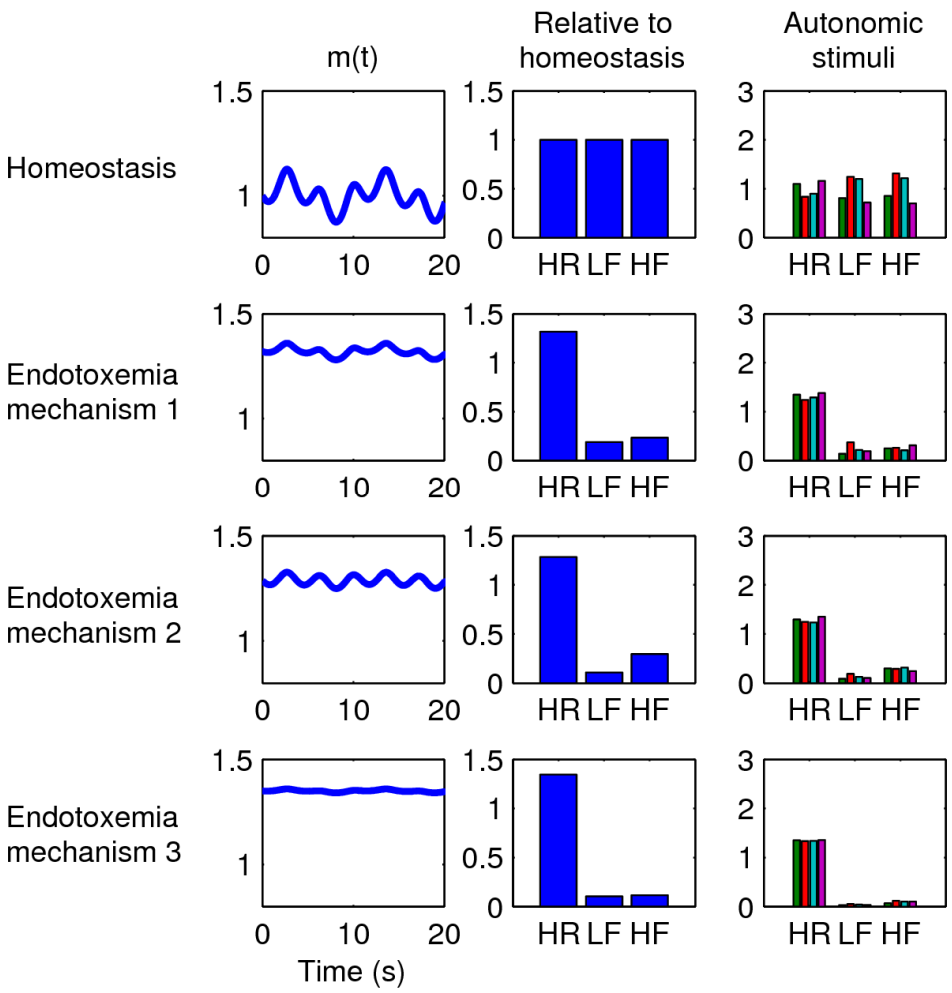

Figure B.4: Mechanisms for HR/HRV changes in endotoxemia. This is the equivalent of Figure 4.15 but with neurotransmitter oscillatory amplitudes proportional to mean values. The last two columns show that there is still significant uncoupling.

B.3: Combined Changes

If these two altered assumptions (different method of HRV calculation and amplitudes depending on mean values) are applied together, as shown in Figure B.5 and Figure B.6, the responses to the hypothetical endotoxemia scenarios remain uncoupled. What this suggests is that, even with a variety of different assumptions, there are still a number of hypothetical scenarios that can equivalently capture experimental results. Furthermore, changing relatively simple assumptions in the model produced significantly

different relationships between mean autonomic signaling and LF and HF powers. In total, these results serve to strengthen the conclusions of Chapter 4 with respect to the function of the autonomic nervous system in endotoxemia and the uncertainty of HR- and HRV-based insight into autonomic function.

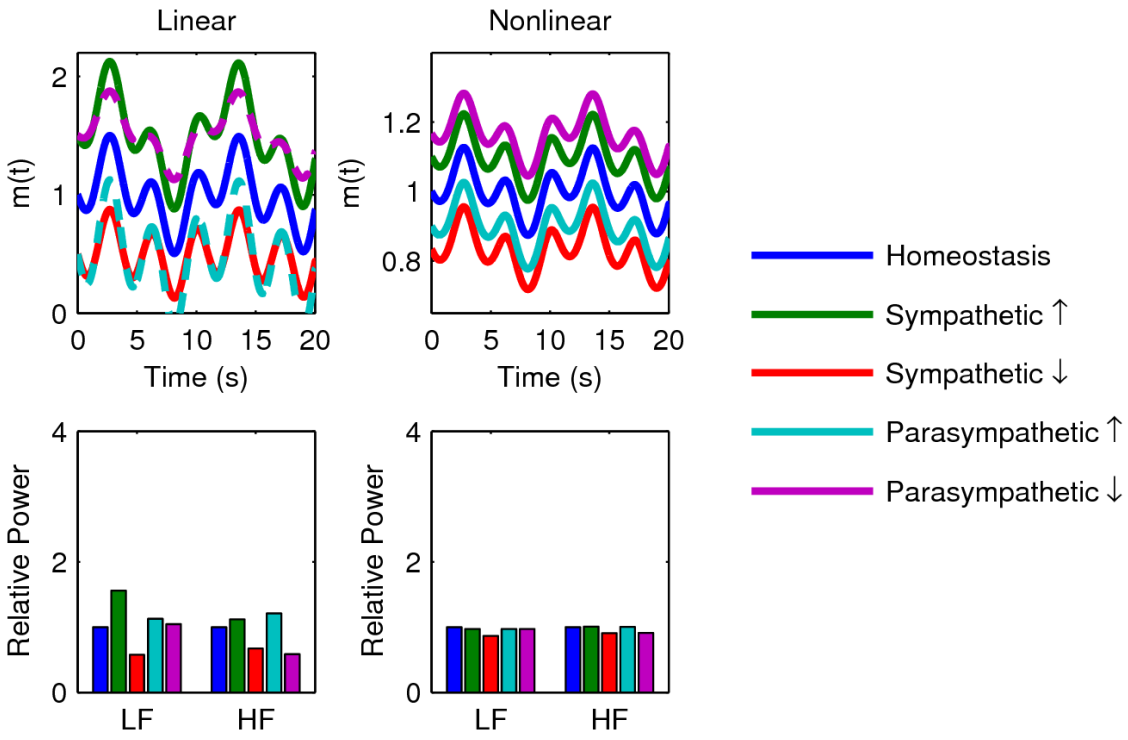

Figure B.5: Relationship between changes in mean autonomic activity and changes in LF power and HF power for both the linear (Eq. 4.4) and nonlinear (Eq. 4.5) models. This is the equivalent of Figure 4.14 but with HR used instead of RR intervals for HRV calculation and neurotransmitter oscillatory amplitudes proportional to mean values.

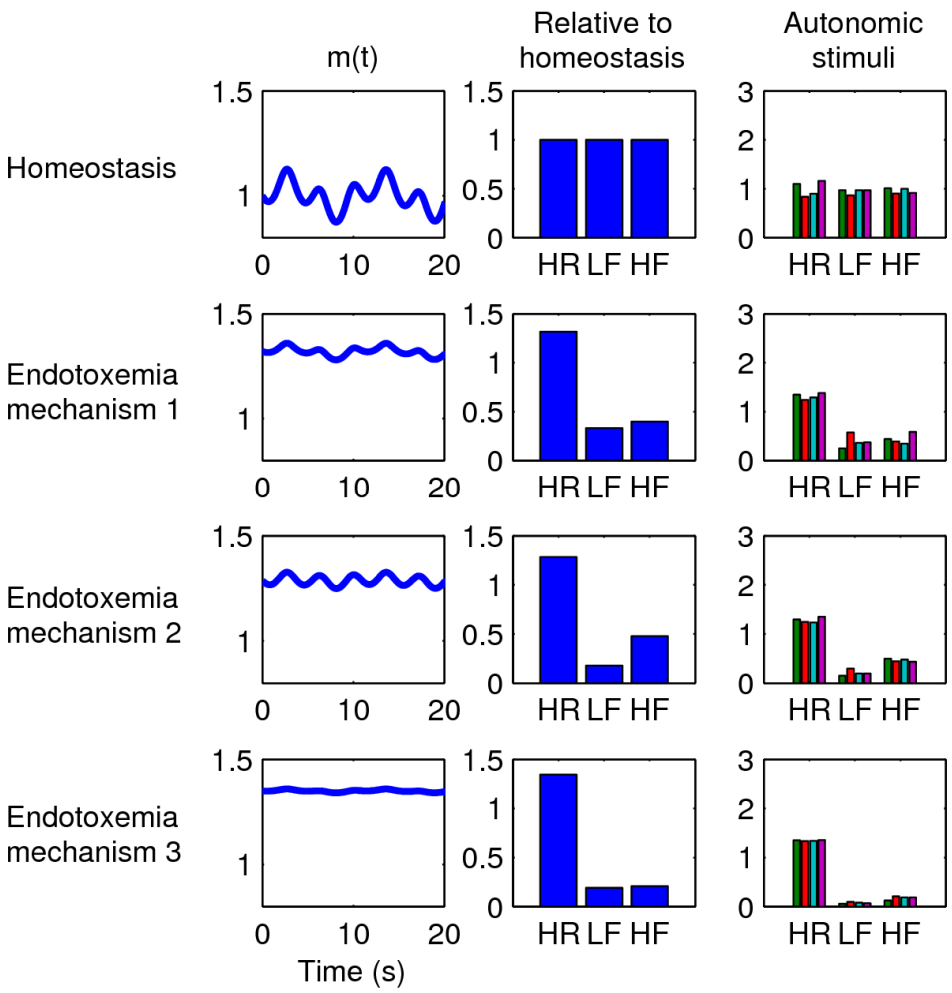

Figure B.6: Mechanisms for HR/HRV changes in endotoxemia. This is the equivalent of Figure 4.15 but with HR used instead of RR intervals for HRV calculation and neurotransmitter oscillatory amplitudes proportional to mean values. The last two columns show that there is still significant uncoupling.

Appendix C: Predicting critical transitions

This appendix serves to elaborate on the methods behind the work presented in Chapter 5.

C.1: Identification of Early Warning Signals for Critical Transitions

Identifying transitions between steady states of a gradually changing dynamical system does not only have value in healthcare, as is discussed in Chapter 5. Conceptually similar problems exist in finance (When will the market crash?), climate (When will an abrupt shift occur?), and ecology (When will the food chain break down as populations change?), to name a few. Statistical analyses of data in these fields has been used to identify early warning signals of critical transitions (Scheffer, Bascompte et al. 2009). The common thread between all of these different types of bifurcations in different types of systems is that characteristic patterns tend to occur as a bifurcation is gradually approached. For example, as a steady state approaches the loss of stability, the system is generally slower to respond to random fluctuations away from the steady state, leading to detectable patterns in the variance or autocorrelation of a state variable; this phenomenon is known as “critical slowing down”.

An intuitive way to think about this is in terms of a locally linearized system of differential equations. In this context, the eigenvalues of the system reflect its stability. If the real parts of all eigenvalues are negative, then small perturbations away from the steady state will decay back to the steady state. If the real part of an eigenvalue becomes positive, then stability is lost and the system will move away from the steady state. However, as the loss of stability is approached, an eigenvalue of the system approaches

zero. The closer it is to zero, the longer it takes to return to the steady state, resulting in the aforementioned patterns in the statistical properties of the state variables. Therefore, the model-based approach discussed here and in Chapter 5 is fundamentally investigating the same phenomenon as this traditional statistics-based approach, it's just that different data and techniques are applied at the same problem of detecting the impending loss of stability.

Additionally, other statistical approaches have been applied to identify patterns in the dynamics of a system as it approaches a bifurcation, such as skewness, flickering, and spatial patterns (Scheffer, Bascompte et al. 2009). One can imagine model-based approaches at achieving the same goal of identifying critical transitions. Given a perfect model of a system, it can simply be simulated into the future to identify when an adverse event will occur. This generally is not feasible, given that the structure and parametrization of a system are typically not known. In systems biology, this is particularly challenging as biological network structures contain significant uncertainty (Shmulevich, Dougherty et al. 2002) and models contain parameters that cannot be identified from reasonable experimental data (Gutenkunst, Waterfall et al. 2007). In the context of a predictive and individualized model, the situation is even more challenging as the goal is to use data from a single patient at one state to predict what will happen in the future, when even multiple subjects with data at multiple steady states might not be sufficient. Recently, Lade and Gross proposed a novel technique for predicting critical transitions based on generalized modeling that works around these issues in typical model-based approaches (Lade and Gross 2012). Below, we discuss and extend this approach.

C.2: Generalized Models

A generalized model is a system of equations comprised of placeholder functions to represent interactions between variables (Gross and Feudel 2006; Kuehn, Siegmund et al. 2012). No assumptions are made about specific functional forms or parametrizations that all correspond to the same network structure. As an example, Eq. C.1 shows the Lotka-Volterra predator-prey model. One can imagine a higher-level form of a predator-prey model that simply describes the relationships between predator and prey in general terms. This is a generalized model, as shown in Eq. C.2.

$$\begin{aligned} \frac{dX}{dt} &= X(\alpha - \beta Y) \\ \frac{dY}{dt} &= -Y(\gamma - \delta X) \end{aligned} \tag{C.1}$$

$$\begin{aligned} \frac{dX}{dt} &= f_1(X) - f_2(X,Y) \\ \frac{dY}{dt} &= f_3(X,Y) - f_4(Y) \end{aligned} \tag{C.2}$$

By appropriately setting all of the f_is in the generalized model, the Lotka-Volterra equations can be derived. However, many other specific predator-prey models with different functional forms are also described by the generalized model. Therefore, mathematical results derived from analysis of Eq. C.2 have broader implications than results derived from analysis of Eq. C.1.

A generalized model (Gross and Feudel 2006; Kuehn, Siegmund et al. 2012) can be constructed for any system with a known network structure. However, for the purposes of predicting critical transitions, there are some practical constraints on the structure of feasible generalized models. As is discussed below in more detail, the ultimate goal is to estimate the stability of the generalized model as a proxy for the

stability of the underlying system. This requires the estimation of the Jacobian matrix, which in turn necessitates the estimation of partial derivatives of the right hand side of every differential equation with respect to every variable it depends on. Therefore, the more variables and connections represented in a generalized model, the more partial derivatives that need to be estimated from limited data. Lade and Gross worked around this problem by considering only relatively small systems such that the dimensionality of the generalized models and the underlying systems could be the same (Lade and Gross 2012). The model of systemic inflammation used here is significantly larger, consisting of 20 differential equations. Real systems are far larger and far more complex. This motivated one of our key methodological questions: is it possible to apply this technique on data generated from a high dimensional system while using a low dimensional generalized model?

Addressing this question first requires network reduction to build the generalized model. Taking motivation from prior studies which simplify network structure by focusing on key measurable components while ignoring intermediate steps (Morris, Saez-Rodriguez et al. 2011), we focused on LPS (*LPS*), pro-inflammatory signaling (*P*), anti-inflammatory signaling (*A*), and cortisol (*F*): *LPS* was chosen because it is the gradually-changing instigator of the inflammatory response in our model. *P* and *A* were chosen because they represent high level quantifications of the state of the inflammatory system as highlighted in Figure 5.2A. The antagonistic relationship between pro- and anti-inflammatory signaling in inflammation and the positive feedback in pro-inflammatory signaling that can lead to runaway inflammation are common motifs in models of inflammation (Kumar, Clermont et al. 2004; Day, Rubin et al. 2006; Reynolds, Rubin et

al. 2006; Foteinou, Calvano et al. 2009; Nieman, Brown et al. 2012). *F* was used because cortisol is an important immunomodulatory hormone that has been widely studied and quantified in a variety of clinical and experimental settings; in contrast, pro- and anti-inflammatory signaling are terms that are somewhat poorly defined in terms of clinical applications, but could plausibly be considered to represent some aggregate metrics derived from levels of cytokines or other inflammatory biomarkers (Foteinou, Calvano et al. 2009; Nieman, Brown et al. 2012).

As this is a somewhat *ad hoc* procedure, to ensure that we are not inappropriately focusing on one particular network structure we considered several different combinations of *LPS*, *P*, *A*, and *F*, ranging from all four variables to just *P* and either *A* or *F*, as is detailed in Figure 5.2. The equations are constructed with production and degradation rates represented by f_i. These functions are never explicitly defined and therefore cannot be simulated forward as would be done with a traditional model, but instead are used to facilitate numerical analyses as described in the following sections. In general, we observed similar results for all of these generalized model structures, suggesting that it is not the specific details in building a generalized model that are important, but it is the higher level principles embedded in a model that are most critical.

C.3: Stability Analysis of Generalized Models

Traditional stability analysis of a system of ODEs is done by assessing the eigenvalues of the Jacobian matrix, which is a local linearization of the system. If the real parts of all eigenvalues at a steady state are negative, then it is stable. If one or more eigenvalues are positive, then it is unstable. This type of stability analysis is valid even in a system with a gradually changing parameter, as is the case in a system approaching a

critical transition, because the time scale of the gradual disturbance is much slower than the time scale of the transition (Lade and Gross 2012). In the context of generalized models, the Jacobian can be found symbolically and numerically estimated. To illustrate this, consider the generalized model containing *LPS*, *P*, *A*, and *F*.

$$\begin{aligned} dLPS/dt &= f_1(\mu) - f_2(LPS) \\ dP/dt &= f_3(LPS, A, P) - f_4(P) \\ dA/dt &= f_5(F) - f_6(A) \\ dF/dt &= f_7(P) - f_8(F) \end{aligned} \tag{C.3}$$

The Jacobian matrix contains partial derivatives of the right sides of the ODEs in Eq. C.3.

$$J = \begin{bmatrix} -f_{2,LPS} & 0 & 0 & 0 \\ f_{3,LPS} & f_{3,P} - f_{4,P} & f_{3,A} & 0 \\ 0 & 0 & -f_{6,A} & f_{5,F} \\ 0 & f_{7,P} & 0 & -f_{8,F} \end{bmatrix} \tag{C.4}$$

In Eq. C.4, $f_{i,j}$ represents the partial derivative of f_i with respect to j. The eigenvalues of J can easily be calculated if numerical values for each $f_{i,j}$ are plugged into Eq. C.4. However, as described above, the f_is do not have defined functional forms, and thus their partial derivatives do not either. From this point, the system can either be analyzed symbolically in order to gain some mathematical insight into the range of its possible behaviors, or the unknowns can be derived from data. We take the latter approach, based on the data generated from the model of systemic inflammation described above.

C.4: Estimation of Partial Derivatives

To directly calculate the partial derivatives $f_{i,j}$ found in the Jacobian matrix defined in Eq. C.4 would require some assumptions that may not always be practical.

Lade and Gross estimated partial derivatives for their generalized models by assuming that some partial derivatives are directly measurable (such as the death rate of a species in an ecological model) and that the production rate in one equation is equal to the degradation rate in another (Lade and Gross 2012). These assumptions facilitate fairly direct estimates of partial derivatives. However, as we assume that the only data available are the state variables sampled at a constant sampling frequency from the model in Appendix A, a less direct approach towards partial derivative estimation must be taken.

Again considering the *LPS-P-A-F* model from Eq. C.3, the available data is measurements of those four state variables sampled at some constant sampling rate. We used the backwards difference method to calculate the derivatives of these state variables over time, as that gives an estimate of the left hand sides of Eq. C.3 that is most updated with the latest data. However, from this limited data, the partial derivatives cannot be directly calculated. To approach this problem, we assumed that each f_i is linear in each of the variables it depends on. While it is known that the system is truly nonlinear, we hypothesized that assuming linearity over a relatively small time window would be sufficient to identify significant changes in the partial derivatives. We used a time window of 10 hours in all of the simulations shown here, although the results do not seem highly sensitive to this parameter choice as long as it is not wildly off by an order of magnitude or so.

We tried two methods for estimating the linear coefficients for f_i (which are the same as the partial derivatives $f_{i,j}$). First, we applied linear regression to fit the numerical derivatives with the linear f_is. For the *A-F-LPS-P* model shown in Eq. C.3, this is

equivalent to treating the system as is shown in C.5, and then each k_i found through linear regression is an estimated partial derivative.

$$\begin{aligned} dLPS/dt &= k_1 \cdot \mu - k_2 \cdot LPS \\ dP/dt &= k_3 \cdot LPS - k_4 \cdot A + k_5 \cdot P \\ dA/dt &= k_6 \cdot F - k_7 \cdot A \\ dF/dt &= k_8 \cdot P - k_9 \cdot F \end{aligned} \tag{C.5}$$

A main drawback of this approach is that it ignores what we know about the directionality of the network. For instance, the degradation rate of a hormone should always be negative, and LPS should always positively stimulate pro-inflammatory signaling. While these relationships typically held in linear regression, they did not always. To fix the signs of partial derivatives with known directionality in the network, the partial derivative estimation can be formulated as the optimization problem. An example for the *A-F-LPS-P* model is shown in Eq. C.6.

$$\begin{aligned} \text{Minimize} \quad & \left(dLPS/dt - k_1 \cdot \mu + k_2 \cdot LPS\right)^2 + \\ & \left(dP/dt - k_3 \cdot LPS + k_4 \cdot A - k_5 \cdot P\right)^2 + \\ & \left(dA/dt - k_6 \cdot F + k_7 \cdot A\right)^2 + \\ & \left(dF/dt - k_8 \cdot P + k_9 \cdot F\right)^2 \\ \text{subject to} \quad & k_1 > 0 \\ & k_2 > 0 \\ & k_3 > 0 \\ & k_4 > 0 \\ & k_6 > 0 \\ & k_7 > 0 \\ & k_8 > 0 \\ & k_9 > 0 \end{aligned} \tag{C.6}$$

Note that the parameter k_5 is unconstrained because it can be positive when the positive feedback term dominates and negative when the degradation term dominates. To solve Eq. C.6, we applied constrained nonlinear optimization via MATLAB's `fmincon`

function. Because this optimization approach makes more intuitive sense due to further taking advantage of known aspects of high-level network structure, we applied it in all the results presented here. Replacing this method with simple linear regression still typically produces estimates that are good enough to estimate the stability of small generalized models (such as the one including only *A* and *P*), but the additional information conveyed by fixing the sign of the partial derivatives becomes more important for larger generalized models (such as the one including *A*, *F*, *LPS*, and *P*).

C.5: Generalized Models for Predicting Critical Transitions

Successful numerical estimation of the Jacobian matrix and calculation of the eigenvalues produces an estimated quantification of the stability of the system at a certain point in time. As new data streams in, this estimate can be updated to produce a signal that evolves over time. However, the ultimate goal is not to assess the current state of the system, it is to make a prediction about the future. The key to the predictive nature of this approach is that these eigenvalues do contain information about the future behavior of the system. In addition to assessing whether an eigenvalue is above or below a threshold, the trajectory of the eigenvalues over time can provide an indication of an impending loss of stability. Furthermore, the phenomenon of bifurcation delay often results in a period of time between the mathematical loss of stability and significant movement from one steady state to another (Kuehn 2011; Lade and Gross 2012). Therefore, the estimation of the stability of a system based on a generalized model can plausibly prove to be predictive of critical transitions.

Given the construction of a generalized model and the estimation of its relevant partial derivatives as described above, the calculation of the eigenvalues is

straightforward. Then, the question is how to interpret them. Lade and Gross wrote that "A warning is raised if at least one of the eigenvalues shows a clear trend toward the stability boundary (for ODEs, zero real part)" (Lade and Gross 2012). Most fundamentally, detecting an eigenvalue-based warning signal is based on movement in the eigenvalues, which in turn is based on movement in the partial derivatives. While it is not immediately clear how to precisely say how much movement is enough to elicit a warning, the information content in the eigenvalues can be seen in relative terms when compared to the state variables of the system or to derivatives of the state variables.

Acknowledgment of Previous Publications

This dissertation contains significant portions of the following publications:

1. Scheff JD, Mavroudis PD, Foteinou PT, Calvano SE, Androulakis IP: **Modeling physiologic variability in human endotoxemia**. *Crit Rev Biomed Eng* 2012, **40**(4):313–322. PMID: 23140122, doi:10.1615/CritRevBiomedEng.v40.i4.60

2. Scheff JD, Mavroudis PD, Foteinou PT, Calvano SE, Androulakis IP: **Translational applications of evaluating physiologic variability in human endotoxemia**. *J Clin Monit Comput*, in press. PMID: 23203205, doi: 10.1007/s10877-012-9418-1

3. Scheff JD, Mavroudis PD, Calvano SE, Lowry SF, Androulakis IP: **Autonomic dysfunction in SIRS and sepsis**. In *Brain Dysfunction in Critical Illness*. Edited by: Stevens RD , Ely EW, Sharshar T: Cambridge University Press; in press.

4. Scheff JD, Calvano SE, Lowry SF, Androulakis IP: **Modeling the influence of circadian rhythms on the acute inflammatory response.** ***J Theor Biol*** 2010, **264**(3):1068-1076. PMID: 20307551, doi:10.1016/j.jtbi.2010.03.026

5. Scheff JD, Calvano SE, Lowry SF, Androulakis IP: **Transcriptional implications of ultradian glucocorticoid secretion, in homeostasis and in the acute stress response**. *Physiol Genomics* 2012, **42**(2):121–129. PMID: 22128089, doi:10.1152/physiolgenomics.00128.2011

6. Scheff JD, Mavroudis PD, Calvano SE, Lowry SF, Androulakis IP: **Modeling autonomic regulation of cardiac function and heart rate variability in human endotoxemia**. *Physiol Genomics* 2011, **43**(16):951–964. PMID: 21673075, doi:10.1152/physiolgenomics.00040.2011

7. Scheff JD, Corbett SA, Calvano SE, Androulakis IP: **On heart rate and heart rate variability in human endotoxemia**. In preparation.

8. Scheff JD, Calvano SE, Androulakis IP: **Predicting critical transitions in a model of systemic inflammation**. *J Theor Biol*, submitted.

References

Ahmad, S., T. Ramsay, et al. (2009). "Continuous multi-parameter heart rate variability analysis heralds onset of sepsis in adults." PLoS One **4**(8): e6642.

Akselrod, S. (1995). Components of heart rate variability: basic studies. Heart Rate Variability. M. Malik and A. J. Camm. Armonk, NY, Futura**:** 147-63.

Alberti, C., C. Brun-Buisson, et al. (2002). "Epidemiology of sepsis and infection in ICU patients from an international multicentre cohort study." Intensive Care Med **28**(2): 108-21.

Almon, R. R., D. C. DuBois, et al. (2002). "Pharmacodynamics and pharmacogenomics of diverse receptor-mediated effects of methylprednisolone in rats using microarray analysis." J Pharmacokinet Pharmacodyn **29**(2): 103-29.

Almon, R. R., D. C. Dubois, et al. (2005). "Pharmacogenomic responses of rat liver to methylprednisolone: an approach to mining a rich microarray time series." Aaps J **7**(1): E156-94.

Almon, R. R., D. C. DuBois, et al. (2007). "A microarray analysis of the temporal response of liver to methylprednisolone: a comparative analysis of two dosing regimens." Endocrinology **148**(5): 2209-25.

Almon, R. R., W. Lai, et al. (2005). "Corticosteroid-regulated genes in rat kidney: mining time series array data." Am J Physiol Endocrinol Metab **289**(5): E870-82.

Alvarez, S. M., M. Katsamanis Karavidas, et al. (2007). "Low-dose steroid alters in vivo endotoxin-induced systemic inflammation but does not influence autonomic dysfunction." J Endotoxin Res **13**(6): 358-68.

An, G. (2008). "Introduction of an agent-based multi-scale modular architecture for dynamic knowledge representation of acute inflammation." Theor Biol Med Model **5**: 11.

Andreasen, A. S., K. S. Krabbe, et al. (2008). "Human endotoxemia as a model of systemic inflammation." Curr Med Chem **15**(17): 1697-705.

Angus, D. C. (2011). "The search for effective therapy for sepsis: back to the drawing board?" Jama **306**(23): 2614-5.

Angus, D. C., W. T. Linde-Zwirble, et al. (2001). "Epidemiology of severe sepsis in the United States: analysis of incidence, outcome, and associated costs of care." Crit Care Med **29**(7): 1303-10.

Annane, D., F. Trabold, et al. (1999). "Inappropriate sympathetic activation at onset of septic shock: a spectral analysis approach." Am J Respir Crit Care Med **160**(2): 458-65.

Atkinson, H. C., S. A. Wood, et al. (2008). "Corticosteroids mediate fast feedback of the rat hypothalamic-pituitary-adrenal axis via the mineralocorticoid receptor." Am J Physiol Endocrinol Metab **294**(6): E1011-22.

Bairagi, N., S. Chatterjee, et al. (2008). "Variability in the secretion of corticotropin-releasing hormone, adrenocorticotropic hormone and cortisol and understandability of the hypothalamic-pituitary-adrenal axis dynamics--a mathematical study based on clinical evidence." Math Med Biol **25**(1): 37-63.

Ballard, P. L. (1979). "Delivery and transport of glucocorticoids to target cells." Monogr Endocrinol **12**: 25-48.

Bao, A. M., R. Y. Liu, et al. (2003). "Changes in diurnal rhythms of free cortisol secretion during different phases of menstrual cycle." Sheng Li Xue Bao **55**(5): 547-53.

Barber, A. E., S. M. Coyle, et al. (1993). "Glucocorticoid therapy alters hormonal and cytokine responses to endotoxin in man." J Immunol **150**(5): 1999-2006.

Barnaby, D., K. Ferrick, et al. (2002). "Heart rate variability in emergency department patients with sepsis." Acad Emerg Med **9**(7): 661-70.

Barnes, P. J. (1998). "Anti-inflammatory actions of glucocorticoids: molecular mechanisms." Clin Sci (Lond) **94**(6): 557-72.

Bayly, E. J. (1968). "Spectral analysis of pulse frequency modulation in the nervous systems." IEEE Trans Biomed Eng **15**(4): 257-65.

Bayston, K. F. and J. Cohen (1990). "Bacterial endotoxin and current concepts in the diagnosis and treatment of endotoxaemia." J Med Microbiol **31**(2): 73-83.

Beishuizen, A. and L. G. Thijs (2003). "Endotoxin and the hypothalamo-pituitary-adrenal (HPA) axis." J Endotoxin Res **9**(1): 3-24.

Biggs, R., S. R. Carpenter, et al. (2009). "Turning back from the brink: detecting an impending regime shift in time to avert it." Proc Natl Acad Sci U S A **106**(3): 826-31.

Bone, R. C. (1996). "Immunologic dissonance: a continuing evolution in our understanding of the systemic inflammatory response syndrome (SIRS) and the multiple organ dysfunction syndrome (MODS)." Ann Intern Med **125**(8): 680-7.

Bravi, A., A. Longtin, et al. (2011). "Review and classification of variability analysis techniques with clinical applications." Biomed Eng Online **10**: 90.

Brennan, M., M. Palaniswami, et al. (2001). "Do existing measures of Poincare plot geometry reflect nonlinear features of heart rate variability?" IEEE Trans Biomed Eng **48**(11): 1342-7.

Brennan, M., M. Palaniswami, et al. (2002). "Poincare plot interpretation using a physiological model of HRV based on a network of oscillators." Am J Physiol Heart Circ Physiol **283**(5): H1873-86.

Brown, E. N., P. M. Meehan, et al. (2001). "A stochastic differential equation model of diurnal cortisol patterns." Am J Physiol Endocrinol Metab **280**(3): E450-61.

Buchman, T. G. (1996). "Physiologic stability and physiologic state." J Trauma **41**(4): 599-605.

Buchman, T. G. (2009). "The digital patient: predicting physiologic dynamics with mathematical models." Crit Care Med **37**(3): 1167-8.

Buchman, T. G. (2010). "Novel representation of physiologic states during critical illness and recovery." Crit Care **14**(2): 127.

Burger, A. J., M. Charlamb, et al. (1999). "Circadian patterns of heart rate variability in normals, chronic stable angina and diabetes mellitus." International Journal of Cardiology **71**(1): 41-48.

Burgess, H. J., J. Trinder, et al. (1997). "Sleep and circadian influences on cardiac autonomic nervous system activity." Am J Physiol Heart Circ Physiol **273**(4): H1761-1768.

Buttenschoen, K., M. Kornmann, et al. (2008). "Endotoxemia and endotoxin tolerance in patients with ARDS." Langenbecks Arch Surg **393**(4): 473-8.

Carpenter, S. R., J. J. Cole, et al. (2011). "Early warnings of regime shifts: a whole-ecosystem experiment." Science **332**(6033): 1079-82.

Chakraborty, A., W. Krzyzanski, et al. (1999). "Mathematical modeling of circadian cortisol concentrations using indirect response models: comparison of several methods." J Pharmacokinet Biopharm **27**(1): 23-43.

Charloux, A., C. Gronfier, et al. (1999). "Aldosterone release during the sleep-wake cycle in humans." Am J Physiol **276**(1 Pt 1): E43-9.

Chen, L., R. Liu, et al. (2012). "Detecting early-warning signals for sudden deterioration of complex diseases by dynamical network biomarkers." Sci Rep **2**: 342.

Chiu, H. W. and T. Kao (2001). "A mathematical model for autonomic control of heart rate variation." IEEE Eng Med Biol Mag **20**(2): 69-76.

Chiu, H. W., T. H. Wang, et al. (2003). "The influence of mean heart rate on measures of heart rate variability as markers of autonomic function: a model study." Med Eng Phys **25**(6): 475-81.

Clermont, G., J. Bartels, et al. (2004). "In silico design of clinical trials: a method coming of age." Crit Care Med **32**(10): 2061-70.

Cobb, J. P., E. E. Moore, et al. (2009). "Validation of the riboleukogram to detect ventilator-associated pneumonia after severe injury." Ann Surg **250**(4): 531-9.

Cohen, M. J. (2012). "Use of models in identification and prediction of physiology in critically ill surgical patients." Br J Surg **99**(4): 487-93.

Coogan, A. N. and C. A. Wyse (2008). "Neuroimmunology of the circadian clock." Brain Res **1232**: 104-12.

Couto-Moraes, R., J. Palermo-Neto, et al. (2009). "The immune-pineal axis: stress as a modulator of pineal gland function." Ann N Y Acad Sci **1153**: 193-202.

Dakos, V., S. R. Carpenter, et al. (2012). "Methods for detecting early warnings of critical transitions in time series illustrated using simulated ecological data." PLoS One **7**(7): e41010.

Dallman, M. F., S. F. Akana, et al. (2004). "Chronic stress-induced effects of corticosterone on brain: direct and indirect." Ann N Y Acad Sci **1018**: 141-50.

Dallman, M. F. and F. E. Yates (1969). "Dynamic asymmetries in the corticosteroid feedback path and distribution-metabolism-binding elements of the adrenocortical system." Ann N Y Acad Sci **156**(2): 696-721.

Day, J., J. Rubin, et al. (2006). "A reduced mathematical model of the acute inflammatory response II. Capturing scenarios of repeated endotoxin administration." J Theor Biol **242**(1): 237-56.

Deans, K. J., M. Haley, et al. (2005). "Novel therapies for sepsis: a review." J Trauma **58**(4): 867-74.

deBoer, R. W., J. M. Karemaker, et al. (1987). "Hemodynamic fluctuations and baroreflex sensitivity in humans: a beat-to-beat model." Am J Physiol **253**(3 Pt 2): H680-9.

Decker, T. (2004). "Sepsis: avoiding its deadly toll." J Clin Invest **113**(10): 1387-9.

del Gobbo, V., V. Libri, et al. (1989). "Pinealectomy inhibits interleukin-2 production and natural killer activity in mice." Int J Immunopharmacol **11**(5): 567-73.

Desvergne, B. and C. Heligon (2009). "Steroid hormone pulsing drives cyclic gene expression." Nat Cell Biol **11**(9): 1051-3.

Deuschle, M., U. Schweiger, et al. (1997). "Diurnal activity and pulsatility of the hypothalamus-pituitary-adrenal system in male depressed patients and healthy controls." J Clin Endocrinol Metab **82**(1): 234-8.

Dexter, F., M. N. Levy, et al. (1989). "Mathematical model of the changes in heart rate elicited by vagal stimulation." Circ Res **65**(5): 1330-9.

Dick, T. E., Y. I. Molkov, et al. (2012). "Linking Inflammation, Cardiorespiratory Variability, and Neural Control in Acute Inflammation via Computational Modeling." Front Physiol **3**: 222.

Dimitrov, S., C. Benedict, et al. (2009). "Cortisol and epinephrine control opposing circadian rhythms in T cell subsets." Blood **113**(21): 5134-43.

Donadio, V., P. Cortelli, et al. (2008). "Isolated generalised anhidrosis induced by postganglionic sympathetic skin nerve fibre degeneration: an incomplete Ross syndrome?" J Neurol Neurosurg Psychiatry **79**(8): 959-61.

Dong, X., P. T. Foteinou, et al. (2010). "Agent-based modeling of endotoxin-induced acute inflammatory response in human blood leukocytes." PLoS One **5**(2): e9249.

DuBois, D. C., Z. X. Xu, et al. (1995). "Differential dynamics of receptor down-regulation and tyrosine aminotransferase induction following glucocorticoid treatment." J Steroid Biochem Mol Biol **54**(5-6): 237-43.

Eckberg, D. L. (1997). "Sympathovagal balance: a critical appraisal." Circulation **96**(9): 3224-32.

Elenkov, I. J., R. L. Wilder, et al. (2000). "The sympathetic nerve--an integrative interface between two supersystems: the brain and the immune system." Pharmacol Rev **52**(4): 595-638.

Ellenby, M. S., J. McNames, et al. (2001). "Uncoupling and recoupling of autonomic regulation of the heart beat in pediatric septic shock." Shock **16**(4): 274-7.

Engler, D., T. Pham, et al. (1989). "Studies of the secretion of corticotropin-releasing factor and arginine vasopressin into the hypophysial-portal circulation of the conscious sheep. I. Effect of an audiovisual stimulus and insulin-induced hypoglycemia." Neuroendocrinology **49**(4): 367-81.

Ewing, D. J., J. M. Neilson, et al. (1991). "Twenty four hour heart rate variability: effects of posture, sleep, and time of day in healthy controls and comparison with bedside tests of autonomic function in diabetic patients." Br Heart J **65**(5): 239-44.

Fairchild, K. D., V. Srinivasan, et al. (2011). "Pathogen-induced heart rate changes associated with cholinergic nervous system activation." Am J Physiol Regul Integr Comp Physiol **300**(2): R330-9.

Feldman, D., C. E. Mondon, et al. (1979). "Glucocorticoid and estrogen regulation of corticosteroid-binding globulin production by rat liver." Am J Physiol **237**(6): E493-9.

Fernandes, P. A., B. Bothorel, et al. (2009). "Local corticosterone infusion enhances nocturnal pineal melatonin production in vivo." J Neuroendocrinol **21**(2): 90-7.

Fernandes, P. A., E. Cecon, et al. (2006). "Effect of TNF-alpha on the melatonin synthetic pathway in the rat pineal gland: basis for a 'feedback' of the immune response on circadian timing." J Pineal Res **41**(4): 344-50.

Ferreira, Z. S., P. A. Fernandes, et al. (2005). "Corticosterone modulates noradrenaline-induced melatonin synthesis through inhibition of nuclear factor kappa B." J Pineal Res **38**(3): 182-8.

Flower, A. A., J. R. Moorman, et al. (2010). "Periodic heart rate decelerations in premature infants." Exp Biol Med (Maywood) **235**(4): 531-8.

Foteinou, P. T., S. E. Calvano, et al. (2009). "In silico simulation of corticosteroids effect on an NFkB- dependent physicochemical model of systemic inflammation." PLoS One **4**(3): e4706.

Foteinou, P. T., S. E. Calvano, et al. (2009). "Modeling endotoxin-induced systemic inflammation using an indirect response approach." Math Biosci **217**(1): 27-42.

Foteinou, P. T., S. E. Calvano, et al. (2009). "Translational potential of systems-based models of inflammation." Clin Transl Sci **2**(1): 85-9.

Foteinou, P. T., S. E. Calvano, et al. (2010). "Multiscale model for the assessment of autonomic dysfunction in human endotoxemia." Physiol Genomics **42**(1): 5-19.

Foteinou, P. T., S. E. Calvano, et al. (2011). "A physiological model for autonomic heart rate regulation in human endotoxemia." Shock **35**(3): 229-39.

Freeman, B. D. and C. Natanson (2000). "Anti-inflammatory therapies in sepsis and septic shock." Expert Opin Investig Drugs **9**(7): 1651-63.

Garnier-Suillerot, A. (1995). "Impaired accumulation of drug in multidrug resistant cells. What are the respective contributions of the kinetics of uptake and of P-glycoprotein-mediated efflux of drug?" Curr Pharm Des **1**(1): 69-82.

Garrard, C. S., D. A. Kontoyannis, et al. (1993). "Spectral analysis of heart rate variability in the sepsis syndrome." Clin Auton Res **3**(1): 5-13.

Gherghel, D., S. L. Hosking, et al. (2004). "Autonomic nervous system, circadian rhythms, and primary open-angle glaucoma." Surv Ophthalmol **49**(5): 491-508.

Gholami, M., P. Mazaheri, et al. (2012). "Endotoxemia is associated with partial uncoupling of cardiac pacemaker from cholinergic neural control in rats." Shock **37**(2): 219-27.

Godin, P. J. and T. G. Buchman (1996). "Uncoupling of biological oscillators: a complementary hypothesis concerning the pathogenesis of multiple organ dysfunction syndrome." Crit Care Med **24**(7): 1107-16.

Godin, P. J., L. A. Fleisher, et al. (1996). "Experimental human endotoxemia increases cardiac regularity: results from a prospective, randomized, crossover trial." Crit Care Med **24**(7): 1117-24.

Goldberger, J. J., S. Challapalli, et al. (2001). "Relationship of heart rate variability to parasympathetic effect." Circulation **103**(15): 1977-83.

Griffin, M. P., T. M. O'Shea, et al. (2003). "Abnormal heart rate characteristics preceding neonatal sepsis and sepsis-like illness." Pediatr Res **53**(6): 920-6.

Grivas, T. B. and O. D. Savvidou (2007). "Melatonin the "light of night" in human biology and adolescent idiopathic scoliosis." Scoliosis **2**: 6.

Gross, T. and U. Feudel (2006). "Generalized models as a universal approach to the analysis of nonlinear dynamical systems." Phys Rev E Stat Nonlin Soft Matter Phys **73**(1 Pt 2): 016205.

Guerrero, J. M. and R. J. Reiter (2002). "Melatonin-immune system relationships." Curr Top Med Chem **2**(2): 167-79.

Gupta, S., E. Aslakson, et al. (2007). "Inclusion of the glucocorticoid receptor in a hypothalamic pituitary adrenal axis model reveals bistability." Theor Biol Med Model **4**: 8.

Gutenkunst, R. N., J. J. Waterfall, et al. (2007). "Universally sloppy parameter sensitivities in systems biology models." PLoS Comput Biol **3**(10): 1871-78.

Haimovich, B., J. Calvano, et al. (2010). "In vivo endotoxin synchronizes and suppresses clock gene expression in human peripheral blood leukocytes." Crit Care Med **38**(3): 751-8.

Haimovich, B., M. T. Reddell, et al. (2010). "A novel model of common Toll-like receptor 4- and injury-induced transcriptional themes in human leukocytes." Crit Care **14**(5): R177.

Harbuz, M. S., R. J. Windle, et al. (1999). "Differential effects of psychological and immunological challenge on the hypothalamo-pituitary-adrenal axis function in adjuvant-induced arthritis." Ann N Y Acad Sci **876**: 43-52.

Hermann, C., S. von Aulock, et al. (2006). "Endogenous cortisol determines the circadian rhythm of lipopolysaccharide-- but not lipoteichoic acid--inducible cytokine release." Eur J Immunol **36**(2): 371-9.

Hrushesky, W. J. and P. A. Wood (1997). "Circadian time structure of septic shock: timing is everything." J Infect Dis **175**(5): 1283-4.

Hrushesky, W. J. M., T. Langevin, et al. (1994). "Circadian Dynamics of Tumor-Necrosis-Factor-Alpha (Cachectin) Lethality." Journal of Experimental Medicine **180**(3): 1059-1065.

Hrushesky, W. J. M. and P. A. Wood (1997). "Circadian time structure of septic shock: Timing is everything." Journal of Infectious Diseases **175**(5): 1283-1284.

Huang, J., Y. Wang, et al. (2010). "The sympathetic-vagal balance against endotoxemia." J Neural Transm **117**(6): 729-35.

Huikuri, H. V., M. J. Niemela, et al. (1994). "Circadian rhythms of frequency domain measures of heart rate variability in healthy subjects and patients with coronary artery disease. Effects of arousal and upright posture." Circulation **90**(1): 121-6.

Huston, J. M. and K. J. Tracey (2011). "The pulse of inflammation: heart rate variability, the cholinergic anti-inflammatory pathway and implications for therapy." J Intern Med **269**(1): 45-53.

Ihekwaba, A. E., D. S. Broomhead, et al. (2004). "Sensitivity analysis of parameters controlling oscillatory signalling in the NF-kappaB pathway: the roles of IKK and IkappaBalpha." Syst Biol (Stevenage) **1**(1): 93-103.

Ingram, J. R., J. N. Crockford, et al. (1999). "Ultradian, circadian and seasonal rhythms in cortisol secretion and adrenal responsiveness to ACTH and yarding in unrestrained red deer (Cervus elaphus) stags." J Endocrinol **162**(2): 289-300.

Ito, K., K. F. Chung, et al. (2006). "Update on glucocorticoid action and resistance." J Allergy Clin Immunol **117**(3): 522-43.

Ixart, G., G. Barbanel, et al. (1991). "A quantitative study of the pulsatile parameters of CRH-41 secretion in unanesthetized free-moving rats." Exp Brain Res **87**(1): 153-8.

Jan, B. U., S. M. Coyle, et al. (2010). "Relationship of basal heart rate variability to in vivo cytokine responses after endotoxin exposure." Shock **33**(4): 363-8.

Jan, B. U., S. M. Coyle, et al. (2009). "Influence of acute epinephrine infusion on endotoxin-induced parameters of heart rate variability: a randomized controlled trial." Ann Surg **249**(5): 750-6.

Javorka, M., I. Zila, et al. (2002). "Heart rate recovery after exercise: relations to heart rate variability and complexity." Braz J Med Biol Res **35**(8): 991-1000.

Jelic, S., Z. Cupic, et al. (2005). "Mathematical modeling of the hypothalamic-pituitary-adrenal system activity." Math Biosci **197**(2): 173-87.

Jiang-Shieh, Y. F., C. H. Wu, et al. (2005). "Reactive changes of interstitial glia and pinealocytes in the rat pineal gland challenged with cell wall components from gram-positive and -negative bacteria." J Pineal Res **38**(1): 17-26.

Jin, J. Y., R. R. Almon, et al. (2003). "Modeling of corticosteroid pharmacogenomics in rat liver using gene microarrays." J Pharmacol Exp Ther **307**(1): 93-109.

Jit, M., B. Henderson, et al. (2005). "TNF-alpha neutralization in cytokine-driven diseases: a mathematical model to account for therapeutic success in rheumatoid arthritis but therapeutic failure in systemic inflammatory response syndrome." Rheumatology (Oxford) **44**(3): 323-31.

Jusko, W. J. (1994). "Receptor-mediated pharmacodynamics of corticosteroids." Prog Clin Biol Res **387**: 261-70.

Jusko, W. J., D. DuBois, et al. (2005). "Sixth-Generation Model for Corticosteroid Pharmacodynamics: Multi-Hormonal Regulation of Tyrosine Aminotransferase in Rat Liver." J Pharmacokin Pharmacodyn.

Karemaker, J. M. (1999). "Autonomic integration: the physiological basis of cardiovascular variability." J Physiol **517 (Pt 2)**: 316.

Keenan, D. M., J. Licinio, et al. (2001). "A feedback-controlled ensemble model of the stress-responsive hypothalamo-pituitary-adrenal axis." Proc Natl Acad Sci U S A **98**(7): 4028-33.

Keenan, D. M. and J. D. Veldhuis (2003). "Cortisol feedback state governs adrenocorticotropin secretory-burst shape, frequency, and mass in a dual-waveform construct: time of day-dependent regulation." Am J Physiol Regul Integr Comp Physiol **285**(5): R950-61.

Keller, N., U. I. Richardson, et al. (1969). "Protein binding and the biological activity of corticosteroids: in vivo induction of hepatic and pancreatic alanine aminotransferases by corticosteroids in normal and estrogen-treated rats." Endocrinology **84**(1): 49-62.

Kitano, H. (2002). "Systems biology: a brief overview." Science **295**(5560): 1662-4.

Kleiger, R. E., J. P. Miller, et al. (1987). "Decreased heart rate variability and its association with increased mortality after acute myocardial infarction." Am J Cardiol **59**(4): 256-62.

Kochanek, K. D. and B. L. Smith (2004). "Deaths: preliminary data for 2002." Natl Vital Stat Rep **52**(13): 1-47.

Kohsaka, A. and J. Bass (2007). "A sense of time: how molecular clocks organize metabolism." Trends Endocrinol Metab **18**(1): 4-11.

Korach, M., T. Sharshar, et al. (2001). "Cardiac variability in critically ill adults: influence of sepsis." Crit Care Med **29**(7): 1380-5.

Korpelainen, J. T., K. A. Sotaniemi, et al. (1997). "Circadian rhythm of heart rate variability is reversibly abolished in ischemic stroke." Stroke **28**(11): 2150-4.

Kox, M., B. P. Ramakers, et al. (2011). "Interplay between the acute inflammatory response and heart rate variability in healthy human volunteers." Shock **36**(2): 115-20.

Kronfol, Z., M. Nair, et al. (1997). "Circadian immune measures in healthy volunteers: relationship to hypothalamic-pituitary-adrenal axis hormones and sympathetic neurotransmitters." Psychosom Med **59**(1): 42-50.

Kuehn, C. (2011). "A mathematical framework for critical transitions: Bifurcations, fast-slow systems and stochastic dynamics." Physica D **240**(12): 1020–35.

Kuehn, C. and T. Gross (2011). "Nonlocal generalized models of predator-prey systems." http://arxiv.org/abs/1105.3662.

Kuehn, C., S. Siegmund, et al. (2012). "Dynamical analysis of evolution equations in generalized models." IMA J Appl Math.

Kumar, R., C. C. Chow, et al. (2008). "A mathematical simulation of the inflammatory response to anthrax infection." Shock **29**(1): 104-11.

Kumar, R., G. Clermont, et al. (2004). "The dynamics of acute inflammation." J Theor Biol **230**(2): 145-55.

Kyrylov, V., L. A. Severyanova, et al. (2005). "Modeling robust oscillatory behavior of the hypothalamic-pituitary-adrenal axis." IEEE Trans Biomed Eng **52**(12): 1977-83.

Lade, S. J. and T. Gross (2012). "Early warning signals for critical transitions: a generalized modeling approach." PLoS Comput Biol **8**(2): e1002360.

Lahiri, M. K., P. J. Kannankeril, et al. (2008). "Assessment of autonomic function in cardiovascular disease: physiological basis and prognostic implications." J Am Coll Cardiol **51**(18): 1725-33.

Lake, D. E., J. S. Richman, et al. (2002). "Sample entropy analysis of neonatal heart rate variability." Am J Physiol Regul Integr Comp Physiol **283**(3): R789-97.

Lander, A. D. (2004). "A calculus of purpose." PLoS Biol **2**(6): e164.

Lehrer, P., M. K. Karavidas, et al. (2010). "Voluntarily produced increases in heart rate variability modulate autonomic effects of endotoxin induced systemic inflammation: an exploratory study." Appl Psychophysiol Biofeedback **35**(4): 303-15.

Levi, F. and U. Schibler (2007). "Circadian rhythms: mechanisms and therapeutic implications." Annu Rev Pharmacol Toxicol **47**: 593-628.

Li, N. Y., K. Verdolini, et al. (2008). "A patient-specific in silico model of inflammation and healing tested in acute vocal fold injury." PLoS One **3**(7): e2789.

Lightman, S. L. and B. L. Conway-Campbell (2010). "The crucial role of pulsatile activity of the HPA axis for continuous dynamic equilibration." Nat Rev Neurosci **11**(10): 710-8.

Lightman, S. L., C. C. Wiles, et al. (2008). "The significance of glucocorticoid pulsatility." Eur J Pharmacol **583**(2-3): 255-62.

Lipniacki, T., P. Paszek, et al. (2006). "Stochastic regulation in early immune response." Biophys J **90**(3): 725-42.

Liu, Y. W., Z. H. Hu, et al. (1999). "A dynamical model for the pulsatile secretion of the hypothalamo-pituitary-adrenal axis." Math Comput Model **29**(4): 103-10.

Lombardi, F., A. Malliani, et al. (1996). "Heart rate variability and its sympatho-vagal modulation." Cardiovasc Res **32**(2): 208-16.

Lowry, S. F. (2005). "Human endotoxemia: a model for mechanistic insight and therapeutic targeting." Shock **24 Suppl 1**: 94-100.

Lowry, S. F. (2009). "The stressed host response to infection: the disruptive signals and rhythms of systemic inflammation." Surg Clin North Am **89**(2): 311-26, vii.

Lowry, S. F. and S. E. Calvano (2008). "Challenges for modeling and interpreting the complex biology of severe injury and inflammation." J Leukoc Biol **83**(3): 553-7.

Ma, X. M., A. Levy, et al. (1997). "Rapid changes of heteronuclear RNA for arginine vasopressin but not for corticotropin releasing hormone in response to acute corticosterone administration." J Neuroendocrinol **9**(10): 723-8.

Mager, D. E., N. A. Pyszczynski, et al. (2003). "Integrated QSPR--pharmacodynamic model of genomic effects of several corticosteroids." J Pharm Sci **92**(4): 881-9.

Malliani, A., F. Lombardi, et al. (1994). "Power spectrum analysis of heart rate variability: a tool to explore neural regulatory mechanisms." Br Heart J **71**(1): 1-2.

Marshall, J. C. (2003). "Such stuff as dreams are made on: mediator-directed therapy in sepsis." Nat Rev Drug Discov **2**(5): 391-405.

Marshall, J. C. (2008). "Sepsis: rethinking the approach to clinical research." J Leukoc Biol **83**(3): 471-82.

Martin, G. S., D. M. Mannino, et al. (2003). "The epidemiology of sepsis in the United States from 1979 through 2000." N Engl J Med **348**(16): 1546-54.

Massin, M. M., K. Maeyns, et al. (2000). "Circadian rhythm of heart rate and heart rate variability." Arch Dis Child **83**(2): 179-82.

Matzinger, P. (2002). "The danger model: a renewed sense of self." Science **296**(5566): 301-5.

Mavroudis, P. D., J. D. Scheff, et al. (2012). "Entrainment of peripheral clock genes by cortisol." Physiol Genomics **44**(11): 607-21.

McMaster, A., M. Jangani, et al. (2011). "Ultradian cortisol pulsatility encodes a distinct, biologically important signal." PLoS One **6**(1): e15766.

McNally, J. G., W. G. Muller, et al. (2000). "The glucocorticoid receptor: rapid exchange with regulatory sites in living cells." Science **287**(5456): 1262-5.

Mershon, J. L., C. S. Sehlhorst, et al. (1992). "Evidence of a corticotropin-releasing hormone pulse generator in the macaque hypothalamus." Endocrinology **130**(5): 2991-6.

Mi, Q., B. Riviere, et al. (2007). "Agent-based model of inflammation and wound healing: insights into diabetic foot ulcer pathology and the role of transforming growth factor-beta1." Wound Repair Regen **15**(5): 671-82.

Miyata, T. and M. Torisu (1986). "Plasma endotoxin levels and functions of peripheral granulocytes in surgical patients with respiratory distress syndrome." Jpn J Surg **16**(6): 412-7.

Moorman, J. R., W. A. Carlo, et al. (2011). "Mortality reduction by heart rate characteristic monitoring in very low birth weight neonates: a randomized trial." J Pediatr **159**(6): 900-6 e1.

Mormann, F., R. G. Andrzejak, et al. (2007). "Seizure prediction: the long and winding road." Brain **130**(Pt 2): 314-33.

Mormont, M. C. and F. Levi (1997). "Circadian-system alterations during cancer processes: a review." Int J Cancer **70**(2): 241-7.

Morris, J. A., Jr., P. R. Norris, et al. (2007). "Adrenal insufficiency, heart rate variability, and complex biologic systems: a study of 1,871 critically ill trauma patients." J Am Coll Surg **204**(5): 885-92; discussion 892-3.

Morris, M. K., J. Saez-Rodriguez, et al. (2011). "Training signaling pathway maps to biochemical data with constrained fuzzy logic: quantitative analysis of liver cell responses to inflammatory stimuli." PLoS Comput Biol **7**(3): e1001099.

Mundigler, G., G. Delle-Karth, et al. (2002). "Impaired circadian rhythm of melatonin secretion in sedated critically ill patients with severe sepsis." Crit Care Med **30**(3): 536-40.

Munford, R. S. and K. J. Tracey (2002). "Is severe sepsis a neuroendocrine disease?" Mol Med **8**(8): 437-42.

Nakagawa, M., T. Iwao, et al. (1998). "Circadian rhythm of the signal averaged electrocardiogram and its relation to heart rate variability in healthy subjects." Heart **79**(5): 493-6.

Nakao, M., M. Norimatsu, et al. (1997). "Spectral distortion properties of the integral pulse frequency modulation model." IEEE Trans Biomed Eng **44**(5): 419-26.

Namas, R., R. Zamora, et al. (2011). "Sepsis: Something old, something new, and a systems view." J Crit Care.

Nieman, G., D. Brown, et al. (2012). "A two-compartment mathematical model of endotoxin-induced inflammatory and physiologic alterations in swine." Crit Care Med **40**(4): 1052-63.

Niklasson, U., U. Wiklund, et al. (1993). "Heart-rate variation: what are we measuring?" Clin Physiol **13**(1): 71-9.

Novak, B. and J. J. Tyson (2008). "Design principles of biochemical oscillators." Nat Rev Mol Cell Biol **9**(12): 981-91.

Octavio, J. A., A. E. Rodriguez, et al. (2004). "[Circadian profiles of heart rate and its instantaneous variability in patients with chronic Chagas' disease]." Rev Esp Cardiol **57**(2): 130-7.

Opal, S. M. and V. A. DePalo (2000). "Anti-inflammatory cytokines." Chest **117**(4): 1162-72.

Opal, S. M., P. J. Scannon, et al. (1999). "Relationship between plasma levels of lipopolysaccharide (LPS) and LPS-binding protein in patients with severe sepsis and septic shock." J Infect Dis **180**(5): 1584-9.

Ottesen, J. T. (2011). The mathematical microscope – making the inaccessible accessible. BetaSys. B. Booß-Bavnbek, B. Klösgen, J. Larsen, F. Pociot and E. Renström, Springer. **2:** 97-118.

Pagani, M. (2000). "Heart rate variability and autonomic diabetic neuropathy." Diabetes Nutr Metab **13**(6): 341-6.

Papaikonomou, E. (1977). "Rat adrenocortical dynamics." J Physiol **265**(1): 119-31.

Parrillo, J. E. (1993). "Pathogenetic mechanisms of septic shock." N Engl J Med **328**(20): 1471-7.

Pavlov, V. A., H. Wang, et al. (2003). "The cholinergic anti-inflammatory pathway: a missing link in neuroimmunomodulation." Mol Med **9**(5-8): 125-34.

Peng, C. K., S. Havlin, et al. (1995). "Quantification of scaling exponents and crossover phenomena in nonstationary heartbeat time series." Chaos **5**(1): 82-7.

Petrovsky, N. and L. C. Harrison (1997). "Diurnal rhythmicity of human cytokine production: a dynamic disequilibrium in T helper cell type 1/T helper cell type 2 balance?" J Immunol **158**(11): 5163-8.

Petrovsky, N. and L. C. Harrison (1998). "The chronobiology of human cytokine production." Int Rev Immunol **16**(5-6): 635-49.

Petrovsky, N., P. McNair, et al. (1998). "Diurnal rhythms of pro-inflammatory cytokines: regulation by plasma cortisol and therapeutic implications." Cytokine **10**(4): 307-12.

Piepoli, M., C. S. Garrard, et al. (1995). "Autonomic control of the heart and peripheral vessels in human septic shock." Intensive Care Med **21**(2): 112-9.

Pigolotti, S., S. Krishna, et al. (2007). "Oscillation patterns in negative feedback loops." Proc Natl Acad Sci U S A **104**(16): 6533-7.

Pincus, S. M. (1994). "Greater signal regularity may indicate increased system isolation." Math Biosci **122**(2): 161-81.

Polk, D. E., S. Cohen, et al. (2005). "State and trait affect as predictors of salivary cortisol in healthy adults." Psychoneuroendocrinology **30**(3): 261-72.

Ponikowski, P., S. D. Anker, et al. (1997). "Depressed heart rate variability as an independent predictor of death in chronic congestive heart failure secondary to ischemic or idiopathic dilated cardiomyopathy." Am J Cardiol **79**(12): 1645-50.

Pontes, G. N., E. C. Cardoso, et al. (2006). "Injury switches melatonin production source from endocrine (pineal) to paracrine (phagocytes) - melatonin in human colostrum and colostrum phagocytes." J Pineal Res **41**(2): 136-41.

Pontes, G. N., E. C. Cardoso, et al. (2007). "Pineal melatonin and the innate immune response: the TNF-alpha increase after cesarean section suppresses nocturnal melatonin production." J Pineal Res **43**(4): 365-71.

Prince, J. M., R. M. Levy, et al. (2006). "In silico and in vivo approach to elucidate the inflammatory complexity of CD14-deficient mice." Mol Med **12**(4-6): 88-96.

Pyetan, E. and S. Akselrod (2003). "Do the high-frequency indexes of HRV provide a faithful assessment of cardiac vagal tone? A critical theoretical evaluation." IEEE Trans Biomed Eng **50**(6): 777-83.

Pyetan, E. and S. Akselrod (2004). "A theoretical appraisal of the dependence of respiratory sinus arrhythmia on gradual vagal blockade." Methods Inf Med **43**(1): 52-5.

Pyetan, E., O. Zoran, et al. (2001). "A theoretical model for the dependency of heart rate on gradual vagal blockade by atropine." Comput Cardiol **28**: 653-6.

Raghavendra, V., V. Singh, et al. (2001). "Melatonin enhances Th2 cell mediated immune responses: lack of sensitivity to reversal by naltrexone or benzodiazepine receptor antagonists." Mol Cell Biochem **221**(1-2): 57-62.

Raison, C. L. and A. H. Miller (2003). "When not enough is too much: the role of insufficient glucocorticoid signaling in the pathophysiology of stress-related disorders." Am J Psychiatry **160**(9): 1554-65.

Rajasethupathy, P., S. J. Vayttaden, et al. (2005). "Systems modeling: a pathway to drug discovery." Curr Opin Chem Biol **9**(4): 400-6.

Ramakrishnan, R., D. C. DuBois, et al. (2002). "Fifth-generation model for corticosteroid pharmacodynamics: application to steady-state receptor down-regulation and

enzyme induction patterns during seven-day continuous infusion of methylprednisolone in rats." J Pharmacokinet Pharmacodyn **29**(1): 1-24.
Rassias, A. J., P. M. Guyre, et al. (2011). "Hydrocortisone at stress-associated concentrations helps maintain human heart rate variability during subsequent endotoxin challenge." J Crit Care.
Rassias, A. J., P. M. Guyre, et al. (2011). "Hydrocortisone at stress-associated concentrations helps maintain human heart rate variability during subsequent endotoxin challenge." J Crit Care **26**(6): 636 e1-5.
Rassias, A. J., P. T. Holzberger, et al. (2005). "Decreased physiologic variability as a generalized response to human endotoxemia." Crit Care Med **33**(3): 512-9.
Reddy, T. E., F. Pauli, et al. (2009). "Genomic determination of the glucocorticoid response reveals unexpected mechanisms of gene regulation." Genome Res **19**(12): 2163-71.
Reppert, S. M. and D. R. Weaver (2002). "Coordination of circadian timing in mammals." Nature **418**(6901): 935-41.
Reynolds, A., J. Rubin, et al. (2006). "A reduced mathematical model of the acute inflammatory response: I. Derivation of model and analysis of anti-inflammation." J Theor Biol **242**(1): 220-36.
Richman, J. S. and J. R. Moorman (2000). "Physiological time-series analysis using approximate entropy and sample entropy." Am J Physiol Heart Circ Physiol **278**(6): H2039-49.
Ridley, S. (2005). "The recognition and early management of critical illness." Ann R Coll Surg Engl **87**(5): 315-22.
Rosmond, R., M. F. Dallman, et al. (1998). "Stress-related cortisol secretion in men: relationships with abdominal obesity and endocrine, metabolic and hemodynamic abnormalities." J Clin Endocrinol Metab **83**(6): 1853-9.
Russell, G. M., D. E. Henley, et al. (2010). "Rapid glucocorticoid receptor-mediated inhibition of hypothalamic-pituitary-adrenal ultradian activity in healthy males." J Neurosci **30**(17): 6106-15.
Saito, Y., T. Shimizu, et al. (1996). "Effect of bright light exposure on muscle sympathetic nerve activity in human." Neuroscience Letters **219**(2): 135-137.
Saul, J. P. (1990). "Beat-to-beat variations of heart rate reflect modulation of cardiac autonomic outflow." News Physiol Sci **5**(1): 32-7.
Savić, D. and S. Jelić (2005). "A mathematical model of the hypothalamo-pituitary-adrenocortical system and its stability analysis." Chaos Soliton Fract **26**(2): 427-36.
Sayk, F., A. Vietheer, et al. (2008). "Endotoxemia causes central downregulation of sympathetic vasomotor tone in healthy humans." Am J Physiol Regul Integr Comp Physiol **295**(3): R891-8.
Schaaf, M. J. and J. A. Cidlowski (2002). "Molecular mechanisms of glucocorticoid action and resistance." J Steroid Biochem Mol Biol **83**(1-5): 37-48.
Schaller, M. D., B. Waeber, et al. (1985). "Angiotensin II, vasopressin, and sympathetic activity in conscious rats with endotoxemia." Am J Physiol **249**(6 Pt 2): H1086-92.
Scheff, J. D., S. E. Calvano, et al. (2010). "Modeling the influence of circadian rhythms on the acute inflammatory response." J Theor Biol **264**(3): 1068-76.

Scheff, J. D., A. K. Kosmides, et al. (in press). "Pulsatile glucocorticoid secretion: origins and downstream effects." IEEE Trans Biomed Eng.

Scheff, J. D., P. D. Mavroudis, et al. (2012). "Translational applications of evaluating physiologic variability in human endotoxemia." J Clin Monit Comput.

Scheff, J. D., P. D. Mavroudis, et al. (2011). "Modeling autonomic regulation of cardiac function and heart rate variability in human endotoxemia." Physiol Genomics **43**(16): 951-64.

Scheff, J. D., P. D. Mavroudis, et al. (in press). Autonomic dysfunction in SIRS and sepsis. Brain Disorders in Critical Illness. R. D. Stevens, T. Sharshar and E. W. Ely, Cambridge University Press.

Scheff, J. D., P. D. Mavroudis, et al. (2012). "Modeling physiologic variability in human endotoxemia." Crit Rev Biomed Eng **40**(4): 313-22.

Scheffer, M., J. Bascompte, et al. (2009). "Early-warning signals for critical transitions." Nature **461**(7260): 53-9.

Schmidt, H., U. Muller-Werdan, et al. (2004). "Impaired chemoreflex sensitivity in adult patients with multiple organ dysfunction syndrome--the potential role of disease severity." Intensive Care Med **30**(4): 665-72.

Schmidt, H., U. Müller-Werdan, et al. (2007). Autonomic dysfunction: A relevant component in multiple organ dysfunction syndrome. Yearbook of Intensive Care and Emergency Medicine. J. L. Vincent, Springer**:** 455-467.

Schmidt, H. B., K. Werdan, et al. (2001). "Autonomic dysfunction in the ICU patient." Curr Opin Crit Care **7**(5): 314-22.

Seely, A. J. and N. V. Christou (2000). "Multiple organ dysfunction syndrome: exploring the paradigm of complex nonlinear systems." Crit Care Med **28**(7): 2193-200.

Sephton, S. E., R. M. Sapolsky, et al. (2000). "Diurnal cortisol rhythm as a predictor of breast cancer survival." J Natl Cancer Inst **92**(12): 994-1000.

Seydnejad, S. R. and R. I. Kitney (2001). "Modeling of Mayer waves generation mechanisms." IEEE Eng Med Biol Mag **20**(2): 92-100.

Shampine, L. F. and S. Thompson (2001). "Solving DDEs in MATLAB." Appl Numer Math **37**(4): 441-58.

Shanker, B.-A., S. M. Coyle, et al. (2010). "Modeling the human injury response." Journal of the American College of Surgeons **211**(3, Supplement 1): S53-S54.

Shmulevich, I., E. R. Dougherty, et al. (2002). "Probabilistic Boolean Networks: a rule-based uncertainty model for gene regulatory networks." Bioinformatics **18**(2): 261-74.

Skwarlo-Sonta, K., P. Majewski, et al. (2003). "Bidirectional communication between the pineal gland and the immune system." Can J Physiol Pharmacol **81**(4): 342-9.

Sontag, E. D. (2004). "Some new directions in control theory inspired by systems biology." Syst Biol (Stevenage) **1**(1): 9-18.

Sriram, K., M. Rodriguez-Fernandez, et al. (2012). "Modeling cortisol dynamics in the neuro-endocrine axis distinguishes normal, depression, and post-traumatic stress disorder (PTSD) in humans." PLoS Comput Biol **8**(2): e1002379.

Stavreva, D. A., M. Wiench, et al. (2009). "Ultradian hormone stimulation induces glucocorticoid receptor-mediated pulses of gene transcription." Nat Cell Biol **11**(9): 1093-102.

Sternberg, E. M. (2006). "Neural regulation of innate immunity: a coordinated nonspecific host response to pathogens." Nat Rev Immunol **6**(4): 318-28.

Sun, Y. N., D. C. DuBois, et al. (1998). "Fourth-generation model for corticosteroid pharmacodynamics: a model for methylprednisolone effects on receptor/gene-mediated glucocorticoid receptor down-regulation and tyrosine aminotransferase induction in rat liver." J Pharmacokinet Biopharm **26**(3): 289-317.

Takayama, K., K. Yuhki, et al. (2005). "Thromboxane A2 and prostaglandin F2alpha mediate inflammatory tachycardia." Nat Med **11**(5): 562-6.

Task (1996). "Heart rate variability: standards of measurement, physiological interpretation and clinical use. Task Force of the European Society of Cardiology and the North American Society of Pacing and Electrophysiology." Circulation **93**(5): 1043-65.

Tateishi, Y., S. Oda, et al. (2007). "Depressed heart rate variability is associated with high IL-6 blood level and decline in the blood pressure in septic patients." Shock **28**(5): 549-53.

Tracey, K. J. (2002). "The inflammatory reflex." Nature **420**(6917): 853-9.

van der Poll, T. (2001). "Effects of catecholamines on the inflammatory response." Sepsis **4**(2): 159-67.

van der Poll, T., A. E. Barber, et al. (1996). "Hypercortisolemia increases plasma interleukin-10 concentrations during human endotoxemia--a clinical research center study." J Clin Endocrinol Metab **81**(10): 3604-6.

van der Poll, T., S. M. Coyle, et al. (1996). "Epinephrine inhibits tumor necrosis factor-alpha and potentiates interleukin 10 production during human endotoxemia." J Clin Invest **97**(3): 713-9.

Veldhuis, J. D., A. Iranmanesh, et al. (1989). "Amplitude modulation of a burstlike mode of cortisol secretion subserves the circadian glucocorticoid rhythm." Am J Physiol **257**(1 Pt 1): E6-14.

Veldhuis, J. D., A. Iranmanesh, et al. (2001). "Corticotropin secretory dynamics in humans under low glucocorticoid feedback." J Clin Endocrinol Metab **86**(11): 5554-63.

Veldhuis, J. D., D. M. Keenan, et al. (2008). "Motivations and methods for analyzing pulsatile hormone secretion." Endocr Rev **29**(7): 823-64.

Venegas, J. G., T. Winkler, et al. (2005). "Self-organized patchiness in asthma as a prelude to catastrophic shifts." Nature **434**(7034): 777-82.

Vinther, F., M. Andersen, et al. (2010). "The minimal model of the hypothalamic-pituitary-adrenal axis." J Math Biol **63**(4): 663-90.

Vodovotz, Y. (2010). "Translational systems biology of inflammation and healing." Wound Repair Regen **18**(1): 3-7.

Vodovotz, Y., G. Clermont, et al. (2004). "Mathematical models of the acute inflammatory response." Curr Opin Crit Care **10**(5): 383-90.

Vodovotz, Y., G. Constantine, et al. (2009). "Mechanistic simulations of inflammation: current state and future prospects." Math Biosci **217**(1): 1-10.

Vodovotz, Y., M. Csete, et al. (2008). "Translational systems biology of inflammation." PLoS Comput Biol **4**(4): e1000014.

Walker, J. J., J. R. Terry, et al. (2010). "Origin of ultradian pulsatility in the hypothalamic-pituitary-adrenal axis." Proc Biol Sci **277**(1688): 1627-33.

Warner, H. R. and A. Cox (1962). "A mathematical model of heart rate control by sympathetic and vagus efferent information." J Appl Physiol **17**: 349-55.

Webster, J. I., L. Tonelli, et al. (2002). "Neuroendocrine regulation of immunity." Annu Rev Immunol **20**: 125-63.

Windle, R. J., S. A. Wood, et al. (2001). "Increased corticosterone pulse frequency during adjuvant-induced arthritis and its relationship to alterations in stress responsiveness." J Neuroendocrinol **13**(10): 905-11.

Windle, R. J., S. A. Wood, et al. (1998). "The pulsatile characteristics of hypothalamo-pituitary-adrenal activity in female Lewis and Fischer 344 rats and its relationship to differential stress responses." Endocrinology **139**(10): 4044-52.

Windle, R. J., S. A. Wood, et al. (1998). "Ultradian rhythm of basal corticosterone release in the female rat: dynamic interaction with the response to acute stress." Endocrinology **139**(2): 443-50.

Wolff, M. E., J. D. Baxter, et al. (1978). "Nature of steroid-glucocorticoid receptor interactions: thermodynamic analysis of the binding reaction." Biochemistry **17**(16): 3201-8.

Wurtman, R. J., L. A. Pohorecky, et al. (1972). "Adrenocortical control of the biosynthesis of epinephrine and proteins in the adrenal medulla." Pharmacol Rev **24**(2): 411-26.

Xu, Z. X., Y. N. Sun, et al. (1995). "Third-generation model for corticosteroid pharmacodynamics: roles of glucocorticoid receptor mRNA and tyrosine aminotransferase mRNA in rat liver." J Pharmacokinet Biopharm **23**(2): 163-81.

Yao, Z., D. C. DuBois, et al. (2006). "Modeling circadian rhythms of glucocorticoid receptor and glutamine synthetase expression in rat skeletal muscle." Pharm Res **23**(4): 670-9.

Yehuda, R., M. H. Teicher, et al. (1996). "Cortisol regulation in posttraumatic stress disorder and major depression: a chronobiological analysis." Biol Psychiatry **40**(2): 79-88.

Young, E. A., J. Abelson, et al. (2004). "Cortisol pulsatility and its role in stress regulation and health." Front Neuroendocrinol **25**(2): 69-76.

Young, E. A., N. E. Carlson, et al. (2001). "Twenty-four-hour ACTH and cortisol pulsatility in depressed women." Neuropsychopharmacology **25**(2): 267-76.

Yue, H., M. Brown, et al. (2006). "Insights into the behaviour of systems biology models from dynamic sensitivity and identifiability analysis: a case study of an NF-kappaB signalling pathway." Mol Biosyst **2**(12): 640-9.

Zabel, P., H. J. Horst, et al. (1990). "Circadian rhythm of interleukin-1 production of monocytes and the influence of endogenous and exogenous glucocorticoids in man." Klin Wochenschr **68**(24): 1217-21.

Zorn-Pauly, K., B. Pelzmann, et al. (2007). "Endotoxin impairs the human pacemaker current If." Shock **28**(6): 655-661.

Zuev, S. M., S. F. Kingsmore, et al. (2006). "Sepsis progression and outcome: a dynamical model." Theor Biol Med Model **3**: 8.